University of Siena
Department of Biotechnology, Chemistry and Pharmacy

PhD in Biochemistry and Molecular Biology (BiBiM 2.0)
Ciclo XXXVI

Coordinator: Prof. Lorenza Trabalzini

Development of BSL-2 platforms for the identification of pan-neutralizing human monoclonal antibodies against Coronaviridae

PhD candidate   Thesis Tutor

Elisa Pantano   **Prof.Rino Rappuoli**

Academic Year: 2022/2023

*Alla mia famiglia, sempre accanto a me
in ogni passo importante della mia vita,
compreso questo percorso.*

*E alla mia nuova futura piccola famiglia,
ora in nascita e presto realtà.*

Table of contents

List of abbreviations

2019-nCoV	novel coronavirus 2019
Ab	Antibody
ACE2	Angiotensin-converting enzyme 2
ACoV	Alpaca Coronavirus
BSL-3	Biosafety Level 3
CDR	Complementarity determining regions
CHO	Cells Chinese hamster ovary cells
COVID-19	Coronavirus disease of 2019
CPE-MN	Cytopathic effect-based microneutralization test
CT	Cytoplasmic domain fusion
Dc	Dendritic cells
(E)	Envelope protein
EBOV	Ebola virus
ELISA	Enzyme-Linked Immunosorbent Assays
ERGIC	ER–Golgi intermediate compartment
Fab	Antigen-binding fragment
Fc	Fragment crystallizable
FcR	Fc receptors
FDA	Food and Drug Administration
FP	Fusion Peptide
GFP	Green Fluorescent Protein
HCoV	Human coronaviruses

HIV	Human Immunodeficiency Virus
HR	Heptapeptide repeat sequence
HRR	Hypervariable regions
Ig	Immunoglobulin
INFs	Interferons
ISGs	IFN stimulated genes
LTR	Long terminal repeat
LVs	Lentiviral vectors
(M)	Membrane protein
mAb	Monoclonal antibody
MBCs	Memory B cells
MERS	Middle East Respiratory Syndrome
MOI	Multiplicity of infection
(N)	Nucleocapsid protein
nAbs	Neutralizing antibodies
NF-kB	Nuclear factor kB
nsp	Non-structural proteins
NTD	N-terminal Domain
ORFs	Open reading frames
PBMCs	Peripheral blood mononuclear cells
pDCs	Plasmacytoid dendritic cells
PRRs	Pattern recognition receptors
PVs	Pseudotype virus
RBD	Receptor binding domain
RBS	Receptor binding site

RLSs	RIG-I–like receptors
RSV	Respiratory syncytial virus
(S)	spike protein
SARS	Severe Acute Respiratory Syndrome
SH	Super Hybrid
SN2	Seronegative 2 doses
SN3	Seronegative 3 doses
TAP	Transcriptionally active PCR
TGF-b	Transforming growth factor-b
TLR	Toll-like receptor
TM	Transmembrane
TMPRSS2	Transmembrane protease serine 2
VOC	Variants of Concern
VOI	Variants of Interest
VSV-G	Vesicular stomatitis virus
WHO	World Health Organization
WT	Wild Type
α-CoV	Alphacoronavirus
β-CoV	Betacoronavirus
γ-CoV	Gammacoronavirus
δ-CoV	Deltacoronavirus

Abstract

During the COVID-19 pandemic, the US Food and Drug Administration approved the use of anti-viral neutralizing monoclonal antibodies (mAbs) for emergency purposes in out-of-hospital patients with mild-to-moderate disease [1]. Given the limited availability of these novel therapies, it is imperative to explore their broader potential and devise effective deployment strategies for functional and accurate assays which investigate the ability of mAbs to neutralize the virus.

Live SARS-CoV-2 is categorized as a Biosafety Level 3 (BSL-3) agent due to its high pathogenicity and infectivity; hence, it must be handled under BSL-3 conditions.

The aim of this PhD thesis was to establish accurate and reliable methods to screen and characterize functional mAbs against SARS-CoV-2 and potentially against other viruses, avoiding the use of a BSL-3 laboratory.

Two main tools were implemented during my PhD studies: a spike protein recombinant library, and a third generation lentiviral-pseudotyped-based platform. Both of them can be safely handled in BSL-2 laboratories. The protein library allowed the detection of Spike-responsive antibodies to SARS-CoV-2, SARS-CoV-1, MERS, and other common human coronaviruses (HCoV) (OC43, HKU-1, 229E) using binding assay such the ELISA assay. A mutagenesis approach was implemented to expand this library with the generation of new S variants. On the other hand, the pseudotype virus platform identified and characterized antibodies versus SARS-CoV-2 virus and other HCoV, since the entry of these viruses is mainly mediated by the S glycoprotein, and lentiviral particles pseudotyped with the related S protein can mimic the entry step of the virus of interest, and be studied in BSL-2 settings.

The numerous research projects to which these tools were applied are discussed in the various chapters of this thesis; in particular, three distinct cohorts of COVID-19 patients with different characteristics were examined. These methods allowed to analyze how, over the course of vaccinations and repeated infections, the affinity of mAbs developed by the subjects changed for the different spike variants of SARS-CoV-2 and other HCoV.

Antibodies that neutralized viruses like SARS-CoV-1 and other HCoVs as well as those that showed cross-neutralizing ability against the most recent SARS-CoV-2 variants were characterized using the pseudotype virus platform. Moreover, matrix assays for determining effective antibody combinations to deploy in the fight against SARS-CoV-2 infection have been developed using pseudotyped lentiviral vectors.

Overall, the technologies implemented and applied in this research project can be easily applied to any virus of interest where the main antigens are known and lentiviral vector typing is feasible. By using these techniques, even highly pathogenic viruses that are typically handled in BSL3 facilities can be examined in BSL2 laboratories.

Introduction

1. COVID-19 disease

A cluster of pneumonia cases with unknown etiology was discovered in Wuhan City, Hubei Province, China, on December 31, 2019, according to information sent to the World Health Organization (WHO) [2]. Many potential etiological agents were ruled out in the process of determining its source, including the avian influenza virus, the Middle-East respiratory syndrome coronavirus (MERS-CoV), the severe acute respiratory syndrome coronavirus (SARS-CoV), and other common respiratory pathogens. The WHO revealed on January 12 2020 that the organism causing the illness was a novel coronavirus, temporarily designated as 2019-nCoV. 41 cases of pneumonia, including seven cases of severe illness and one fatality, were reported as of January 11, 2020 [3]. Two infections in individuals infected with 2019-nCoV without physically visiting Wuhan were reported in Guangdong Province on January 20, 2020, as part of epidemiological investigations, confirming the occurrence of human-to-human transmission [4]. Subsequently, 14 medical personnel infected with 2019-nCoV from patients provided additional evidence of human-to-human transmission [5]. The WHO alerted the public to take precautions for their own protection on January 21, 2020, when it revealed that 2019-CoV may have been spread from person to person [2].

WHO officially designated the illness brought on by the new coronavirus as coronavirus disease 2019 (COVID-19) on February 11, 2020, after having declared a public health emergency of international concern on January 30, 2020. At that time, the International Committee on Taxonomy of Viruses reclassified and categorized 2019-nCoV as severe acute respiratory syndrome coronavirus 2 (SARS-CoV-2) based on its genetic similarity to known coronaviruses and established categorization system. Considering the continuous ongoing cases, the economic effects of the virus, and the exponential rise in hospital admissions, WHO on March 11, 2020 formally declared the global spread of the novel COVID-19 as a global pandemic, the first to be caused by a coronavirus.

1.1 History of coronaviruses

The virus that causes COVID-19 is the severe acute respiratory syndrome coronavirus 2 (SARS-CoV-2), a member of the Coronaviridae family that may infect both people and animals[6].

Members of the Coronaviridae family of viruses, coronaviruses, cause respiratory infections in birds and animals, including camels, bats, and masked palm civets. Depending on the host species, coronavirus infections might have distinct symptoms and tissue tropisms. Human coronavirus infections can either be asymptomatic or present with symptoms such as fever, cough, dyspnea, and gastrointestinal distress. Coronavirus infections can sometimes result in severe pneumonia and death, especially in older and immunocompromised persons[7].

The significant emerging and re-emerging status of these viruses has been proven by the 2019 appearance of this highly pathogenic human coronavirus in China.

The official name of coronavirus, an enveloped, RNA-positive single-stranded virus, comes from the spikes on its surface.

Alphacoronavirus (α-CoV), Betacoronavirus (β-CoV), Gammacoronavirus (γ-CoV), and Deltacoronavirus (δ-CoV) are the four genera into which coronaviruses are classified. Mammals are typically infected by α-CoVs and β-CoVs, birds by γ-CoVs, and both mammals and birds by δ-CoVs[8]. Prior to 2019, there were six coronaviruses known that could infect humans: the severe acute respiratory syndrome coronavirus (SARS-CoV)[9], the Middle East respiratory syndrome coronavirus (MERS-CoV) [10], the human coronaviruses 229E [10], NL63 [11] , HKU1 [12], and OC43[13]. While HCoV-229E, HCoV-NL63, HCoV-HKU1, and HCoV-OC43 are responsible for the common cold, infection with SARS-CoV and MERS-CoV, both β-CoVs, can lead to pneumonia and potentially fatal outcomes (**Figure 1**).
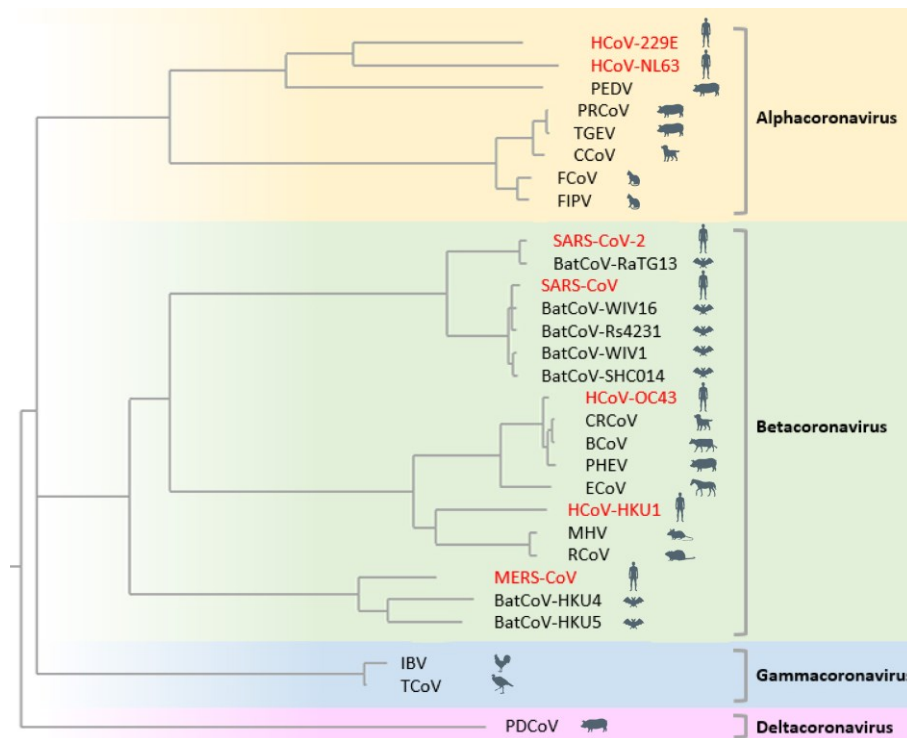
Figure 1. Classification of coronaviruses. *Alpha and Betacoronaviruses. Seven types of coronaviruses (Alpha and Beta) which are known to infect humans are indicated in red: HCoV-229E, HCoV-NL63, HCoV-OC43, HCoV-HKU1, SARS-CoV, MERS-CoV, and SARS-CoV-2. HCoV stands for human coronavirus where HCoV-229E and HCoV-NL63 are alpha-CoVs while HCoV-OC43 and HCoV-HKU1 are beta-CoVs.*

In 1966 human respiratory virus 229E was discovered. A similar sequence of 229E was discovered in a Californian alpaca breed in 2007. Alpaca Coronavirus (ACoV) is the scientific name for it. With 92.2% nucleotide identity throughout the entire genome, HCoV 229E and ACoV share the most genetic similarity.

Further investigation revealed that 229E has many features in common with the bat coronavirus [10]. This indicates that alpacas are most likely the intermediate host through which the original 229E virus strain spread from bats to people [14].

One kind of β-coronavirus is the human coronavirus OC43 [15]: a molecular clock analysis revealed that the 1890s recorded the isolation of the recent common ancestor of OC43 and bovine

coronavirus (BCoV). This indicates that BCoV crossed the species barrier and infected humans around 1890. It might be the place where OC43 was born[13].

The Severe Acute Respiratory Syndrome (SARS) outbreak that struck the Guangdong Province of China in 2002–2003 was caused by a virus part of β-coronavirus known as SARS-CoV. It is the most serious illness that a coronavirus has ever caused in humans. A mortality rate of 9% was achieved during the 2002–2003 outbreak, with about 8,098 cases and 774 deaths. With mortality rates for those over 60 approaching 50%, this rate was far greater for the elderly [9]. Over two dozen countries were affected by the pandemic, which started in a hotel in Hong Kong. Closely related viruses were recovered from many exotic animals during the outbreak, such as Himalayan palm civets and raccoon dogs [16].

A 7-month-old child was admitted to the hospital in Amsterdam in January 2003 due to fever, conjunctivitis, and coryza [17]. Following the initial report of HCoV-NL63, another research team found the same virus, known as HCoV-NL, in the supernatant of Vero-E6 cell culture.

The first case of coronavirus HKU-1 (CoV HKU-1) was reported in a Hong Kong adult patient who had pneumonia in 2005. Despite being a well-known respiratory tract infection, little is known about its function in adult hospitalized patients, particularly in Europe.

Ten years after SARS-CoV initially appeared, in June 2012, a man in Saudi Arabia passed away from severe pneumonia and renal failure. His expectorate was used to isolate a new coronavirus known as Middle East respiratory syndrome coronavirus (MERS-CoV) [18]. Retrospective diagnosis of MERS was made for a cluster of severe respiratory disease patients that had occurred in a Jordanian hospital in April 2012, and in September 2012, three MERS cases in the UK were found [19,20]. Travel by infected individuals caused MERS-CoV to continue to arise and spread; frequently, these imported MERS cases led to nosocomial transmission. A single person returning from the Middle East ignited a nosocomial MERS outbreak in South Korea in May 2015, affecting 16 hospitals and 186 patients[21]. As of April 26, 2016, 624 MERS deaths had been reported from 1,728 confirmed cases in 27 countries [21].

1.2 Novel Coronavirus disease evolution

The replication process of RNA viruses, including the coronavirus, influenza virus, and HIV, as well as the absence of viral RNA polymerase proofreading activity, are known to result in exceptionally high rates of mutation [22,23]. The key components of evolution are aminoacidic mutations, which enable natural selection to favour features that are advantageous to the virus, such as increased virulence, adaptability, and evolvability. SARS-CoV-2 was shown to have crossed the species barrier from bats sold at the Huanan South China Seafood Market in Wuhan, Hubei Province, China, according to a phylogenetic research by Lu et al [24]. Additionally, compared to SARS-CoV (79%) or MERS-CoV (51.8%), the study found that the genomic sequences of SARS-CoV-2 were more similar to the SARS-like bat coronaviruses RaTG13 (96.2% identity) that were recovered from bats in Yunnan, therefore suggesting bats as the main source of SARS-CoV-2.
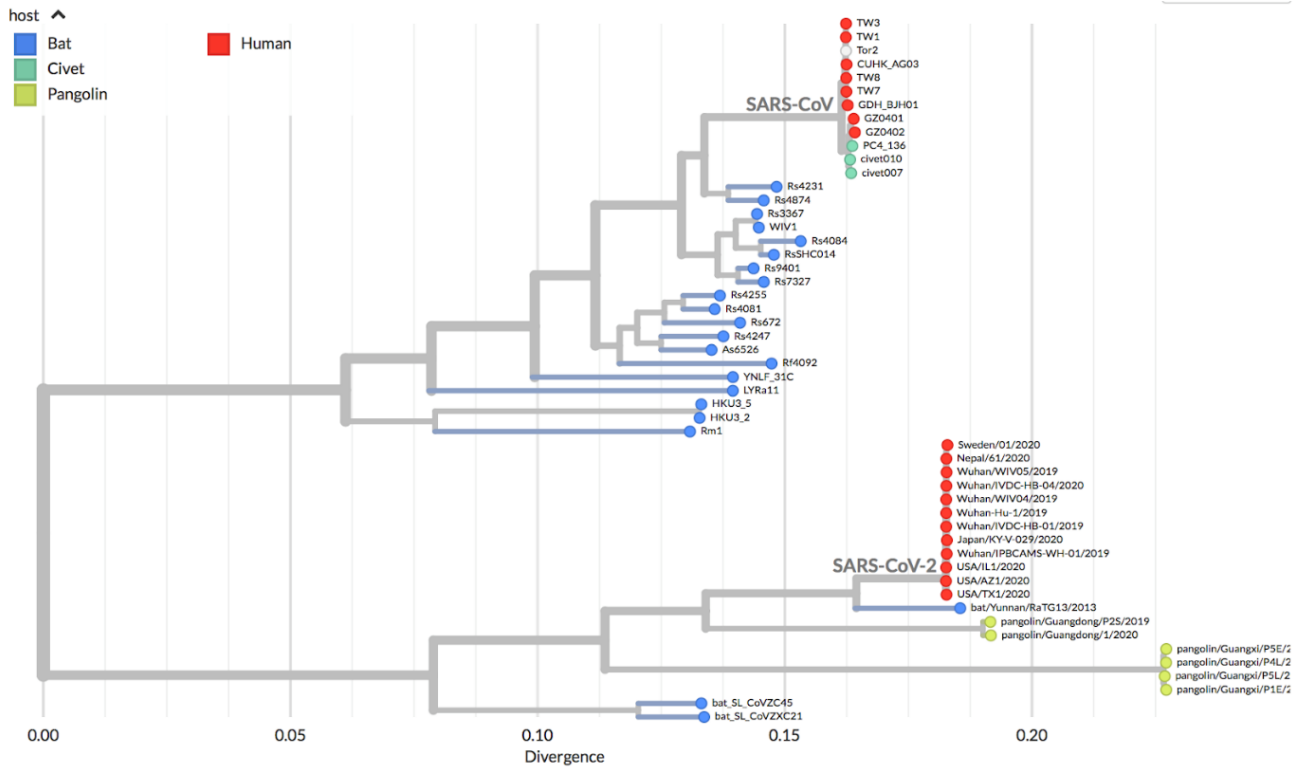
Figure 2. Phylogenic tree of coronaviruses isolated during the years. *Phylogeny demonstrating similarity of 'SARS-like' Betacoronaviruses (or 'Sarbecovirus') to SARS-CoV-2 samples isolated from China, USA, and Japan. Each circle 'tip' of the phylogenetic tree represents a virus sample, color coded by type of host. Figures from nextstrain.com.*

Researchers hypothesise that an intermediate animal, such as snakes, pangolins, birds, or other mammals, may have contributed to the current COVID-19 outbreak because of the wide diversity of animals sold in the Huanan Seafood Market [25]. For the first eight months following SARS-CoV-2 first appearance in humans, the virus appeared to be evolving very slowly. This was caused by a combination of factors, including a small worldwide virus population at the time of the outbreak—which was still not widespread—later non-pharmaceutical actions in many regions of the world, and an artefact of virus undersampling [26]. At the time, predictions were that SARS-CoV-2 would evolve slowly and that evolution would not have a significant impact on the progression and handling of the pandemic. These assumptions were based on known information about the coronavirus polymerase enzyme's proofreading ability.

During April 2020, the most prominent evolutionary change was the D614G substitution. There were few examples of viral variety and evolution during this time. The anticipated substitution rate of SARS-CoV-2 dropped by almost half throughout this time frame. This was mostly caused by imperfect purifying selection[27], which over short durations leaves an excess of harmful mutations in the viral population that have not yet been eliminated. Over the course of epidemic waves, this phenomenon is probably also in charge of changing the predicted substitution rate of other viruses.

1.3 Transmission of COVID-19

It was discovered that the Pangolin-CoV spike protein's sole receptor-binding domain (RBD) differed by just one amino acid from that of SARS-CoV-2. These findings suggested that, prior to infecting humans, Pangolin-CoV and Bat-nCoV may have undergone viral recombination to produce SARS-CoV-2.[25]

This emphasises the potential for initial animal-to-animal transmission.

It soon became clear that respiratory droplets released by an infected person were the primary means of human-to-human transmission. As a result, coughing and sneezing can spread SARS-CoV-2, increasing the risk of infection among those who are not affected [28]. Additionally, data has shown that contact with contaminated inanimate items, commonly referred to as fomite transmission, can also result in SARS-CoV-2 infection [29].

Hospitals are recognised as one of the hubs for secondary SARS-CoV-2 transmission due to the high number of infected patients they treat[30]. The COVID-19 epidemic has presented issues for hospital critical care units (ICUs). In addition to the pressing need to address the demand for healthcare, reducing the viral spread from COVID-19 ICU patients to other patients and medical staff has proven to be a difficulty. To address this issue, strategies for controlling ICU capacity, staffing levels, and infrastructure for infection prevention have been suggested and included into ICU rules [30].

1.4 Immunopathology and clinical presentation of COVID-19

Different pattern recognition receptors (PRRs) are used by the innate immune system to identify viruses, specifically those belonging to the *Betacoronavirus* genus.

There are two distinct pathways for detecting RNA viruses, like coronaviruses [31]. Toll-like receptor 7 (TLR7) is one way by which specialised immune cells, such as plasmacytoid dendritic cells (pDCs), identify the incoming viral genomic RNA in the endosome. Different cell types express endosomal TLR3 (variety of cells) and TLR8 (myeloid cells), which are also capable of identifying endocytosed dsRNA and ssRNA, respectively. Alveolar macrophages are the first line of defence, surveying the respiratory tract lumen [31].

The other strategy comprises viral recognition inside infected cells. dsRNA intermediates can be recognized throughout viral replication by cytosolic RNA sensors such as RIG-I and MDA5, or RIG-I–like receptors (RLRs).

The IRF3/IRF7-dependent transcription of type I and type III interferons (IFNs), as well as nuclear factor kB (NF-kB)-dependent proinflammatory cytokines and chemokines, are activated by downstream signalling upon activation of TLRs and RLRs.

Through the production of viral proteins that interfere with these pathways, SARS-CoV-2 can avoid innate recognition, signalling, IFN induction, and IFN stimulated genes (ISGs) [32].

As a result, compared to other respiratory viruses, SARS-CoV-2-infected people have lower amounts of IFN-I or IFN-III in their peripheral blood or lungs [33,34].

While IFN-l2 and type I IFNs—but not ISGs—can have enhanced expression in the upper airways of patients who develop severe COVID-19, IFN-III (IFN-l1 and IFN-l3) and ISGs are expressed in the upper airways of individuals with reduced disease risk or severity [35].

Furthermore, the number of immunological sentinel cells, such as pDCs and conventional DCs (cDCs), in the blood[36] and lungs [37] significantly decreases in conjunction with COVID-19.

Effector cells are activated by innate immune responses triggered by PRR signalling, which facilitates viral clearance. For example, NK cells help identify and eradicate cells that are infected with viruses. But in individuals with severe COVID-19, transforming growth factor-b (TGF-b) causes NK cells to be reduced in the blood and dysfunctional, which reduces their ability to fight infection [38]. The lungs of patients with severe illness have significantly reduced alveolar macrophage counts, which are crucial sentinel cells in the lungs as they detect and activate strong antiviral immunity [39]. Proinflammatory cytokines and chemokines are markedly enhanced [40], in contrast to the compromised early antiviral defence mediated by IFN-I and IFN-III.

The scientific community has invested heavily in the study of humoral antibody (Ab) and cell-mediated immunity with the goal of defining correlates of protection, developing immune-based therapies, and optimising vaccine design and administration, given the critical role that adaptive immunity plays in protection from viral infection and disease[41,42] .

The amount of antigen and the duration of the germinal centre reaction, where the response matures, are related to the quantity and quality of the Ab response[43]. Ab responses of varying intensities have been observed in preimmune, vaccinated, and infected people; these findings most likely correspond to fluctuations in antigenic load and exposure [36]. The prolonged persistence of the virus, which favours the selection of variants, has been linked to immunosuppressed patients and dialysis patients' generally inadequate Ab response [44].

Moreover, *de novo* immune responses to SARS-CoV-2 as well as progression of the disease may be influenced by cross-reactive Abs induced by seasonal coronaviruses [45].

Similar to SARS-CoV, SARS-CoV-2 is thought to have two phases in its pathogenesis, and the two viruses are 73% similar [46]. Viral replication that causes direct tissue damage is the first hallmark of the viral phase. The course of events of the secondary phase, which is marked by the recruitment of effector immune cells generating a systemic and local inflammatory response that may endure even after viral clearance, is contingent upon the degree of this damage. In addition to a variety of systemic symptoms, such as olfactory dysfunction, which affects about half of people diagnosed with COVID-19 but has not been linked to SARS-CoV, gastrointestinal symptoms [47], cardiac, hepatobiliary, and renal dysfunction, the development of pulmonary disease is linked to excess vascular permeability leading to microthrombi deposition and vascular permeability [31].

The aetiology of extrapulmonary manifestations is probably multifactorial, involving direct viral damage to neurons, arteries, or tissue cells in addition to cytokine production, auto-Ab-induced tissue damage, vascular damage, or dysbiosis of the gastrointestinal tract in the case of GI symptoms. While a few risk factors for severe COVID-19 have been discovered, the pathophysiological mechanisms underlying these factors and their contribution to disease severity remain still not fully understood (**Figure 3**).

The most significant risk factor for developing critical pneumonia is age, as the chance of developing a potentially fatal illness rises substantially after the age of 65. Remarkably, children under the age of two who are frequently susceptible to influenza infections are typically shielded from serious illness [48].

Male patients have a significantly higher chance of developing severe COVID-19 than female patients. This may be because to increased levels of afucosylated anti-SARS-CoV-2 Abs [49], stronger innate immunity, and poorer T cell activation in males compared to females [50]. Chronic kidney disorders, obesity, diabetes, and hypertension are significant risk factors for severe COVID-19.
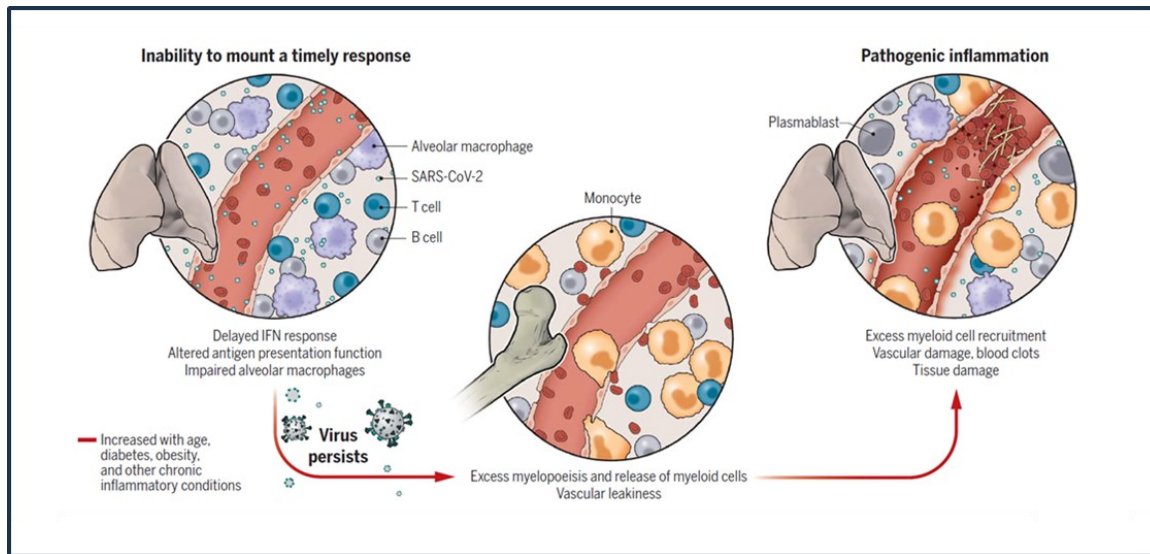
Figure 3. COVID-19 pathogenesis. *Incapacity to mount a prompt and efficient antiviral response due to delayed interferon-β synthesis, modified antigen presentation function, or altered tissue resident macrophage pool—common in the elderly—promotes the persistence of the virus and prolonged tissue damage, which in consequently causes the prolonged release of blood and the recruitment of inflammatory myeloid cells that cause damage to the infected site. The increased release of inflammatory myeloid cells from the bone marrow to the blood circulation and their recruitment to the site of infection leading to profound tissue damage, vascular lesions, and blood clots common in patients with severe disease are further facilitated by enhanced myelopoiesis and vascular damage, which are common in older people and patients with chronic inflammatory diseases. The Figure is from Merad et al., "The immunology and immunopathology of COVID-19, 2022"* [31].

2. SARS-CoV-2 Virus

2.1 Virion structure and maturation

SARS-CoV-2 is a positive-sense, enveloped, single-stranded RNA virus belonging to the Betacoronavirus genus 1. Of the 14 open reading frames (ORFs) in its genome, two thirds encode the 16 nonstructural proteins (nsp 1–16) that make up the replicase complex. Angiotensin-converting enzyme 2 (ACE2), the obligatory receptor for SARS-CoV-2, is necessary for the virus to enter cells. ACE2 was first discovered in 2003 as the receptor for SARS–CoV[51]. The structural proteins nucleocapsid (N), membrane (M), envelope (E), and spike (S) constitute the coronavirus virion (**Figure 4**). The S glycoprotein mediates the entrance phases of the virus particles, which include fusion and adhesion to the host cell membrane. The homotrimer-like S protein is made and placed into the virion's membrane in numerous copies, giving it a crown-like appearance. The entry-glycoproteins of many viruses, (HIV-1, Ebola virus and avian influenza viruses), when penetrate in the infected cells are cleaved into two subunits, the extracellular one and the transmembrane. Similar to this, some coronaviruses cleave their S protein into S1 and S2 subunits during the biosynthesis process in the infected cells, whilst other coronaviruses cleave their S protein only after they arrive at their next target cell. Analogous to SARS-CoV and MERS-CoV, SARS-CoV-2 falls within the first category, as protein convertases such as furin in the virus-producing cells cleave its S protein [52] (**Figure 4**).

Consequently, the two non-covalently linked subunits that together make up the mature virion's S protein are the S1 subunit, which binds ACE2, and the S2 subunit, which anchors the S protein to the membrane. Along with other components required to promote membrane fusion upon infection of a new cell, the S2 subunit also contains a fusion peptide [7].

Viral entrance glycoproteins bind receptors, usually in conjunction with other stimuli, causing both subunits to undergo drastic conformational changes that fuse the viral and cellular membranes and, in the process, open a fusion pore through which the viral genome can enter the cytoplasm of the cell. The cleavage of an extra site inside the S2 subunit, known as the "S2' site," is one such activator for SARS-CoV-2. The S2' location is exposed when the virus interacts with ACE2. When the S2' site is broken, the fusion peptide is released, which starts the creation of the fusion pore. This can happen by transmembrane protease serine 2 (TMPRSS2) [53] at the cell surface or by cathepsin L in the endosomal compartment after ACE2-mediated endocytosis[54]. Every stage of this procedure is crucial because the viral genome needs to access the cytoplasm, and it can only do so when this aperture widens and the viral and cell membranes merge together.

By interacting with other viral proteins (nsp), the E and M proteins support virus assembly and budding [55]. Viruses that have assembled bud into the ERGIC (ER–Golgi intermediate compartment) lumen travel through the secretory pathway to the plasma membrane, where they are released into the extracellular space created when the plasma membrane and virus-containing vesicles fuse.
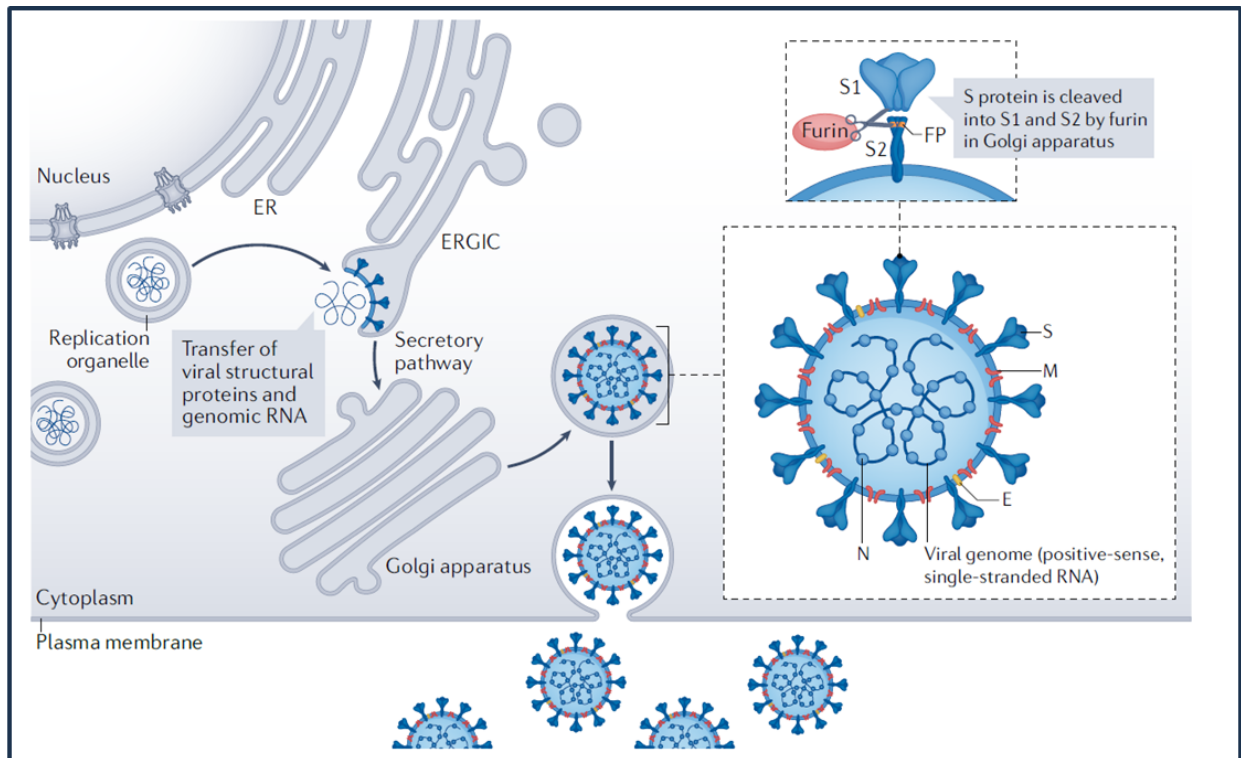
Figure 4. Coronavirus maturation. *The spike (S), envelope (E), membrane (M), and nucleocapsid (N) proteins are the only four viral proteins that are present in the virion. The structural proteins S, E, and M are integrated into the virion membrane, whereas the N protein bound to the viral genomic RNA is packed inside the virion. The Figure is from Jackson et al., "Mechanisms of SARS- CoV-2 entry into cells", 2022 [56].*

2.2 Functional and structural characteristics of SARS-CoV-2 spike protein

The S protein, which has a molecular weight of 180–200 kDa, is made up of a brief intracellular C-terminal segment, an extracellular N-terminus, and a transmembrane (TM) domain that is anchored in the viral membrane [57]. Normally, S is found in a metastable, prefusion conformation. However, when the virus encounters the host cell, it undergoes significant structural changes that enable it to fuse with the membrane of the host cell. To avoid being detected by the host immune system upon entry, the spikes are covered by polysaccharide molecules[58].

Spike of SARS-CoV-2 is 1273 aa long and is made up of the S1 subunit (14–685 residues), the S2 subunit (686–1273 residues), and a signal peptide (amino acids 1–13) at the N-terminus. The last two regions are responsible for membrane fusion and receptor binding, respectively. The S2 subunit is made up of the fusion peptide (FP) (788–806 residues), heptapeptide repeat sequence 1 (HR1) (912–984 residues), HR2 (1163–1213 residues), TM domain (1213–1237 residues), and cytoplasm domain (1237–1273 residues).

2.3 S1 Subunit

The S1 subunit contains the N-terminal domain (14–305 residues) and the receptor-binding domain (RBD, 319–541 residues).

Visually, the viral particle is enveloped by a distinctive, bulbous, crown-like halo made of S protein trimers. The bulbous head and stalk region of the coronavirus are formed by the S1 and S2 subunits, according to the structure of the S protein monomers [59]. Atomic level cryo-electron microscopy has determined the structure of the SARS-CoV-2 trimeric S protein, revealing distinct conformations of the S RBD domain in opened and closed states and their associated functions [60]. Prefusion S1 subunit folds into four domains in the prefusion conformation: the RBD, two carboxy-terminal (C-terminal) domains (CTD1 and CTD2), and the amino-terminal (N-terminal) domain (NTD). It then wraps around the prefusion S2 subunit, which forms a central helical bundle with heptad repeat 1 (HR1) bending back towards the viral membrane. The S protein has two different conformations, 'up' for a receptor-accessible state and 'down' for a receptor-inaccessible state, which are obtained by the three RBDs of the S trimer, which form the apex of the protein (**Figure 5**).

Four stacked β-sheets and several flexible loops that connect and carry multiple N-linked glycans are the main components that form the NTD. It is unknown whether the NTD is functionally involved in SARS-CoV-2 entry into cells.
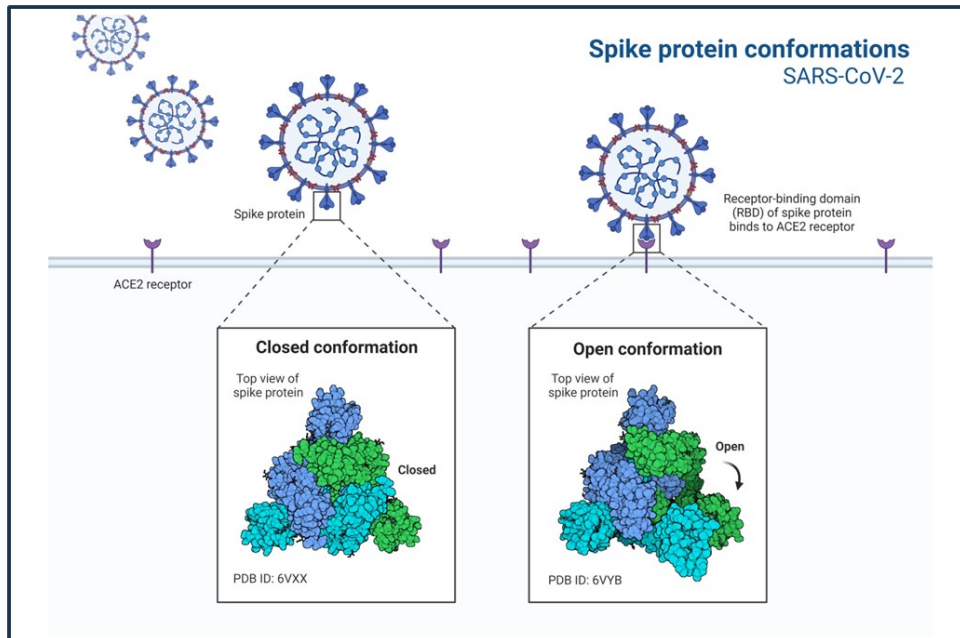
Figure 5. Conformational change of RBD. *The figure shows a 3D conformational change of the SARS-CoV-2 virus spike protein as it binds the human ACE2 receptor* [61].

2.4 S2 Subunit

Viral fusion and entry are mediated by the S2 subunit, which is composed of an FP, HR1, HR2, TM domain, and cytoplasmic domain fusion (CT) in that order.

When the S protein assumes the pre-hairpin conformation, a short segment of 15–20 conserved amino acids known as FP is formed, mostly, of hydrophobic residues like glycine (G) or alanine (A), which serve as an anchor to the target membrane. According to earlier studies, FP is crucial for mediating membrane fusion because it breaks and rejoins the lipid bilayers of the host cell membrane [62]. The repeating heptapeptide HPPHCPC, which makes up HR1 and HR2, has three types of residues: C is another charged residue, P is polar or hydrophilic, and H is hydrophobic or typically bulky [63].

The six-helical bundle (6-HB), which is formed by HR1 and HR2 (**Figure 6**), is necessary for the S2 subunit ability to fuse with viruses and enter host cells. A hydrophobic FP C-terminus is home to HR1, and the TM N-terminus domain is home to HR2 [64]. The S protein is anchored to the viral membrane by the downstream TM domain, and the S2 subunit terminates in a CT tail [63].

After the RBD binds to ACE2, S2 inserts FP into the target cell membrane, exposing the pre-hairpin coiled-coil of the HR1 domain and causing the HR2 domain and HR1 trimer to interact to form 6-HB. This brings the cell membrane and viral envelope closer together for viral fusion and entry [63].

Three highly conserved hydrophobic grooves on the surface of HR1 form a homotrimeric assembly and bind to HR2. To interact with the HR1 domain, the HR2 domain forms both a flexible loop and a rigid helix. The helical region inside the post-fusion hairpin conformation of CoVs is called the "fusion core region" (HR1core and HR2core regions, respectively) because of the numerous strong interactions between the HR1 and HR2 domains.
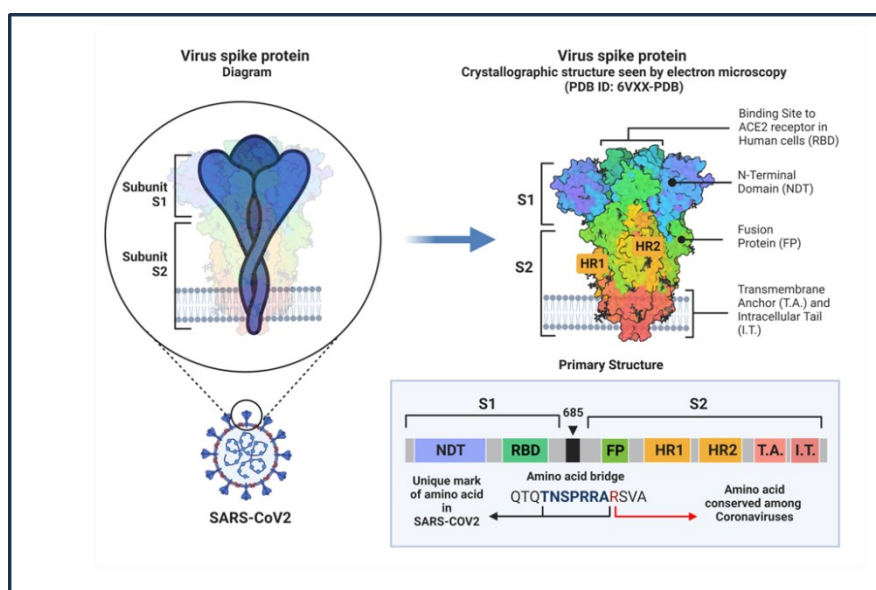
Figure 6. PDB Model of spike Glycoprotein. *The Protein Data Bank (PDB) model of this glycoprotein reveals how the subunits are comprised of different regions that are fundamental to the infection process. S1 and S2 are linked together by a polybasic amino acid bridge. Figure from Andersen et al. "The proximal origin of SARS-CoV-2" , 2020* [65].

2.5 S protein function

The fundamental unit through which the S protein attaches to the receptor is the trimer of the protein that is present on the surface of the viral envelope [66].

The SARS-CoV-2 S protein binds to the host cell through its recognition of the ACE2 receptor, as was previously mentioned. Angiotensin I is converted into angiotensin 1–9 by ACE2, an ACE homolog. The lung, gut, heart, and kidney are the organs where ACE2 is primarily found, and the cells that express it the most are alveolar epithelial type II cells [67].

SARS-CoV-2 can enter cells through endocytosis or membrane fusion at the cell surface; the route utilised in a particular cell type is primarily determined by the expression of proteases, specifically TMPRSS2 (**Figure 7**). When TMPRSS2 is expressed, the membrane fusion pathway is favoured; in the absence of this protease, the virus will enter the body through endocytosis; in this case the most well-characterized pathway is clathrin-mediated endocytosis (CME), which results in the formation of clathrin-coated vesicles and the absorption of extracellular materials within them. (**Figure 7**). In this case the cytoplasmic tail and enzymatic activity of ACE2 are not necessary.
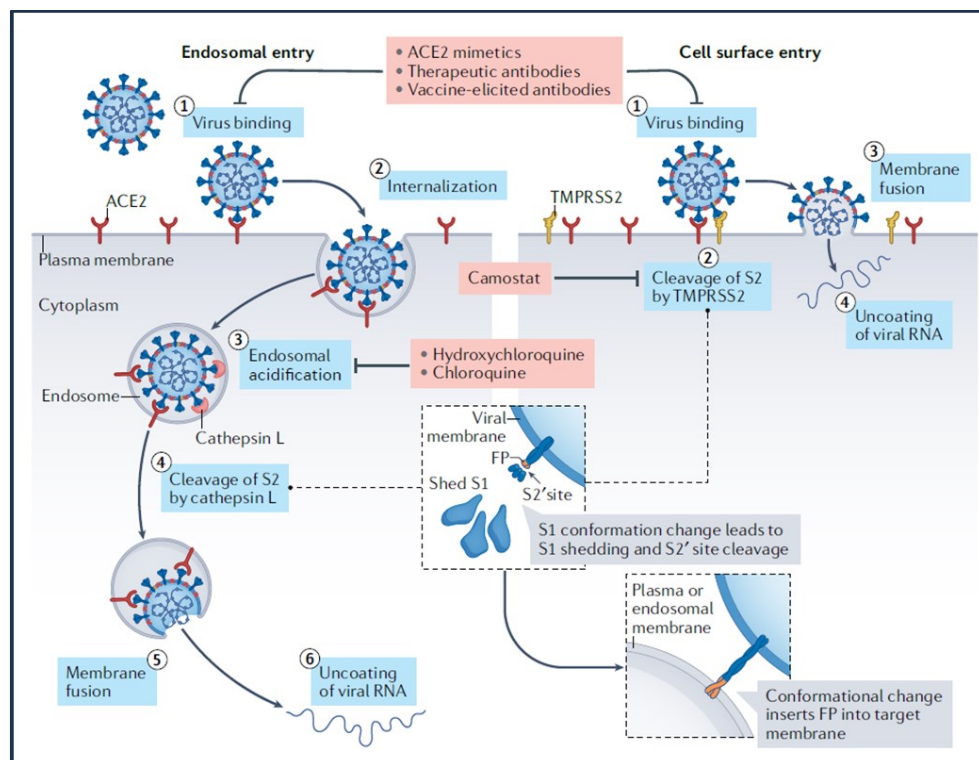
Figure 7. The two possible entry pathways of SARS-CoV-2. *Usually, two spike (S) protein cleavage events—one at the intersection of the S1 and S2 subunits and the other at the S2' site, which is*

internal to the S2 subunit—are required for the coronavirus entry process. The SARS-CoV-2 virus matures in an infected cell, cleaving the polybasic sequence at the S1–S2 boundary. However, the S2' site cleaves at the target cell after angiotensin-converting enzyme 2 (ACE2) binding.

The S1 subunit undergoes conformational changes upon binding to ACE2, and in the S2 subunit, S2's cleavage site is made visible. Different proteases cleave the S2 site in response to the entry pathway that SARS-CoV-2 takes. The virus-ACE2 complex enters through clathrin-mediated endocytosis (step 2) if the target cell expresses insufficient transmembrane protease serine 2 (TMPRSS2), or if it does not come into contact with TMPRSS2. Cathepsins then cleaves the S2' molecule in the endolysosomes, which requires an acidic environment to be active (steps 3 and 4).

TMPRSS-2 promoted pathway: S2' cleavage takes place at the cell surface when TMPRSS2 is present (step 2). The fusion peptide (FP) is exposed in both entry pathways by cleavage of the S2' site, and the S2 subunit undergoes significant conformational changes upon dissociation of S1 from S2, particularly in HR1, which drives the fusion peptide forward into the target membrane, starting the fusion of the membranes (steps 3 and 5 on the left and right, respectively). Steps 6 on the left and 4 on the right show how the fusion of the viral and cellular membranes creates a fusion pore, which allows the release of viral RNA into the cytoplasm of the host cell for uncoating and replication. The Figure is from Jackson et al., "Mechanisms of SARS- CoV-2 entry into cells", 2022 [56].

2.6 SARS-CoV-2 evolution during the first four years of spread: emergency of variants of concern

Starting from December 2020 the rate of evolution matched with the acquisition of approximately two mutations per month in the world population. The first mutation observed was the D614G in the RBD domain of the spike protein. This first mutation was responsible for the increased fitness of the virus conferring a major ability to bind the ACE2 human receptor thanks to an open conformational state of the spike protein, so that this mutation is still conserved in all the emerging variants of the SARS-CoV-2 virus. D614G may also be responsible for an increase of the number of spike proteins per virion and increasing the frequency of S1/S2 cleavage [68].

A novel SARS-CoV-2 lineage with several mutations in the spike region [69] was found to be spreading quickly in several areas of the United Kingdom towards the end of December 2020. The WHO named firstly this VOC Alpha, then reclassified with its Pango reference as B.1.1.7.

Two further fast expanding lineages, VOCs Beta (Pango lineage B.1.351) and Gamma (Pango lineage P.1), were discovered in the following weeks in South Africa and Brazil. Each of them had a significant number of genetic variations from the baseline virus population, some of which showed signs of increased transmissibility or immune escape capabilities [70].

The Delta lineage (Pango lineage B.1.617.2), was first detected in India in late 2020. The Delta variant was named on 31 May 2021 and had spread to over 163 countries by 24 August 2021; it promptly replaced previous VOCs and headed a radical wave in cases around the world [71].

It is important to mention together with the B.1.617.2 variant the concomitant variant which occurred, the B.1.617.1 (Kappa) variant. This shows a very similar spike protein to the B.1.617.2, but in this variant the mutation E484Q showed up together with the L452R located in the S2 portion.

New global waves of infection were sparked in November 2021 by the discovery of Omicron [72] (Pango lineages BA.1–BA.5) in South Africa and Botswana. N501Y, E484K, and ΔH69/V70 are examples of shared sets of mutations that these VOCs exhibited while emerging from different parts of the world, suggesting the possibility of convergent evolution [73]. Compared to their preceding variations, each of these VOCs exhibited a substantially greater growth advantage [74].

Omicron variants maintain some of the mutations typical of the Delta variant and the Gamma variant, such as D405N, E484K, N501Y. Q493R is another mutation characteristic in all the Omicron variants, present in each of the Omicron sub lineages, associated with high-level resistance to several nAbs. Differently, G496S is present in the Omicron BA.1 variant but not in the BA.2 and BA.4/5 variants and is associated with about 5-fold reduced nAbs susceptibility [26].

In the last few months circulation of a new Omicron subvariant has being observed: XBB is a recombinant of BA.2.10.1 and BA.2.75 sublineages, and although there has been a broad increase in prevalence of XBB in regional genomic surveillance, it has not yet been consistently associated with an increase in new infections. This subvariant conserves all the typical mutations of the BA.2 Omicron, with the addition of some mutation which until now were classified as BA.4/5 variant or its subvariants, such as the R346T, G446S, N460K and F486V.

It is still up for debate what the evolutionary origins of VOCs are. A few theories have been proposed as reasons for their emergence: persistent latent transmission of SARS-CoV-2 in humans in regions with inadequate genomic surveillance; zoonotic transmission of SARS-CoV-2 in animal reservoirs; and persistent SARS-CoV-2 infections in specific immunocompromised individuals (**Figure 7**).
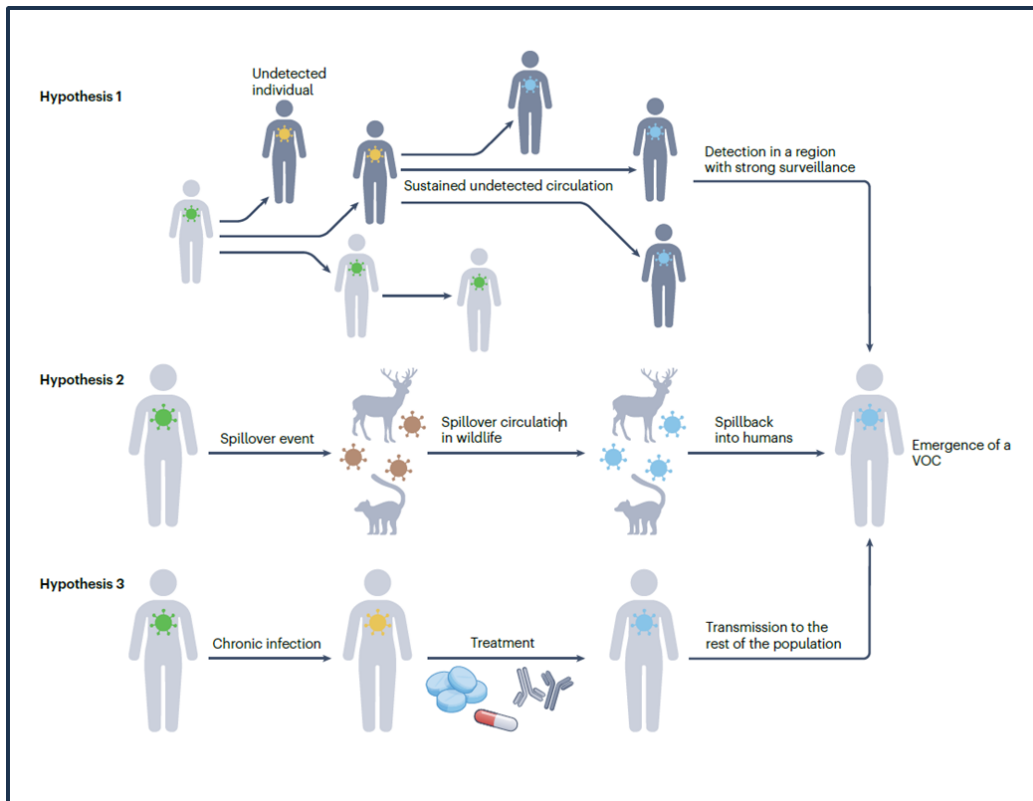
Figure 7. Hypothetical origin of VOCs. *Hypothesis 1: the virus can spread, causing severe illness for an extended period of time in an area with insufficient genomic surveillance and gradually gaining adaptive modifications unreported until it reaches a location with more robust genomic surveillance. Hypothesis 2: Individuals who have close interactions with domestic or untamed animals, like deer or mink, may spread the virus to these categories. There, the SARS-CoV-2 virus may develop extra adaptive modifications in the animal populations before spreading to humans and giving rise to variants of concern (VOCs). Hypothesis 3: When the virus continues to exist in a person with a chronic infection for an extended duration, it might undergo alterations that serve as adaptations to the host's immune system reactions. If the patient is receiving treatment (such as convalescent plasma or monoclonal antibodies) to eradicate the infection, further adaptive changes might take place, which might speed up the selection process for mutations that escape antibodies. The Figure is from V. Markov et al., "The evolution of SARS-CoV-2, 2023* [26].

3. COVID-19 Control Measures

3.1 Vaccines against SARS-CoV-2

The four most important structural proteins of the coronavirus, E, M, S, N are the primary targets for potential vaccines.

Specifically, the spike protein, because of its key role in interacting with the ACE2 receptor and thus promoting infection, is the focus of vaccines to date on the market and in development. The recent pandemic was contained thanks to the rapidly development of the COVID-19 vaccines, and research on COVID-19 treatments is still moving extraordinarily quickly. There are two types of vaccine platforms: one based on individual viral components and another based on the entire virus. Protein subunits, virus-like particles, DNA- and RNA-based viral vectors, replicating and non-replicating viral vectors, and virus-like particles are examples of viral components. On the other hand, both live-attenuated and inactivated vaccines are part of the entire virus-based platform.

Currently, more than 200 vaccine studies are underway, and many vaccines across multiple platforms have been approved for clinical trials despite a number of limitations [75].

Pfizer-BioNTech's BNT162, Oxford-AstraZeneca's AZD1222, Sinovac's CoronaVac, Moderna's mRNA-1273, Johnson & Johnson's Ad26.COV2.S, Sputnik-V, vector vaccines (Gamaleya National Research Centre for Epidemiology and Microbiology), and adjuvanted recombinant protein nanoparticles (Novavax) are among the top-performing pharmaceutical companies at the moment for COVID-19 [76] [77].

Another effective vaccination mechanism involves the use of a recombinant antigen to promote immunity in the subject. The RBD portion of the spike protein, or even just the protein itself, is the primary antigen of interest in the case of SARS-CoV-2 (the RBD is specifically targeted by the majority of antibodies produced during immunisation).

The antigenic portion of the virus used in recombinant COVID-19 vaccines reduces the risk of side effects that come with live or attenuated vaccinations while simultaneously enhancing their safety and effectiveness. Recombinant vaccines have shown very promising results thus far and are undergoing extensive study. Numerous new vaccine candidates are undergoing clinical trials; a few have successfully completed phase III studies and received authorization to proceed with additional procedures[78].

3.2 COVID-19 vaccines' efficacy against SARS-CoV-2 variants of concern

Immune escape can also be facilitated by vaccination in addition to innate immunity. For SARS-CoV-2 in particular, the absence of mucosal protection after parenteral immunisation is a critical distinction.

Given that the virus is still capable of replicating and spreading within the upper respiratory tract mucosa, vaccination may have a less significant effect in the evolution of SARS-CoV-2 than spontaneous infection does[79]. The majority of widely used vaccines target the spike protein or even

only the RBD, a far more limited antigenic area than that in a normal infection. This naturally restricts the pressure for escape to these specific areas. Nonetheless, vaccination-related immune escape has been demonstrated for Omicron [26,80] and Beta, primarily due to antibodies produced by RBD. Besides natural immunity, vaccination can also be a driver for immune escape, for the lack of mucosal immunity following parenteral vaccination. The Delta variant[81] was shown to be immune to vaccine-induced humoral immunity. The distribution and continuing evolution of the virus make natural immunity a far more dynamic selective force, even though mass vaccination with ancestral strains may produce a more steady and predictable immunological pressure. A SARS-CoV-2 variant with a high degree of escape from its immune landscape will always proliferate quickly throughout the population due to the shifting immune landscape, and it may even be able to prevail over variants that produce immunity[26].

3.3 Passive immunization: monoclonal antibodies to prevent and treat the infection

Emil von Behring discovered that immune serum could prevent and cure diphtheria, which led to the development of passive immunisation and modern medicine. The most obvious method for curing COVID-19 in the absence of targeted medications and vaccinations was the presence of SARS-CoV-2 antibodies in the plasma of convalescent patients who had recovered from illness. Transfusion of plasma with high titres of neutralising antibodies from patients who were convalescing to those who were hospitalised was the first use of antibodies during the COVID-19 pandemic. Plasma therapy was the first medication approved by the FDA for use in an emergency, and a number of trials have shown modest benefit [82] [83].

Prior to the COVID-19 pandemic, the application of monoclonal antibodies (mAbs) as treatments for infections received less attention, even though over 100 of them had been approved as cancer, autoimmune, and inflammatory medicines [83].

This was mostly due to their expensive price, which prevented them from being used for larger applications. Cloning powerful neutralising antibodies from memory B cells of convalescent patients after SARS infection changed the game in the field of mAbs for infectious illnesses[84]. Since then, a number of techniques for isolating and cloning mAbs from B cells have been established. They were widely employed, for example, in HIV research, where mAbs aided in the identification of highly conserved epitopes, guiding the creation of vaccines and passive antiviral and therapeutic treatments. The field of isolating mAbs was established when the COVID-19 pandemic broke out in January 2020. The discovery and development of mAbs specifically targeted against the SARS-CoV-2 virus was the primary focus of several research institutes and pharmaceutical corporations. Potent, ultrapotent, and extremely potent mAbs that target the RBD of the spike protein have been quickly described. These mAbs neutralised the virus *in vitro* at concentrations of 100 ng/ml or below. Only very rare antibodies can neutralise the virus at concentrations below 10 ng/ml. Within the first six months of the pandemic, several mAbs entered clinical trials and showed positive results. Early administration of the medication after infection was shown to accelerate viral clearance and reduce hospitalisation by 75% [85,86]. The administration of mAbs as therapy for COVID-19 may have even

greater benefits than classical vaccination, and thus than triggering active immunity. In fact, for active vaccinations to work in a regulated and advantageous way, the adaptive immune system must be intact. However, a lot of people lack a strong immune system to react appropriately to vaccinations because of conditions like cancer, autoimmune diseases, immunological immaturity or senescence, medical immunosuppression. Conversely, immunity can be transferred to almost anyone by passive immunisation with antibodies, irrespective of age, immunological state, or medical condition. Lastly, it is important to note that while active vaccinations usually take weeks or months to reach peak immunity and require numerous administrations (boosters) to reach that peak, passively transferred antibodies attain peak immunity in a variety of tissues within hours to days since administration [87,88].

When discussing mAbs as therapeutics, it is also crucial to note that they may have prophylactic effects as well, providing protection and avoiding possible infections.

For this reason, mAbs might have the best use case in emergency medicine.

4. Antibodies

The antibody, also called immunoglobulin, is an essential component of the immune response and has been utilised to investigate immunity and aid in the creation of treatments. Antibodies are naturally occurring proteins produced by the immune system to protect the body against infections and illnesses like cancer.

They are the secreted form of the B-cell receptor. Except for a tiny piece of the heavy-chain constant region's C-terminus, an antibody is the same as the B-cell receptor of the secretor cell. The C-terminus is a hydrophilic sequence that permits secretion in the case of an antibody while it presents a hydrophobic sequence that anchors the membrane in the case of a B-cell receptor [89]. They can only be produced by B lymphocytes, which are essential components of the adaptive immune system, together with T lymphocytes [90]. A vast and varied repertoire of antibodies, each with a unique amino acid sequence and antigen-binding site, can be produced by B lymphocytes.

Passive "serum therapy," or using sera obtained from sick animals (immunised animals) to protect non-immunized humans, was the first demonstration of the protective effect of antibodies [91]. To cure illnesses like diphtheria and tetanus, Behring and Kitasato made the initial discovery of target specific antibodies that could bind bacterial toxins in the early 1890s. By immunising a horse with *Corynebacterium diphtheriae*, Emil Adolf von Behring and Erich Wernicke created the first potent antitoxin serum against diphtheria. Originally known as "Antitoxin," the anti-infective compound in the serum was eventually renamed as antibody [92]. For his work and discovery in medical fields, in 1901, when the Nobel Prizes were awarded for the first time, Behring received the Prize in Physiology or Medicine.

4.1 Antibody structure and function

IgG antibodies are big molecules composed of two distinct types of polypeptide chains, with a molecular weight of about 150 kDa. The terms "heavy" (about 50 kDa) and "light" (about 25 kDa)

refer to the two different chains. Two heavy chains and two light chains make up each IgG molecule. Disulfide bonds connect the two heavy chains, and they also connect each heavy chain to a light chain (**Figure 8**). The two light and heavy chains of every immunoglobulin molecule are identical, providing an antibody molecule with two identical antigen-binding sites and the capacity to bind to two identical structures at the same time.
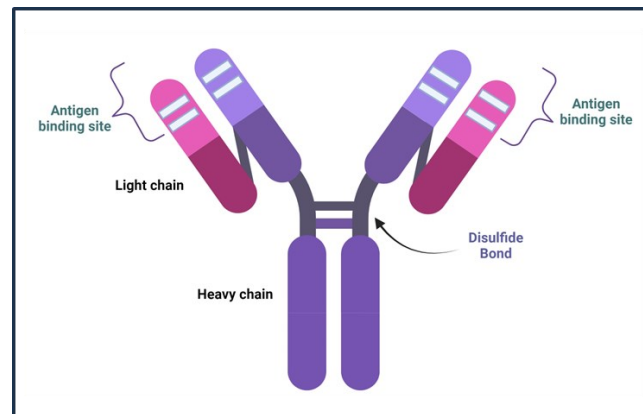
Figure 8. Schematic structure of immunoglobulins. *Heavy chain is coloured in purple while light chains are in pink. At the centre of the structure is evident the disulfide bond which joins the chains. The antigen binding sites are present in each heavy and light chain, here displayed in white color.*

Antibodies contain two different types of light chains, known as lambda (λ) and kappa (κ). An immunoglobulin can include one or two λ or κ chains, but never both. There is no discernible functional distinction between antibodies with λ or κ light chains, and antibodies belonging to any of the five primary classes can contain either kind of light chain. The proportion between the two kinds of light chains differs between species.[89]

Immunoglobulins consist of a Fab region with antigen-binding sites and an Fc region that mediates biological functions (such as the ability to interact to cellular receptors). The domains are the areas where the chains are folded. Depending on the class, there are four or five domains in the heavy chain and two in the light chain. The antigen-binding sites are found in the hypervariable regions (HRR). Each light and heavy chain has three HRRs in its V domains. These fold into areas at the tip of each monomer to form two antigen-binding sites. Every antibody possesses one or more bifunctional roles, such as stimulating the complement system, making microorganisms more easily phagocytosed, preventing the adhesion of bacteria to mucosal surfaces, and neutralising toxins and viruses [93].

Throughout the immune response, both Fc and Fab regions undergo fast change: the Fc transforms into five distinct isotypes to elicit distinct effector actions, while the Fab evolves to strengthen the affinity to the foreign antigen. IgM, IgD, IgA, IgE, and IgG are these isotypes. IgM is the first class of antibodies to emerge during the main immune response; it has broad specificity but poor affinity to the antigen since it is still developing. It co-expresses with IgD on the surface of mature B cells (prior to activation). Additionally, IgD has the ability to attach to basophils and release antimicrobial substances through secretion in blood and mucosal secretions [94].

The predominant isotype found in secretions is IgA, which is particularly significant in the mucus produced by the intestinal and respiratory tract epithelium. Blood or extracellular fluid contain very low concentrations of IgE, which binds to mast cell receptors to cause the mast cells to release potent chemical mediators. Lastly, IgG is mostly found in serum and blood, and acts by activating the complement system and by opsonizing pathogens for phagocytosis. In humans, the isotype is further classified into four subclasses (IgG1, IgG2, IgG3, and IgG4)[95].

Antibody molecules are divided into three pieces by limited digestion with the protease papain (**Figure 9**). The two identical arms of the antibody molecule, which comprise the entire light chains paired with the VH and CH1 domains of the heavy chains, are represented by the Fab fragments. The other fragment was initially found to crystallise easily despite having no antigen-binding function; for this reason, it was given the designation Fc fragment, which stands for fragment crystallizable. This portion of the antibody molecule, which interacts with effector molecules and cells, is matched to the paired CH2 and CH3 domains. The Fc is primarily responsible for the functional variations between heavy-chain isotypes.
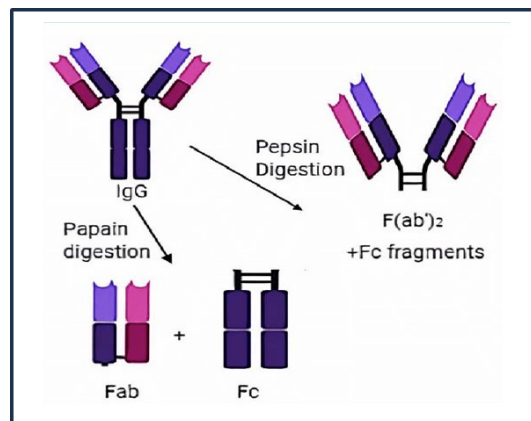
Figure 9. Schematic structure of an immunoglobulin. *The Fab portion and the Fc portion of the immunoglobulin have two distinct roles.*

While the antibody antigen-binding fragment (Fab) region attaches to antigen directly, the Fc region determines the antibody isotype and regulates interactions with FcR [94].

The immunoglobulin fold is a structure formed by the folding of immunoglobulin domains. This structure is composed of two beta sheets that are "sandwiched" together and contain antiparallel beta strands joined by loops. There are two varieties of immunoglobulin folds seen in antibodies, with seven or nine beta strands (plus an additional loop) in each. While the latter is located in the variable region, the former serves as the structural unit of the constant areas.

Consequently, the complementarity determining regions (CDRs) are represented by the loops that join the antiparallel beta strands of the VL and VH domains. There is significant variation in both the length and composition of the CDR sequences. This heterogeneity results from various mechanisms that occur throughout the production of antibodies, including recombination of the V(D)J genes, nucleotide additions or deletions in junctions, and somatic hypermutations in the recombined genes. These processes are designed to produce a large variety of antibodies from a small number

of antibody genes [96]. The quantity and kind of amino acids that constitute up the CDRs loops, which define the surface topography of the binding site, affect the particular interactions that antibodies have with their antigen; the affinity is promoted by non-covalent forces between the paratope and epitope [97].

The specificity of the antigen is determined by antigen binding, which can also affect how the antibody interacts with the Fc receptor. The interaction of Fc with the Fc receptor is connected to the antigen binding of the Fab portion of antibodies. Because antigen binding alters the Fc domain and hinge regions' conformation, it can allosterically increase Fc receptor recognition. Different receptors can be engaged by the Fc, and the intracellular signalling that results can either activate or inhibit activity. The FcγRI, a high affinity receptor that recognises monovalent antibodies, and the FcγRIIa, IIc, FcηRIIIa, and IIIb, which have lower affinity and necessitate avidity-based interactions, are examples of activating receptors. Conversely, FcγRIIb is an inhibitory receptor [98].

4.2 Antibodies to contrast viral infections

The full theoretical potential of mAbs in treating infectious diseases has not really been explored until now. In fact, only a small number of mAbs have been authorised for the treatment of infectious illnesses (Table 1). 1998 saw the licencing of Palivizumab, a humanised murine mAb, in high-risk newborns to avoid lower respiratory tract sickness brought on by the respiratory syncytial virus (RSV). October 2020 saw the licencing of a combination of antibodies known as REGN-EB3 for the treatment of Zaire ebolavirus infection, and two months later, a monotherapy for the same virus. The latest COVID-19 pandemic promoted the authorization for   the Emergency use of a number of SARS-CoV-2 antibodies.

Regarding bacteria, three antibacterial mAbs have been authorised. As of the writing of this thesis in 2023, the FDA had fully approved six mAbs that target viral or bacterial pathogens (Table 1). These indications include the treatment of Ebola virus (EBOV) infection, the prevention of anthrax infection, the prevention of *Clostridium difficile* infection recurrence, and the prevention of respiratory syncytial virus (RSV) infection.

**Table 1. mAbs available as drug therapy by December 2023**

Drug (brand name; company)	Target	Format	Technology	Indication	Year of FDA approval
Palivizumab (Synagis; MedImmune/AbbVie)	RSV	Humanized IgG1	Hybridoma	Prevention of RSV infection	1998
Raxibacumab (ABthrax/Anthrin; GlaxoSmithKline/Human Genome Sciences)	*Bacillus anthrasis* PA	Human IgG1	Human scFv phage display library	Anthrax infection	2012
Bezlotoxumab (Zinplava; Merck & Co.)	*Clostridioides difficile* enterotoxin B	Human IgG1	Transgenic mice	Prevention of *C. difficile* infection recurrence	2016
Obiltoxaximab (Anthim; Elusys Therapeutics)	*B. anthrasis* PA	Chimeric IgG1	Hybridoma	Prevention of inhalational anthrax	2016
Ibalizumab[a] (Trogarzo; TaiMed Biologics)	CD4 receptor (domain 2)	Humanized IgG4	Mice	Treatment of HIV-1 infection	2018
Ansuvimab (Ebanga; MedImmune/Ridgeback Biotherapeutics)	Ebola glycoprotein	Human IgG1	Human	Prevention and treatment of Ebola infection	2020
Atoltivimab, maftivimab and odesivimab (Inmazeb; Regeneron Pharmaceuticals)	Ebola glycoprotein	Human IgG1	Transgenic mice	Prevention and treatment of Ebola infection	2020

Because of properties including their high specificity and capacity to boost immune responses, mAbs are attractive as possible treatments and preventative measures against viral infections. Additionally, antibody engineering can be utilised to increase effector functions and extend the half-life. Developments in structural biology have made it possible to select and optimise powerful neutralising mAbs by identifying susceptible regions in viral proteins, which may also have implications for vaccine development. Neutralising monoclonal antibodies (nAbs) against SARS-CoV-2 have been developed in large part because of the COVID-19 pandemic. With the approval of many mAbs for use in emergency situations, these treatments not only constitute a crucial part of COVID-19 prevention and treatment programmes, but also advance the use of mAbs in other infectious disease scenarios.

The use of antibodies as drugs is particularly interesting in the case of pathogens such as viruses and specifically SARS-CoV-2, since mAbs can inhibit viral replication at multiple steps in the virus life cycle, through different mechanisms **(Figure 10c)**. In details they can use several mechanisms to:

1) avoid virions from attaching to cells, as strongly neutralising antibodies frequently prevent viruses from attaching to cell receptors by identifying the receptor-binding domain (RBD) or receptor-binding site (RBS);

2) stop the virus and cell membrane from fusing, primarily inhibiting the spike protein action since the spike protein binds to attachment factors on the surface of the host cell, such as the cell surface protease TMPRSS2 (which cleaves the viral protein to allow entry) and receptor ACE2;

3) prevent virion particles from exiting infected cells: at some point, viruses have to exit an infected cell. This process, which is also known as egress, consists of budding, release, and assembling. Preventing this action leads to an inhibition of virus pathogenicity;

4) attract and activate cells expressing Fc receptors to boost immunity.
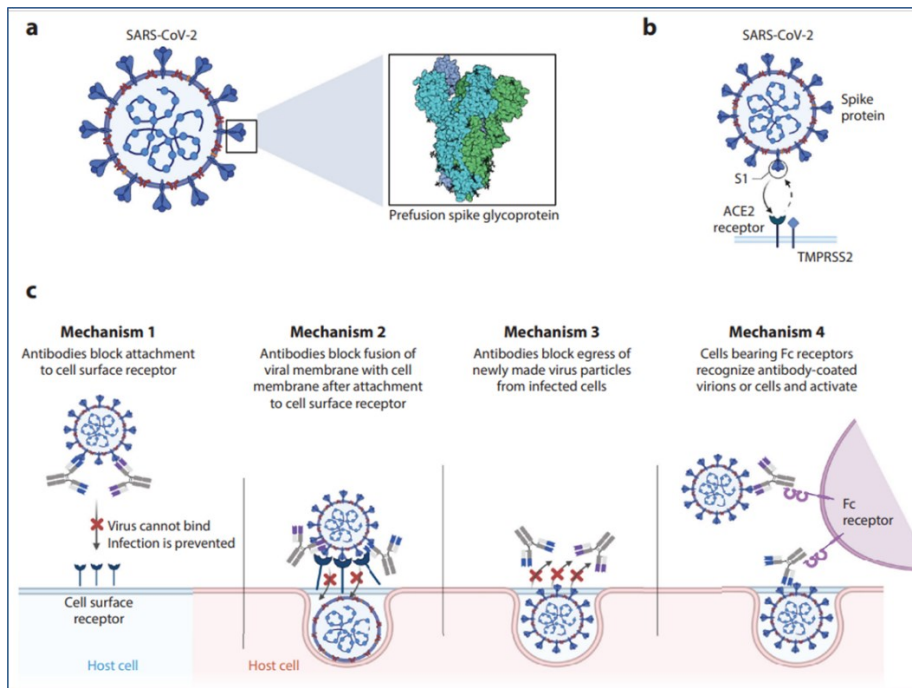
Figure 10. Four typical mechanisms of inhibition of virus infection mediated by antibodies.
A. Representation of SARS-CoV-2 virus with the spike proteins on the envelope; B. Interaction between SARS-CoV-2 virus and ACE2 receptor, indispensable for the incipit of the infection. C. The four mechanisms used by the mAbs to avoid virus infection and proliferation. The Figure is from Pantaleo et al. "Antibodies to combat viral infections: development strategies and progress", 2022[99].

In conclusion, in viral infection antibodies can have a variety of structural consequences, from completely disrupting the protein's oligomeric structure to stabilising a viral fusion protein by locking or stapling it in the prefusion state.

4.3 Strategies to generate human therapeutic antibodies for SARS-CoV-2 infections

During the last 50 years many strategies have been developed to discover and isolate mAbs versus viral infections. Five different procedures are the most effective and the more used worldwide, summarized in **Figure 11**.

In details, the phage bio-panning library is a library of phages with genes encoding for variable light (VL) and variable heavy (VH) domains, which produce antibodies on phage surfaces. The process of selecting antibodies derived from phages requires immobilising the target ligand on a solid support (the spike protein of the SARS-CoV-2), after which the phage display library is applied to the immobilised ligand to enable binding of specific variants. Multiple rounds of washing are often carried out to remove adhering non-binders, and any residual bound phages are then eluted and re-amplified (**Figure 11a**).

The sorting method involves the use of fluorescence-activated flow cytometry, where recombinant antigens conjugated to a fluorescent marker are incubated with class-switched memory B cells and sorted based on their ability to bind the target antigen (the S protein of SARS-CoV-2) and the antibodies they produce. Subsequently, on a feeder layer, single B cells are seeded in the presence of a TLR activator and a cytokine mixture. After checking the culture supernatant for neutralisation activity, representative clones are extracted and sequenced (**Figure 11b and 11c**).

There has been recent news of a functional organotypic system for production of antibodies. This system implicates a procedure for reconstituting organoids from human tonsils to create an *in vitro* system that mimics important characteristics of the germinal centre, such as the generation of antibodies specific to antigens, somatic hypermutation, and affinity maturation (**Figure 11d**). Lastly, workflow for single cell immune profiling barcoded gel beads are used to encapsulate B cells in a single partition, after which they go through reverse transcription and PCR. Every cDNA is extracted from its unique cell of origin, barcoded, and prepared for next-generation sequencing (**Figure 11e**)[99].
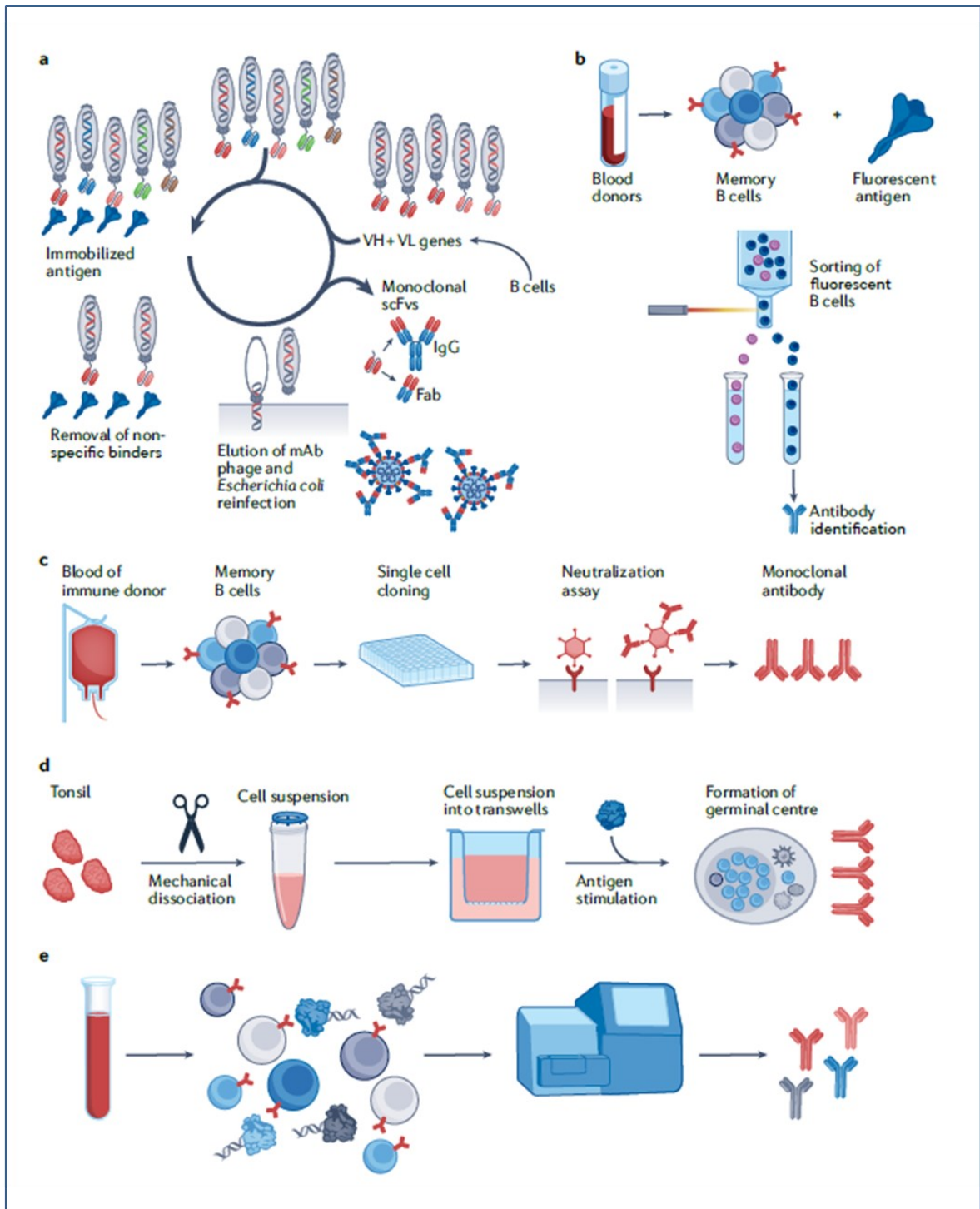
Figure 11. Several approaches to isolate mAbs versus viruses. *The phage bio-panning library (a), the sorting strategy (b, c), the organoid system (d) and the single cell immune profiling method are shown step by step. The Figure is from Pantaleo et al. "Antibodies to combat viral infections: development strategies and progress", 2022*[99].

4.4 mAbs for vaccine discovery: Reverse vaccinology 2.0

In pathways like viral infection and antibody response to virus entry, a focal point is represented by the interaction between the Fab of the neutralizing antibody and the paratope of the antigen

involved. Apart from therapeutic uses, the antigen-antibody interface can be investigated and antibodies and their binding epitope can be templated and subsequently assessed. This may offer a novel method for locating protective antigens to design vaccines that effectively stimulate B-cell immunity. Characterising the Fab complexed with the target antigen, commonly referred to as conformational epitope mapping investigations, is now feasible thanks to structural biology methods. The mAb-identified protective epitopes' atomic features can be obtained by three-dimensional characterisation.

The typical flow of vaccinations to antibodies can be reversed by isolating mAbs from seropositive people and using them as a guide to create new vaccines. Reverse Vaccinology 2.0 is the term used to describe this strategy (**Figure 12**) [100].

This development of reverse vaccination, known as "reverse vaccinology 2.0," uses bioinformatics to identify protective antigens, in the case where the infection is well – known, but still the main antigen responsible of the illness has not been identified yet. Furthermore, this can be especially helpful for infections where vaccine development is difficult or in case of bacterial infection, for which a vaccination is required to counteract antibiotic resistance.
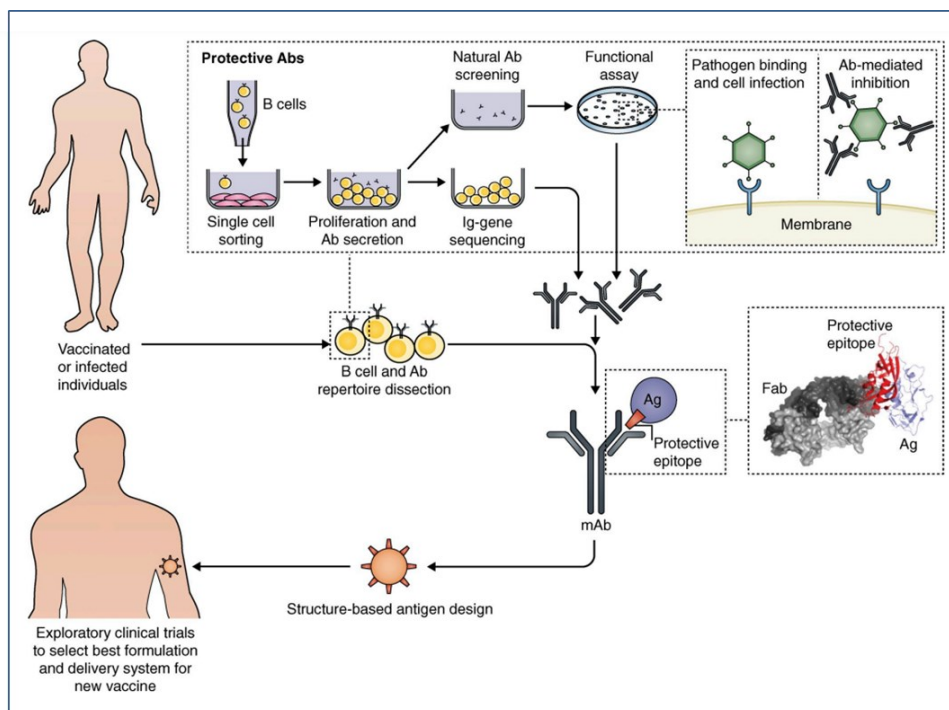
Figure 12. Reverse vaccinology 2.0. *It is possible to directly test and choose mAbs with the required functionality by single B cell sorting and culture from vaccinated or infected people. By thoroughly defining the protective epitope, which may subsequently be tailored for presentation as an optimal immunogen, the structural characterisation of the mAbs bound to their target antigen is made possible. Figure taken from Rappuoli et al. "Reverse vaccinology 2.0: Human immunology instructs vaccine antigen design", 2016* [100].

5. Pseudotype virus

The method of creating viruses or viral vectors combined with foreign viral envelope proteins is known as pseudotyping. A pseudovirus, also known as a pseudotyped virus particle, is the final product. By using this technique, host tropism or the stability of the virus particles can be changed by manipulating the foreign viral envelope proteins.

The primary goal of producing pseudotype virus in the lab is to produce viral vectors [101].

In laboratory-created viral vectors derived from infectious viruses, genes of interest are substituted for the original viral genes. As a result, the viral vectors are no longer able to replicate and spread on their own, but they can still infect and transfer their genetic material into the host cell. Retroviral vectors were utilised in the initial approach, but lentiviral vectors (LV vectors) have gradually replaced them. This is primarily because LV vectors activate a lower level of innate immune response than retroviral vectors , and it is also because of biosafety concerns [102]. Since LVs can integrate into the genome of mammalian cells regardless of their proliferative state, ensuring long-term expression of the transgene, they are currently regarded as one of the most useful gene transfer vectors for both research and gene therapy applications. LVs are derived from viruses that belong to the retrovirus family (**Figure 13**) (Retroviridae; genus lentivirus)[103].
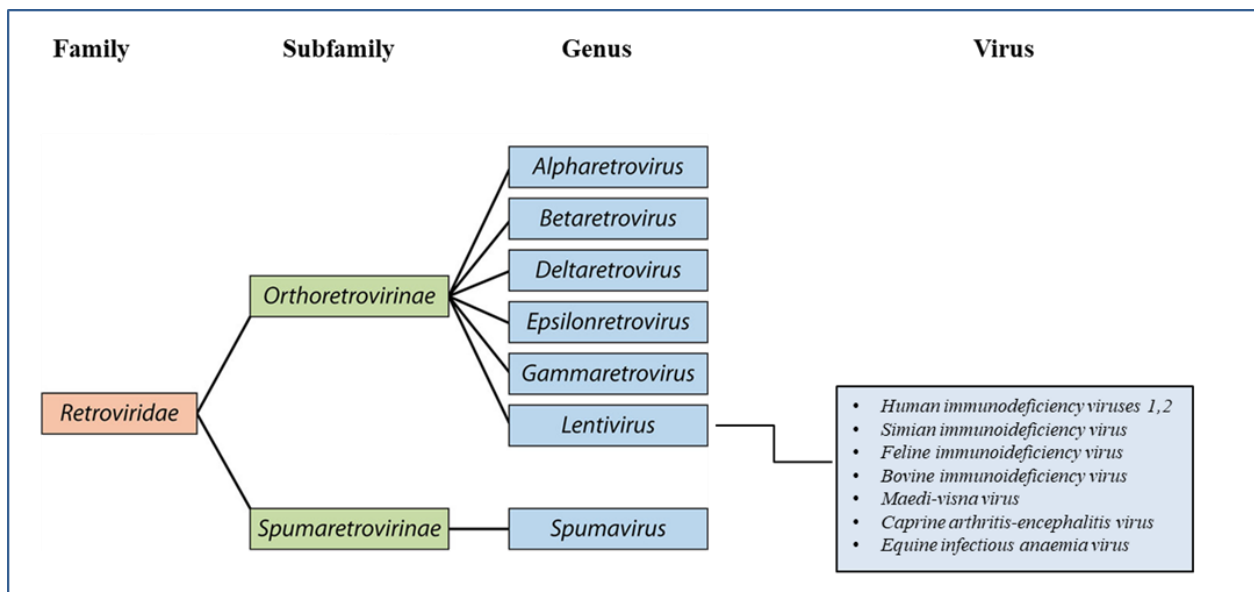
Figure 13. Classification of viruses according to the International Committee on Taxonomy of Viruses (ICTV).

LVs find application both in *vitro* for the transduction of eukaryotic cells and the production of recombinant proteins, and in *vivo*, in animal models, for the pre-clinical and clinical development of vectors used in gene therapy, but also for the development of new delivery systems for production of next-generation vaccines.

5.1 Molecular Biology of Lentivirus (HIV)

The genus of lentiviruses bears the name Lentus, which means "slow" in Latin. They are members of the retrovirus family, and they received the designation because many of them cause slow-moving degenerative diseases in their host. Lentiviruses have a diameter of 80–100 nm and they are enveloped single-stranded RNA viruses. They exhibit strong host specificity and live a lifetime in their host. For instance, the feline immunodeficiency virus (FIV) only infects domestic and large cats, whereas the bovine immunodeficiency virus (BIV) only infects cows. With its two forms, HIV-1 and HIV-2, the human immunodeficiency virus (HIV) is likely the most well-known member of the retrovirus family and is the virus known to cause AIDS in humans.

Lentiviruses possess *gag*, *pol*, and *env* genes, which code for viral proteins in the following order: 5´-gag-pol-env-3´, identical to all other retroviruses. However, lentiviruses have two regulatory genes, *tat* and *rev*, in contrast to other retroviruses. Depending on the virus, they might also have other accessory genes (for example, *vif*, *vpr*, *vpu*, and *nef* in the case of HIV-1), the products of which are involved in controlling synthesis, digesting viral RNA, and other replicative activities.[104] The *nef* gene produces an intracellular protein that can downregulate the CD4 receptor, preventing it from being visible on the cell surface [105]. This causes the host immune system to deteriorate, which promotes the spread of infection. Reduced CD4-positive cell counts suggest a far more severe immunological deficit. Finally, about 600 nt make up the long terminal repeat (LTR), of which 450 nt are in the U3 region, 100 nt are in the R sequence, and 70 nt are in the U5 region (**Figure 14**).
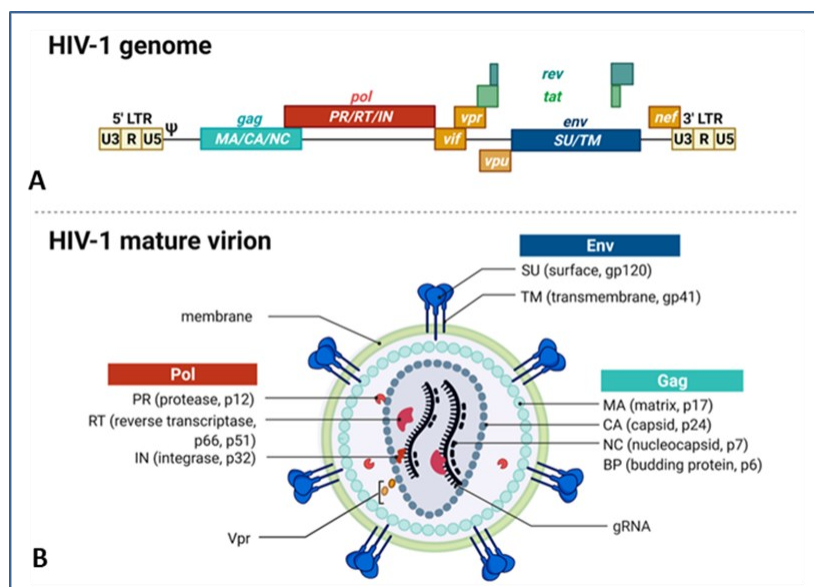
Figure 14. A. *Basic scheme of the wild-type human immunodeficiency virus type-1 (HIV-1) genome. B. Representation of HIV-virion structure. The Figure is from Heuvel et al., "Infectious RNA: Human Immunodeficiency Virus (HIV) Biology, Therapeutic Intervention, and the Quest for a Vaccine", 2022* [106].

Lentiviruses have a replication cycle comparable to other retroviruses (**Figure 15**). A virus-specific reverse transcriptase must first convert the viral RNA into DNA before the viral genome can be integrated into the genome of the host cell. Unlike other viruses, such as gamma-retroviruses, lentiviruses are able to penetrate the infected cell's nuclear membrane "on their own" and do not require the aid of the cell's division to incorporate their genetic material into the host's genome [105]. Their unique characteristic renders them highly intriguing as viral vectors for both scientific and medicinal purposes. Lentiviruses can therefore transfect cells at any stage of the cell cycle when they are employed as vectors.
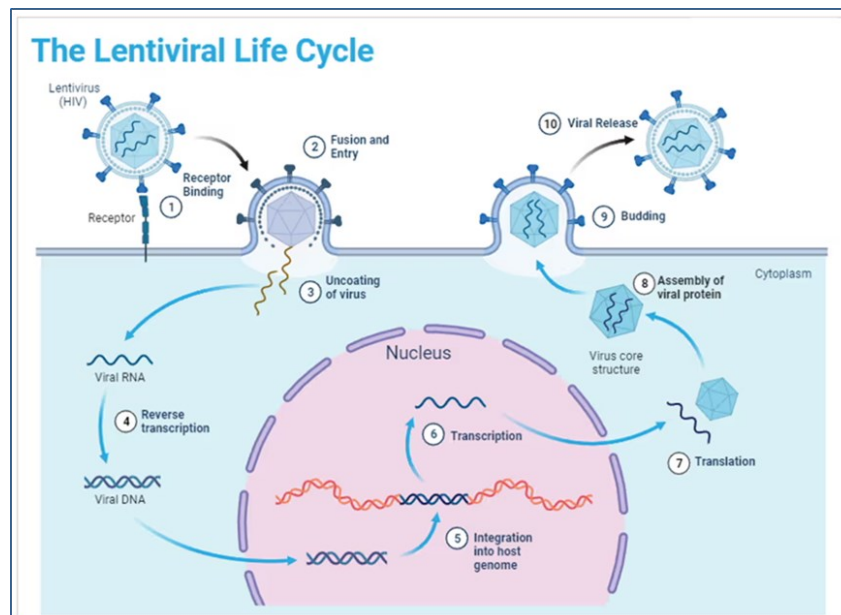
Figure 15. **The Lentiviral life cycle.** *A sequence of events in the lentiviral life cycle allows the virus to infiltrate target cells, transfer its genetic material, and multiply: 1-2. The first step provides the binding and entry through the envelope glycoprotein. 3-4**. When inside the cell, the viral core carries out reverse transcription 5-6. Transcription and Translation: Integrated proviral DNA serves as a guide for transcription promoted by the host cell's RNA polymerase II. 7-10. After translation, the virion defines its final structure through the assembly and budding process. After budding, the freshly formed virus particles go through maturation and are from the host cell so that are ready to infect other new cells (maturation and release). The Figure is from Assay Genie website* [107].

5.2 History: Lentivirus in gene therapy and vaccines

Since the beginning of their use, lentiviral vectors have been studied mainly for gene therapy. When it comes to gene therapy, the use of VLs is intended to correct the disease-causing gene mutation by means of targeted inhibition of gene expression, targeted gene insertion, or targeted removal of target cells. Treatment for X-linked Adrenoleukodystrophy (ALD), a severe brain disease brought on by demyelination of neuronal cells due to a lack of the ALD protein, which is encoded by the ABCD1 gene, is one example of this. Blockade of the demyelination process was noted in the patients 16 months following LV therapy[87]

In the field of vaccination, LVs, in particular those with deficient integration, i.e., those with a mutation in the integration gene that prevents them from integrating in the host's body, found use in the vaccination regimen for pathogen infections for which the traditional vaccination regimen (inactivated, attenuated, subunitized, recombinant) has not produced satisfactory results.[108]

5.3 When the clothes make the virus: pseudotyping

All of the *cis* elements required for encapsulation, reverse transcription, and integration of the viral genome are preserved during the construction of a lentiviral vector. The expression of the vector can be regulated by the LTR or given to an external promoter inserted into the vector; the *gag*, *pol*, and *env* genes are removed instead, and their products are supplied *in trans* through the use of multiple plasmids or by the use of engineered helper cells, or packing cells, that are able to express the viral proteins necessary for the formation of viral particles. The viral genome is split into three or four different plasmids: [109]

- a packaging plasmid, which supplies *in trans* the products of the HIV-1 *gag*, *pol* and *rev* genes necessary for particle production, but lacks all the *cis*-agent sequences necessary for encapsidation, reverse transcription and integration;
- an envelope plasmid, which provides a heterologous *env* gene not derived from HIV-1 and which serves to increase the tropism of the vector;
- a plasmid transfer, containing the genetic material to be expressed in the target cell, all the *cis*-agent sequences necessary for the reverse transcription of the viral genome, for transcription of the transgene, for integration, and the ψ packaging sequence (psi), which is required for production of lentiviral particles.

This sequence is used to encapsulate the genome in the virion and thus produce the VL, which will not have the ability to replicate in the host cell as it does not contain the genes necessary for replication. In the latest generation of vectors, the *rev* gene is produced from a fourth plasmid.

This type of strategy, involving the use of several plasmids, is necessary to increase the safety of the vector as it decreases the risk of recombination that could reconstitute a replication-competent genome [110]. It is also possible to modify the host spectrum of the virus by providing a heterologous envelope protein in the viral particle, as the G protein of vesicular stomatitis virus (VSV-G) or the spike protein of the SARS-CoV-2 virus.
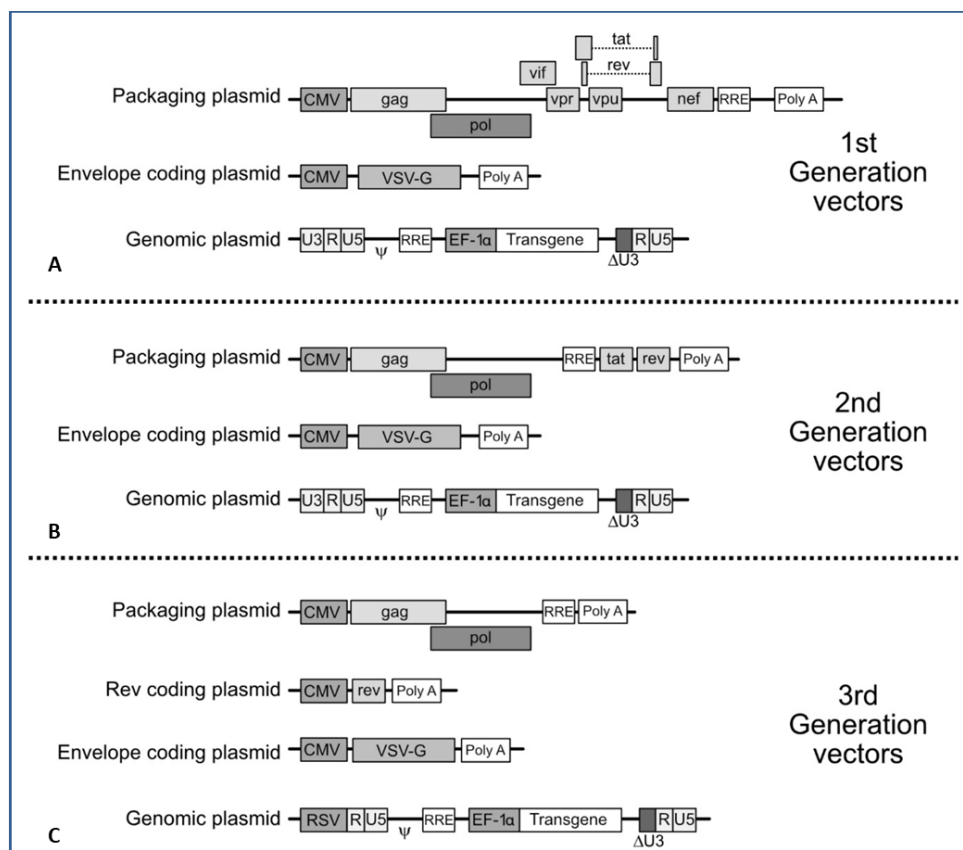
A number of generations of lentiviral vectors have been produced in an effort to reduce the likelihood of generating replication competent particles (RCLs, or replication competent viruses)[101]. The lentiviral vectors that split the system into three distinct plasmids are known as first-generation vectors (**Figure 15A**):

1. a packaging construct (packaging plasmid) expressing all HIV-1 *gag/pol* genes, *tat*, *rev*, *nef*, *vif*, *vpr* and v*pu*. The LTR sequences and the packaging sequence ψ are deleted and the ORF of *env* is blocked. Expression of the plasmid is driven by the CMV cytomegalovirus promoter, which replaces the LTR at the 5' end. The LTR sequence at the 3' end has also been replaced. This plasmid is therefore devoid of the *cis*-acting sequences required for packaging (ψ), for reverse transcription (PBS) and for integration (LTR).

2. an envelope construct (envelope plasmid) expressing a heterologous viral glycoprotein, such as VSV-G or spike protein, in such a way as to obtain viral particles that have a ubiquitous membrane receptor.

3. a transfer construct (transfer plasmid) containing the transgene and the elements in *cis* necessary for particle formation (packaging sequence ψ), reverse transcription of the viral genome and its

integration (LTRs, ψ, RRE), but not expressing any of the HIV-1 viral proteins. The transgene of interest is placed under the control of a specific internal promoter.

Otherwise, a single packaging plasmid encoding the *gag*, *pol*, *rev*, and *tat* genes is present in the second generation lentiviral vector system. The auxiliary genes *vif*, *nef* and *vpr* are absent. The viral LTRs and the ψ packaging signal are located on the transfer plasmid. The 5'LTR, a weak promoter that needs *Tat* to activate expression, drives gene expression in the absence of an internal promoter. A third, distinct envelope plasmid encodes the envelope protein Env, which is typically VSV-G because of its broad infectivity. In the case of this Thesis, spike protein from SARS-CoV-2 and other HCoV has been used to pseudotyping the envelope of the pseudotype viruses. (**Figure 15B**). In the case of the second generation of pseudotype virus the transgene expression from the LTR is *tat*-dependent.

In several important aspects, the third generation system outperforms the second generation in terms of safety. The packaging system is first divided into two plasmids, one of which encodes *rev* and the other *gag* and *pol*. Secondly, by introducing a chimeric 5' LTR linked to a heterologous promoter on the transfer plasmid, *tat* is removed from the third generation system. Expression of the transgene from this promoter is no longer dependent on *tat* transactivation (**Figure 15C**).

Figure 15. *The several generations of lentiviral vectors. In the first generation all the HIV genes are maintained in the packaging plasmid. Starting from the second generation, several HIV genes that are not necessary for the formation of virion are removed, and the LTR sequences are altered to provide additional biosafety.* The Figure is from Duverge et al. "*Pseudotyping Lentiviral Vectors: When the Clothes Make the Virus*", 2020 [101].

Background and aim of the project

My PhD project was part of a research effort that began in the Monoclonal Antibody Discovery Laboratory at Fondazione Toscana Life Sciences in April 2020, at the height of the COVID-19 emergency. The purpose of the COVID-19 research project consisted in the identification of mAbs directed against SARS-CoV-2 that could be developed as prophylactic and/or therapeutic tools.

As mentioned in the Introduction, the COVID-19 pandemic has had a dramatic impact on the global public health and economic systems [4]. In addition, the ability of SARS-CoV-2 to mutate and the emergence of new variants has hampered the development of new therapeutics. Human mAbs have shown great potential in the field of infectious diseases, and their use in the initial phase of the COVID-19 pandemic is a focal example. However, despite numerous mAbs received emergency use authorization for the treatment of COVID-19, they all fell short with the emergence of the SARS-CoV-2 Omicron variants and its sublineages thus highlighting the need for new therapeutics. To address this challenge, in our laboratory we isolated hundreds of neutralizing human monoclonal antibodies (nAbs) from single cell sorting of memory B cells collected from different cohorts of COVID-19 convalescent and vaccinated donors.

This thesis describes three distinct projects that I carried out in cooperation with my research group. These projects involved isolation and screening of mAbs from various donor cohorts by means of experimental tools that I developed during my PhD studies.

In 2020 we sorted over 1,100 S-protein specific memory B cells from fourteen COVID-19 convalescent donors to find effective mAbs against SARS-CoV-2. We screened mAbs against the S1/S2 subunits and the S-protein trimer stabilized in its prefusion conformation. We found mAbs that targeted both the S trimer and S-protein linear epitopes [111].

In 2021, we examined the memory B cells of five convalescent people vaccinated with the BNT162b2 mRNA vaccine (classified as "seropositive") and other five people who had not experienced the infection but just the vaccination with the same vaccine (classified as "seronegative"). Over 3,000 cells developed mAbs against the spike protein, over 400 cells neutralized the original SARS-CoV-2 virus that was first discovered in Wuhan, China [111,112].

In 2023 we isolated hundreds of nAbs from single cell sorting of memory B cells collected from COVID-19 convalescent and vaccinated donors. Class-switched memory B cells were isolated, single-cell sorted using the prefusion S protein trimer-specific (S protein+), and then incubated to allow the mAbs to be naturally produced and released into the supernatant.

Anti-Spike-specific mAbs were selected by Enzyme-Linked Immunosorbent Assays (ELISA) using the spike recombinant protein in its trimeric form. The selected candidates were cloned and expressed on the high-throughput format in 96-well plates and then a cytopathic effect-based microneutralization test (CPE-MN) was conducted to assess the neutralization activity of discovered nAbs against SARS-CoV-2 wild type virus.

Furthermore, since it is reported that antibodies produced against the common cold-causing human seasonal coronaviruses (sCoVs) cross-react with SARS-CoV-2 antigens[113], we explored the cross-neutralizing properties of the antibodies against well-known HCoVs. Indeed, from a scientific and therapeutic perspective, understanding the rationale behind mAb broad neutralizing activity would

yield a wealth of information regarding SARS-CoV-2 infection and other viruses belonging to the Coronaviridae family.

To rapidly evaluate mAb binding and neutralization activity I implemented two platforms based on recombinant S protein and lentiviral vectors that rely on the generation of a panel of SARS-CoV-2 spike (S) proteins from existing variants and from other Coronaviridae members. A spike protein library was constructed and included the S recombinant proteins of the various COVID-19 variants as well as those of other coronaviruses belonging to the α-coronaviridae family and β-coronaviridae family. Additionally, the pseudo-typing platform allowed evaluation of the SARS-CoV-2 neutralizing mAbs on viruses not available in the live-wild type form such as SARS-CoV-1 and additional Alpha and Beta coronaviruses. The same pseudotyped viruses were exploited to optimize a synergy neutralization assay that evaluates the potency of mAb combinations.

In details, in Chapter 1 of the Results section I describe the generation of a spike protein library which includes h-CoV and SARS-CoV proteins. In Chapter 2 I describe the pseudotyping process and the neutralization assay using pseudotyped viruses. In Chapter 3 I report an approach I have explored to assess the synergy of antibodies using the pseudotype virus neutralization assay. An overview of the screenings done in BSL3 on each cohort is provided in Chapter 4.

Chapters

## 1. Constructing a spike protein library: h-CoV and SARS-CoV S proteins

1.1 Introduction

The S (Spike) protein on the viral surface is crucial for successful cell infection. It is a trimeric class I transmembrane (TM) glycoprotein involved in viral entry and is found in all HCoVs as well as other viruses including HIV (HIV glycoprotein 160, Env), influenza virus (influenza hemagglutinin, HA), paramyxovirus (paramyxovirus F), and Ebola (Ebola virus glycoprotein)[114].

The S protein of SARS-CoV-2, like most other coronaviruses, binds to the ACE2 receptor thus mediating viral attachment and host cell entry. Because of its critical functions, it has been (and still is) one of the most essential targets for the development of COVID-19 vaccines and therapies. [66]

The quaternary structure of the S protein that interacts with the receptor is a trimer located on the surface of the viral envelope [115].Each monomer includes the Receptor Binding Domain (RBD), which is part of the S1 domain and is primarily important for viral binding to the ACE2 receptor, and the HR domain, including HR1 and HR2, in the S2 domain and strongly associated to fusion of the viral membrane with the host cell membrane [116].

Similar spike proteins are expressed by the other previously listed HCoVs: E229, NL63, HKU-1, and OC43 [117]
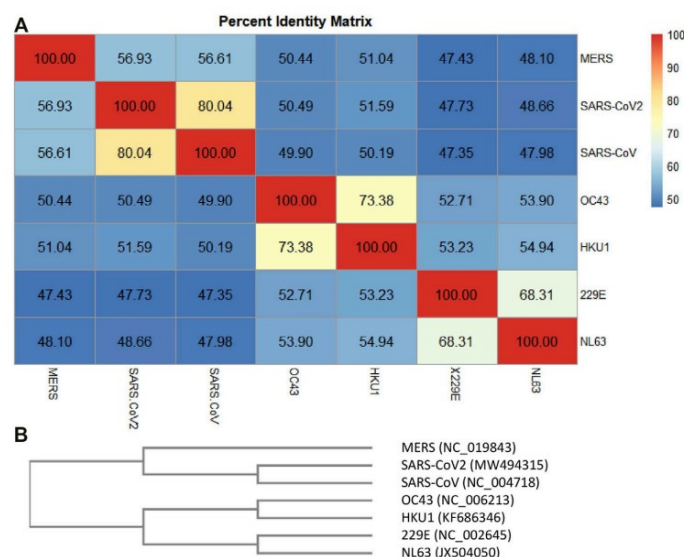
Figure 16. **Percent identity matrix.** *(A). The table shows the percent identity matrix, which indicates the % of identities among the HCoVs. In (**B**), the similarity phylogram tree is reported. The number of nucleotide substitutions, or the number of evolutionary events that occurred after the branching*

point, is directly correlated with the branch length. (Image taken from the paper of Cicaloni et al.,2022)[117]

Given the key role played by the S proteins in viral pathogenesis and in eliciting immune responses upon infection, I focused the first part of my work on the generation of an S protein library which included recombinantly expressed S proteins of NL-63, OC-43, HKU-1, 229E, SARS-CoV-1, and MERS viruses. In addition, I developed a mutagenesis platform to create an accurate and complete library of recombinant spike proteins that reflected all of the SARS-CoV-2 Variants Of Concern (VOCs) appeared from 2020 to the present. These recombinant proteins were mostly employed in ELISA experiments for assessing the presence and the affinity of monoclonal antibodies (mAbs) capable of binding the various S proteins. Specifically, the S proteins used in the assay differed according to the patient cohorts analyzed (**Figure 17**): for the *Covid -19 convalescent donors cohort*, the wild-type (WT) spike protein was primarily used for ELISA; for the *Hybrid cohort* (i.e. people who were infected once and vaccinated twice), we studied binding not only to the WT spike protein but also to the S proteins of other HCoVs (SARS, MERS, 229E, OC43, NL63 and HKU-1). The same approach was followed for the *Super Hybrid cohort* subjects who had received 3 vaccine doses. Furthermore, with the advent of the various Omicron sublineage, in 2023 we decided to investigate the possible binding of antibodies derived from the Hybrid Cohort and the Super Hybrid Cohort also versus the spike XBB 1.5 and the spike 2.86.
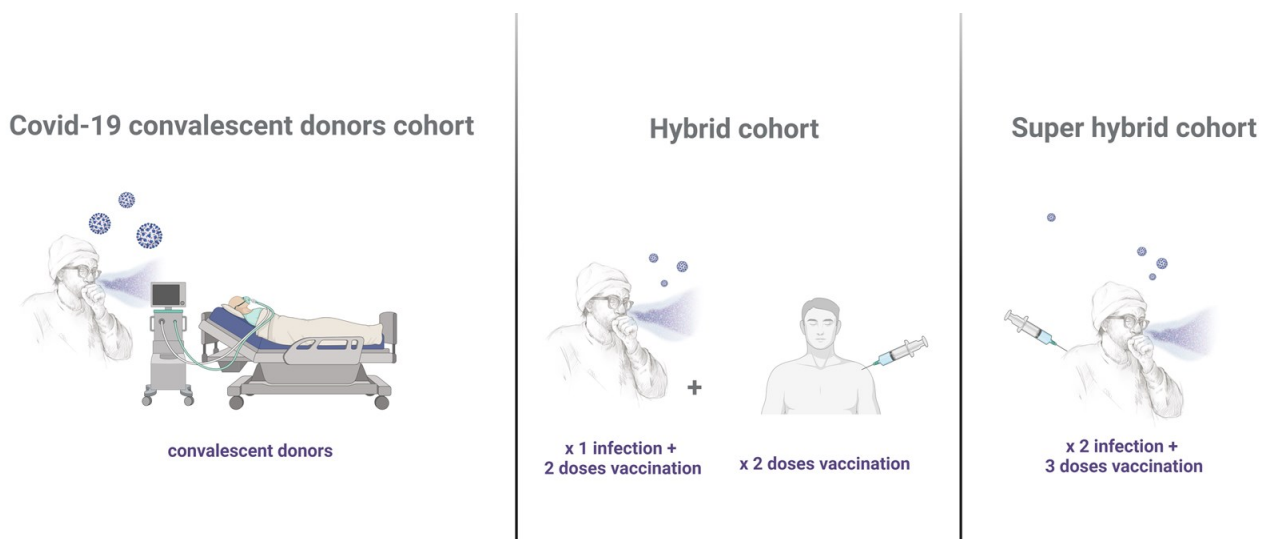
Figure 2. Three different donor cohorts were included in this study.

- *Covid -19 convalescent donors cohort: a cohort of 14 convalescents patients recovered from Covid-19 infection.*

- *Hybrid cohort: five convalescent patients vaccinated with the BNT162b2 mRNA vaccine (classified as "seropositive") and five people who had not experienced infection but were vaccinated twice with the same vaccine (classified as "seronegative").*

- *Super Hybrid cohort: six COVID-19 convalescent donors who had had the COVID-19 infection twice and were vaccinated with 3 doses of the BNT162b2 mRNA vaccine.*

This first chapter explains how plasma from donors who have either been vaccinated against COVID-19 or been infected by SARS-CoV-2, or both, can be analysed using recombinant proteins to identify antibodies endowed with cross-binding properties to the various Spikes of SARS-CoV-2 variants and of distinct HCoV. The final goal here was the identification of pan cross-neutralizing antibodies.

1.1.2 Optimization of expression and purification of recombinant S protein of SARS-CoV-2

In early 2020, the DNA plasmid encoding the 2P stabilized S protein of SARS-CoV-2 was kindly provided to our laboratory by Prof. Jason McLellan. Using a previous stabilization strategy that proved efficient for other beta-coronavirus S proteins [118] [119], the McLellan's laboratory expressed ectodomain residues 1 to 1208 of SARS-CoV-2 S, adding two stabilizing proline residues in positions 986 and 987 of the C-terminal S2 fusion domain. Wrapp and colleagues described the recombinant construct expressing S and the methodology used for purification. [60]

Figure 18A displays the map of the expression construct while **Figure 18B** shows the plasmid where the sequence of the spike protein is inserted and **Figure 18C** illustrates the purification process optimized by the McLellan group. The reported yield was ~0.5 mg/L of recombinant prefusion-stabilized S ectodomain from FreeStyle 293 cells purified by affinity chromatography followed by size-exclusion chromatography. [60]
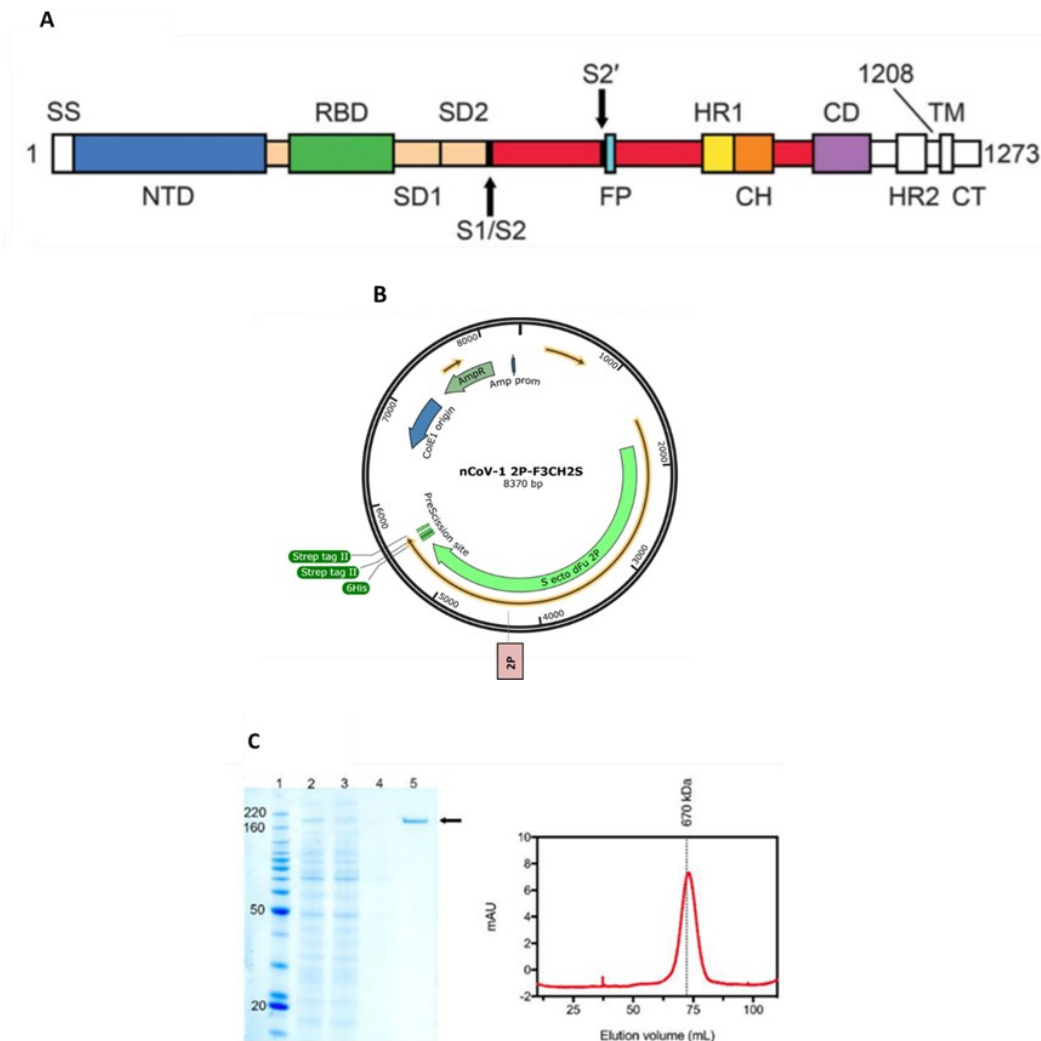
Figure 18. S protein expression construct and purification procedure. *A*. *Representation of SARS-CoV-2 S primary structure coloured by domain. Domains that were excluded from the ectodomain expression vector or could not be present in the final map are colored white. SS, signal sequence; S2', S2' protease cleavage site; FP, fusion peptide; HR1, heptad repeat 1; CH, central helix; CD, connector domain; HR2, heptad repeat 2; TM, transmembrane domain; CT, cytoplasmic tail. The black-arrows denote protease cleavage sites [120]. **B**. Construct of spike 2P recombinant protein. The sequence of the spike protein from residue 1- 1208 is indicated by the green arrow and is expressed under control of a CMV promoter. Residues 986 and 987 have been replaced by prolines to confer improved stability to the protein. A TwinStrepTag and an 6XHisTag have been added to simplify the purification process by using appropriate affinity columns. Plasmid map was obtained with SnapGene. **C**. SARS-CoV-2 S expression and purification. SDS-PAGE analysis is shown on the left. Lane 1: Ladder with molecular weights, relevant bands are indicated in kilodaltons; lane 2: filtered supernatant from transfected cells; lane 3: supernatant after passing through StrepTactin resin; lane 4: wash of StrepTactin resin; lane 5: elution from StrepTactin resin. The band corresponding to SARS-CoV-2 S is denoted by a black arrow. The panel on the right reports the result of a size-exclusion chromatography of the affinity-purified S protein. The column used is a Superose 6 10/300. The elution volume of a 670 kilodalton molecular weight standard is shown as a black dotted line. Images were taken from Cryo-EM structure of the 2019-nCoV spike in the prefusion conformation, Wrapp et al., Science 2020 [60].*

To express the S protein in our laboratory, the plasmid encoding SARS-CoV-2 S-2P was transiently transfected into Expi293F™ cells (Thermo Fisher) using ExpiFectamine™ 293 Reagent.

Initially, 50 mM NaH_2PO_4, 300 mM NaCl, 10 mM Imidazole pH 7.4 was used as Equilibration buffer and 50 mM NaH_2PO_4, 300 mM NaCl, 500 mM Imidazole pH 7.4 was employed as Elution buffer, used in a gradient elution. In this first attempt a 80 mL supernatant volume was purified (**Figure 19A).**

The eluted material was collected in fractions of 1 mL each which were then analyzed by SDS-PAGE (**Figure 19B).**
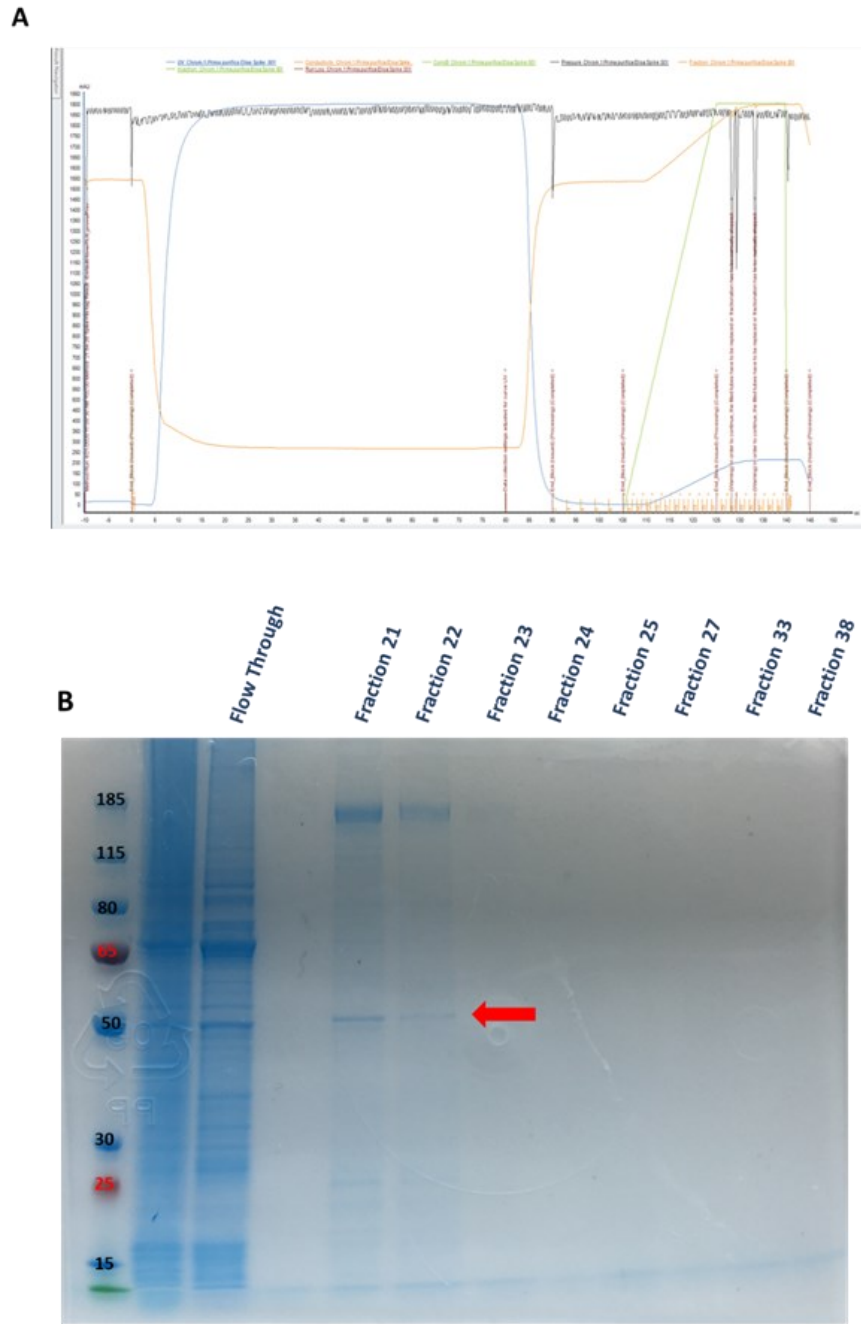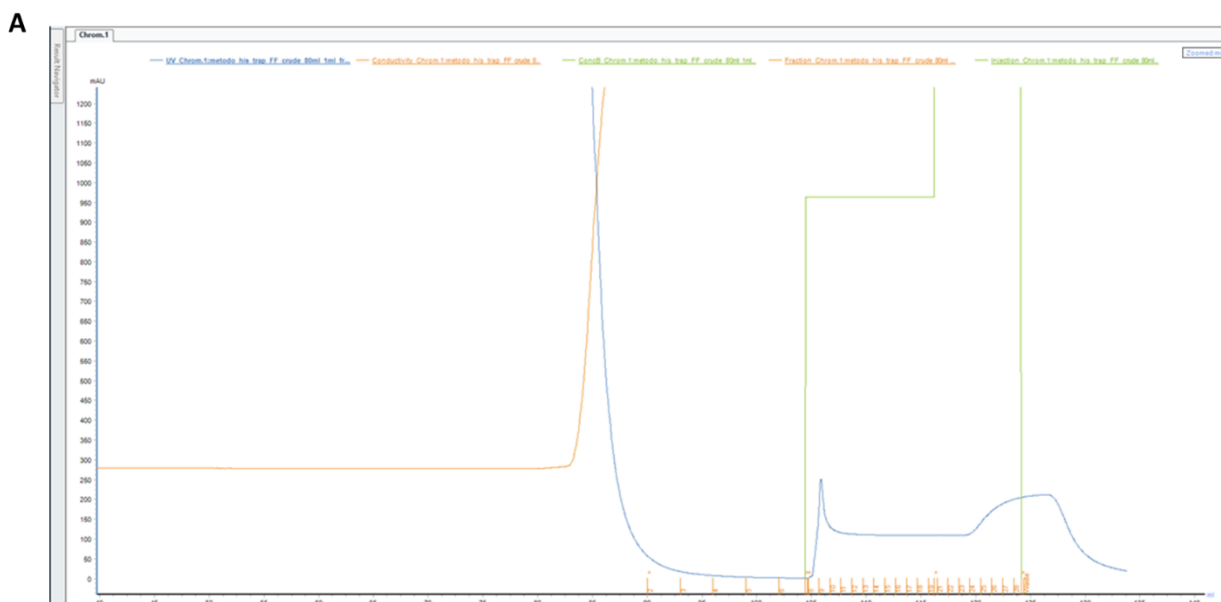
Figure 19. First purification of the SARS-CoV-2 S protein. *A*. *Affinity chromatogram of the first attempt of purification of the Spike-2P recombinant protein. The blue line corresponds to the mAU absorption of the sample loaded and eluted; the orange line represents the conductivity of the buffer used in the procedure; the black line denotes the pressure of the column used during the purification; the green line characterises the percentage of buffer elution used for each collected fraction. Elution followed a gradient from 0% concentration to 100% concentration in 33 fractions (from fraction 9 to fraction 41). **B**. SDS PAGE of the eluted fractions of spike 2P recombinant protein. Since at its lowest concentration Imidazole absorbs around 100 mAu, I decided to run the elution fractions that in the chromatogram had an absorbance equal to or greater than this. In this denaturing but not reducing SDS PAGE, elution fractions ranging from number 20 to 27 were run, and to assess further presence of the protein I randomly ran some elution fractions between number 30 and 38. As observed from*

the SDS PAGE, the only elution fractions where the protein was present corresponded to fractions number 21 and 22, that is, where the imidazole gradient used corresponded to 250 mM. In addition, the highlighted fractions appeared to still have, despite elution in imidazole, a background residue perhaps corresponding to proteins naturally present in the cell supernatant, probably containing histidines (red arrow).

Based on these findings, I decided to modify the expression and collection protocols, as well as the purification technique.

First, transfected cells were collected at a different timepoint: 5 days instead of 6. Second, I increased the initial transfection volume to 150 mL, which was purified upon single collection and centrifugation. Moreover, I changed the equilibration buffer by increasing the molarity of the imidazole from 10 mM to 30 mM to eliminate as many contaminants as possible during sample loading on column. Finally, I decided to employ a single elution step with 250 mM imidazole since fractions with the spike protein in the SDS PAGE in **Figure 3B** contained imidazole at that molarity.

The outcomes of these modifications to the protocol are showed in **Figure 20**. The protein elution peak is now clearly visible in the chromatogram (**Figure 20A**), and several elution fractions, devoid of impurities, can be observed in the SDS PAGE. The bands stained by Coomassie Blue matched the spike 2P molecular weight (**Figure 20B**).
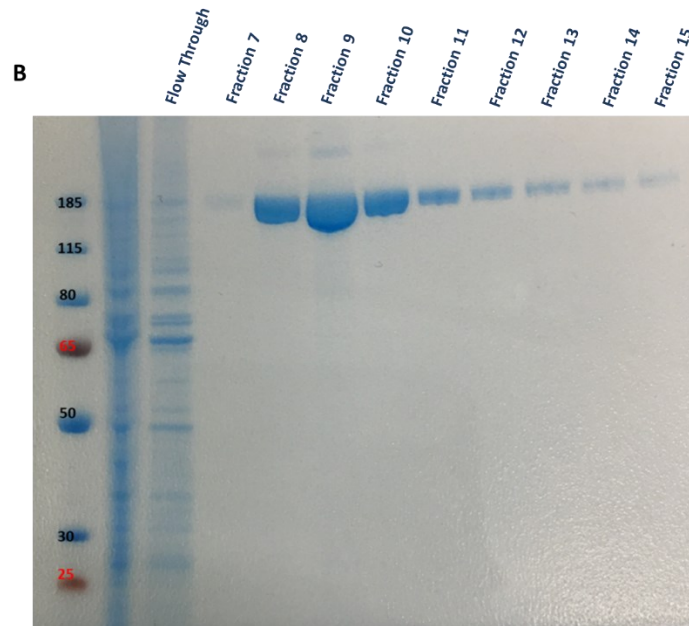
Figure 20. Second purification of the SARS-CoV-2 S protein with protocol optimization. *A*. *Chromatogram showing the elution peak of the spike 2P recombinant protein. The blue line represents the peak height corresponding to the elution fractions containing the protein; the spike protein absorbs at around 250 mAu, as shown in the graph. **B**. SDS PAGE of the eluted fractions of spike 2P recombinant protein. The spike protein is present in fractions from number 8 to number 15, in a decreasing amount. No background is observed in this gel: the equilibration buffer with 30 mM Imidazole allowed for upstream cleaning of the sample before the protein of interest was eluted from the column.*

Since the SARS-CoV-2 S protein purification process was successful, I applied the procedure to the spike proteins of the other HCoVs: NL63, E229E, OC43, HKU-1, SARS-CoV-1 and MERS. In these cases too, the proteins were stabilized by addition of two prolines and the constructs were kindly gifted by Prof. Jason McLellan (**Figure 21**).
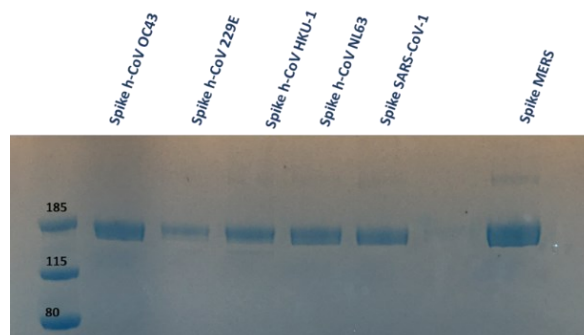
Figure 21. *SDS PAGE of the spike 2P recombinant protein of the several h-CoV and of the spike of SARS-CoV-1 and MERS coronaviruses*. *Each spike protein revealed high purity after purification. The SDS-PAGE reported is normalized to 1 mg/ml for each protein.*

Table 2. List of purified spike proteins 2P with their respective yields.

Spike protein expressed and purified	Final yield mg/l
H-CoV OC43	1 mg/l
H-CoV 229E	0.6 mg/l
H-CoV HKU-1	0.8 mg/l
H-CoV NL63	0.8 mg/l
SARS-CoV-1	2 mg/l
MERS	3.2 mg/l

1.1.3 Moving from a 2P construct to a 6P construct for the SARS-CoV-2 WT S protein

In September 2020, Hsieh and co-workers [120] reported the identification of 26 aminoacidic substitutions that improved S protein yields and stability upon recombinant expression. The so-called spike HexaPro, i.e. a spike version with six proline substitutions, was characterized by higher expression levels than the parental construct and by the ability to withstand heat stress, room temperature storage, and three freezing-thawing cycles [120]. **Figure 22** illustrates the map of the vector encoding spike HexaPro (6P).
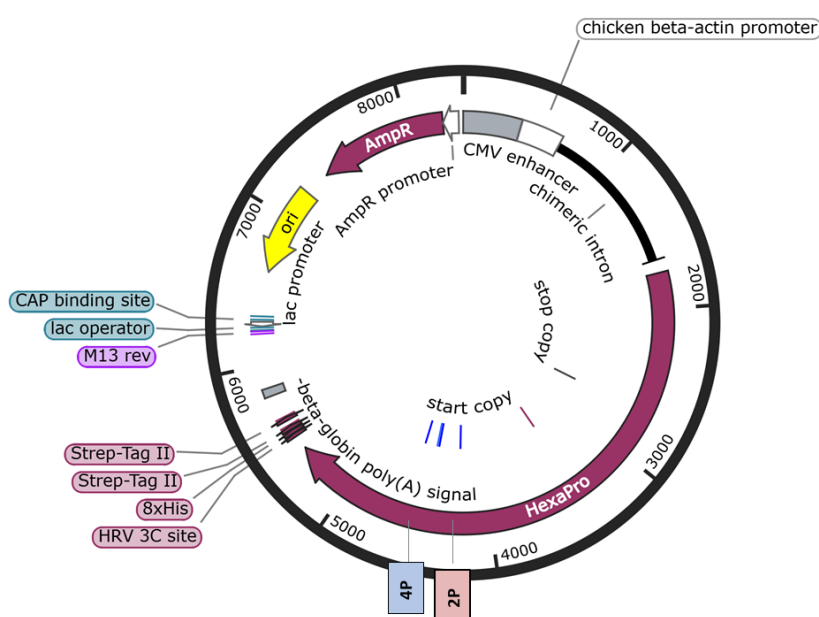
Figure 22. Map of the plasmid encoding spike 6P. *DNA corresponding to aminoacid sequence 1-1208 of SARS-CoV-2 S (GenBank: MN908947) with 2 Proline residues in positions 986 and 987 and 4 additional Proline residues in positions 817, 892, 899, 942 was cloned into the expression vector (purple arrow). A TwinStrepTag and an 8XHisTag have been added. The map was obtained with SnapGene.*

The same article reported the use of a different cell line, CHO cells, a suspension cell line optimized for the production of complex recombinant proteins, due to their ability to generate appropriate protein N-glycans, even with the most difficult templates such as the trimeric spike protein.

We therefore decided to try the expression of spike 6P using the new plasmid and cell line expression system. The protein purification procedure relied on the use of the His tag and was not changed compared to that described in the previous section.

The new construct in CHO cells resulted in significantly better spike protein expression, probably thanks to the stabilization by the additional 4 prolines (**Figure 23**). Overall, the yield was about 30 mg/l.
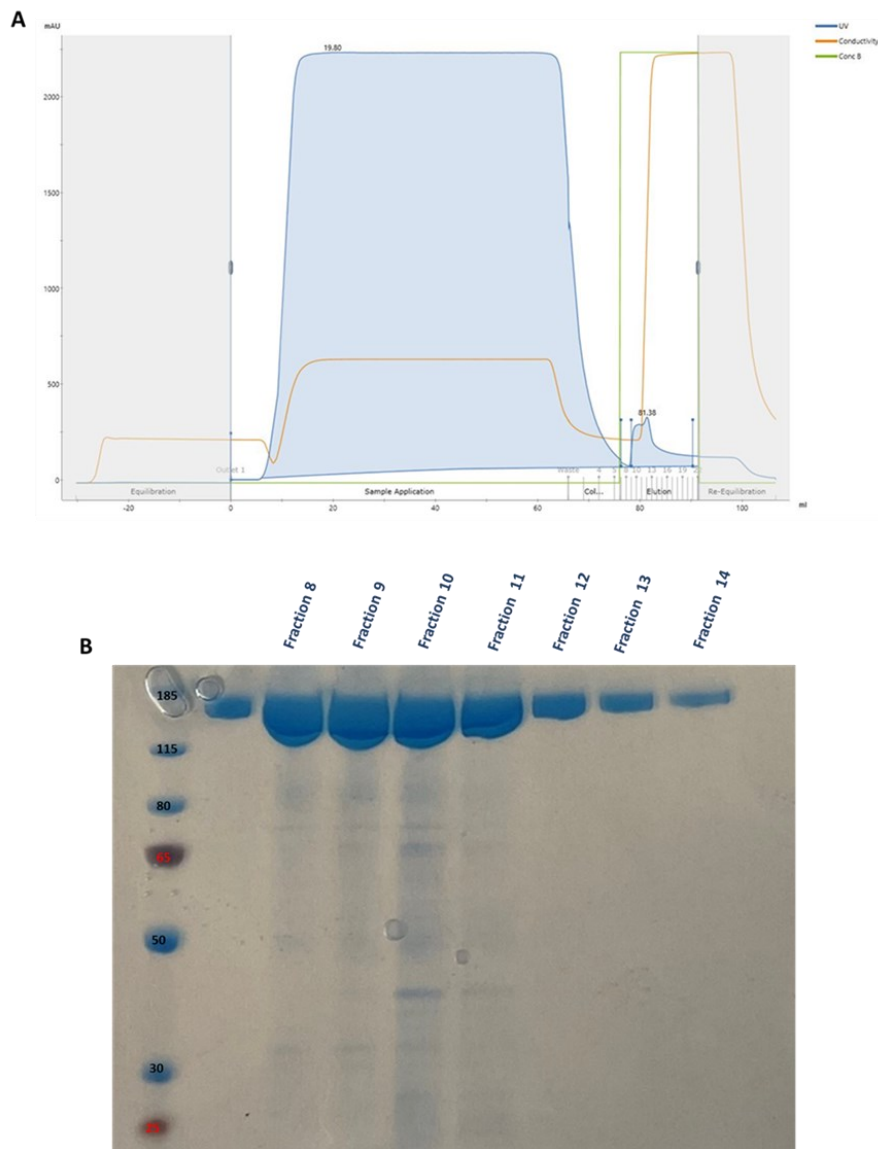
Figure 23. Purification of the SARS-CoV-2 S 6P protein. *A. Chromatogram showing the elution peak of the Spike 6P recombinant protein. The blue line represents the peak height corresponding to the elution fractions containing the protein; in this chromatogram, it is evident that the absorbance is slightly higher and that the peak is more extended than the peak presented in Figure 4A. This correlates with higher expression and yield of the Spike 6P protein. B. SDS PAGE of the eluted fractions of Spike 6P recombinant protein. Spike 6P is present in significant amounts in all of them.*

1.1.4 Developing a SARS-CoV-2 S protein modular mutagenesis platform to construct a library of SARS-CoV-2 VOCs

Like the majority of viruses, SARS-CoV-2 has acquired various mutations during its evolution which provided selective advantage and possibly improved fitness and/or adaptation to the human host [116]. Specifically, amino acid substitutions, insertions, and deletions conferred benefits to SARS-CoV-2 and resulted in the selection of different dominant strains.

SARS-CoV-2 variants have been categorized by the World Health Organization (WHO) as Variants Of Concern (VOC), Variants Of Interest (VOI) or variants under monitoring based on their transmissibility, immunity and infectivity. Starting from December 2019 the rate of evolution paralleled the acquisition of approximately two mutations per month in the world population [121] [122]. The first mutation observed was the D614G in the RBD domain of the spike protein. This first mutation was responsible for the increased fitness of the virus which could bind the ACE2 human receptor thanks to an open conformational state of the spike protein [122]. Indeed, this mutation is still conserved in all of the emerging variants of the SARS-CoV-2 virus. D614G may also be responsible for an increase in the number of spike proteins per virion [123] and for the higher frequency of S1/S2 cleavage [122].

The D614G mutation was the first of thousands of mutations that appeared in the spike protein sequence over the years: in fact, at the beginning in 2020, the WHO decided to introduce a systematic classification and ranking of the new variants according to their transmission rate and associated risk of mortality.

Given the acceleration in variant detection, we decided to update our library of S protein expression constructs by designing and then producing the spike variants corresponding to the VOCs reported by SARS-CoV-2 epidemiologists.

The plasmid encoding the WT S 6P protein served as the backbone where the different mutations were introduced by exploiting the following modular strategy. The gene encoding the WT spike 6P can be divided into five restriction fragments, indicated in **Figure 24** and identified by the enzymes KpnI, EcoRI, AgeI, NheI, XbaI, BamHI. Variant-specific mutations, extracted from the website https://outbreak.info/situation-reports (**Figure 25**), were mapped to these fragments which were then synthesized in their mutated version by an external company and used to replace the corresponding wild type portion. Plasmids encoding mutated S proteins were thus obtained.
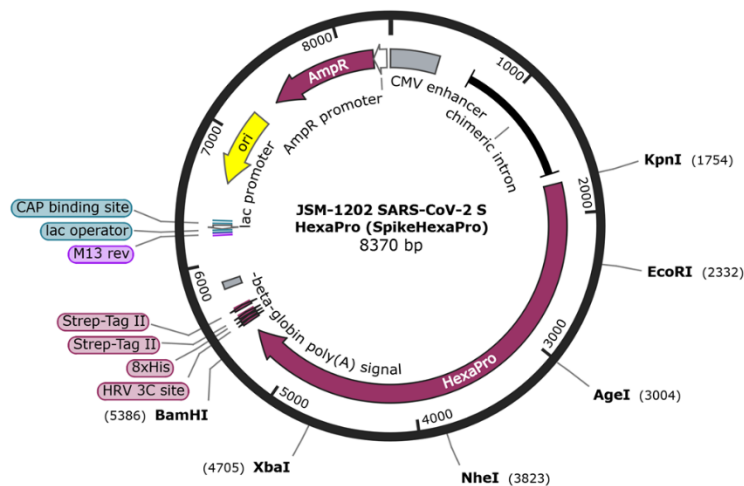
Figure 24. Plasmid encoding spike 6P wild type with the restriction sites that define 5 restriction fragments. *Five restriction sites, generated by enzymes KpnI, EcoRI, AgeI, NheI, XbaI and BamHI, were identified in the S encoding gene. The restriction sites are 800-1000 bp spaced. The map was obtained with SnapGene.*
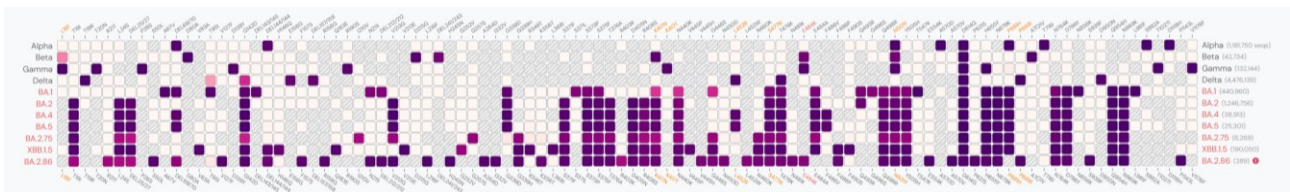
Figure 25. Single point mutations in the spike gene of the SARS-CoV-2 Variants of Concern. *In the Figure the VOC which we chose to reproduce in our laboratory are shown. Starting from the **B.1.1.7** variant (Alpha) until the latest BA.2.86, we identified the more representative single point mutations (coloured in dark-purple) for each lineage. We decided to include in the final construct the mutations which had 75% prevalence in at least the 80% of the lineage.*

Each spike variant was then expressed using CHO cells using the same expression protocol that was developed for the spike WT HexaPro.

As a result of this effort, our laboratory now possesses a library of recombinant spike proteins that correspond to the various VOCs. These proteins have been employed during my PhD studies to describe and categorize the most potent mAbs discovered in our laboratory, allowing for a comprehensive and in-depth analysis.

Table 3. List of spike recombinant proteins VOC 6P available in our lab with their respective yields

Spike VOCs protein expressed and purified	Final yield mg/l
B.1.1.7	7 mg/l
B.1.351	8.5 mg/l
P1	6.3 mg/l
B 1.617.1	5.4 mg/l
B 1.617.1	6.2 mg/l
BA.1	6.8 mg/l
BA.2	5.9 mg/l
BA 4/5	7 mg/l
XBB 1.5	12 mg/l
BA 2.86	13 mg/l

1.2 Results

SARS-CoV-2 convalescent and vaccinated donors' S-protein specific antibodies were isolated and characterized using spike recombinant proteins

The recombinant spike proteins previously described were employed in the early stages of research on mAbs isolated from peripheral blood of convalescent or vaccinated patients in our laboratory.

As previously explained in the Background section, this thesis reports results from three studies conducted on three different donor cohorts:

- *COVID-19 convalescent donors cohort*: a cohort of convalescent patients recovered from COVID-19 infection.

- *Hybrid cohort*: convalescent patients vaccinated with the BNT162b2 mRNA vaccine (classified as "seropositive") and five people who had not experienced infection but were vaccinated with the same vaccine (classified as "seronegative").

- *Super Hybrid cohort:* COVID-19 convalescent donors who had COVID-19 infection twice and were vaccinated with 3 doses of BNT162b2 mRNA vaccine.

Although the cohorts included patients with various infection-vaccination history, the experimental workflow was the same for all of them: **Figure 26** describes Phase 1 of the research pipeline, where recombinant spike proteins were used.

To recover mAbs specific for SARS-CoV-2 S-protein, peripheral blood mononuclear cells (PBMCs) were collected and stained with fluorescently labeled S-protein trimer to identify antigen specific memory B cells (MBCs) from recovered and/or vaccinated patients.
The sorting strategy was designed to identify class-switched MBCs (CD19$^+$CD27$^+$IgD$^-$IgM$^-$) and to detect only memory B lymphocytes that had undergone the maturation process[111].
Following the sorting process, S-protein+ MBCs were cultured for two weeks over a layer of 3T3-CD40L feeder cells in the presence of IL-2 and IL-21 stimuli to facilitate natural immunoglobulin production [124] (**Figure 26B**).
Next, MBC supernatants containing IgG or IgA were evaluated by enzyme linked immunosorbent assay (ELISA) for their ability to bind either the SARS-CoV-2 S-protein trimer in its prefusion conformation or, specifically for the *Hybrid cohort* and *Super Hybrid cohort,* the ability to bind spike recombinant proteins from other HCoV (SARS-1, MERS, NL63, 229E, OC43, HKU-1) (**Figure 26C**).
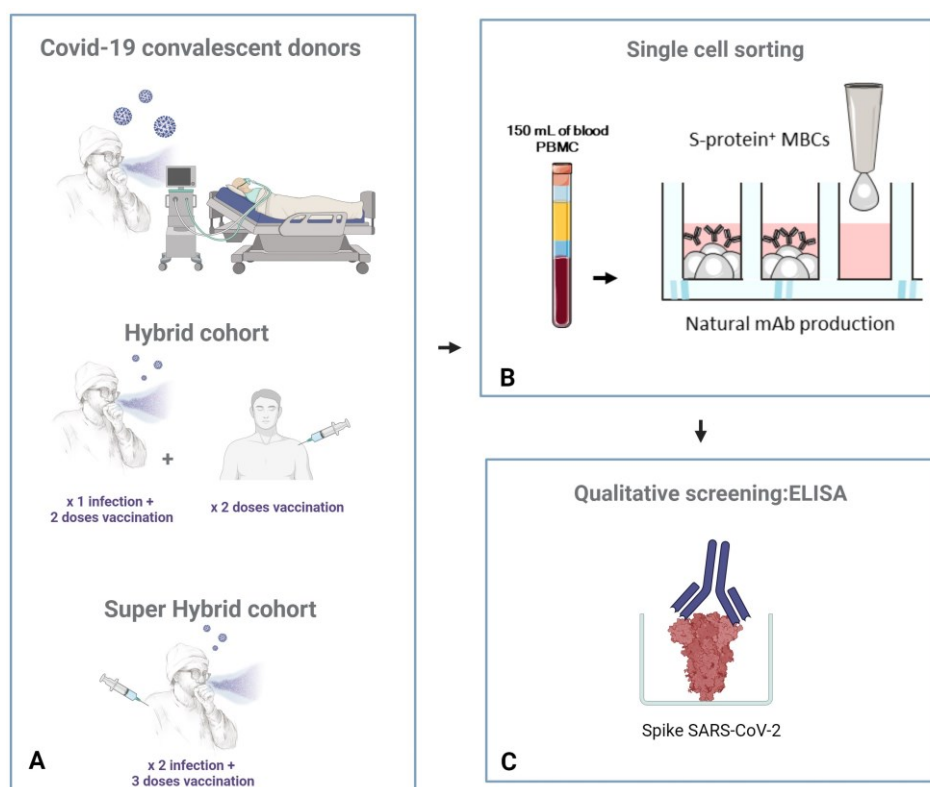
Figure 26. Phase 1 workflow for the identification of SARS-CoV-2 neutralizing antibodies. *The scheme depicts the first part of the process that resulted in the identification of neutralizing antibodies (nAbs). The first phase involved enrolling COVID-19 patients from which PBMC was obtained (A). Memory B cells were single cell sorted (B), and antibodies were tested for binding specificity against the S-protein trimer and the S protein from the other HCoV viruses after a 2-week incubation (C). Once S-protein specific mAbs were identified, they entered the characterization phase with assessment of their neutralization potency.*

COVID-19 convalescent donors cohort: a total of 4,277 S-protein-binding MBCs were successfully retrieved from this cohort. A panel of 1,731 mAbs specific for the SARS-CoV-2 WT S-protein was identified showing a broad range of signal intensities (**Figure 27**). For these donors, the ELISA was performed using the S protein of SARS-CoV-2, since the research was conducted during the height of the pandemic, and the main necessity at that time was to find a mAb that would work primarily on the SARS-CoV-2 wild type virus, which was responsible for the majority, if not all, infections [111].
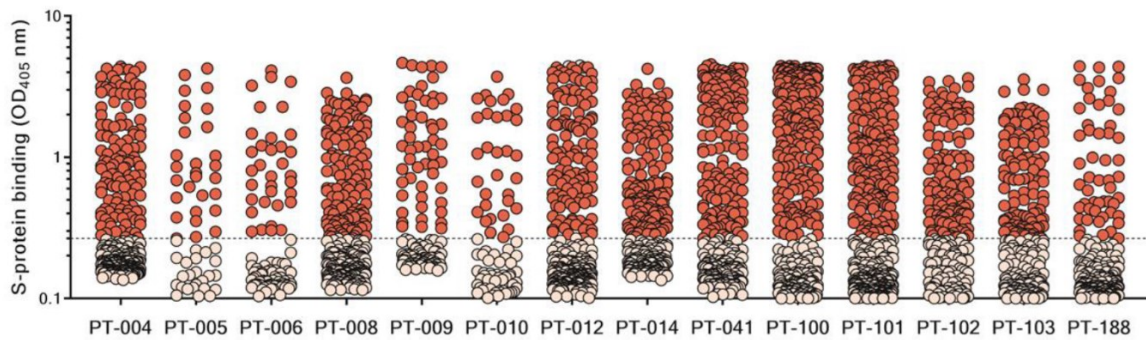
Figure 27. Monoclonal antibodies from COVID-19 convalescent donors cohort: binding to SARS-CoV-2 prefusion trimer. The graph shows MBC supernatants tested for binding to the SARS-CoV-2 S protein stabilized in its prefusion conformation. Threshold of positivity has been set as two times the value of the blank (dotted line). Red dots represent mAbs that bind to the S protein, while pink dots represent mAbs that do not bind. Patients are listed on the X axis.

Hybrid cohort: a total of 2,352 and 3,532 S protein-specific MBCs were isolated from seronegative and seropositive vaccinees, respectively. In ELISA, the mAbs released in the supernatants were first tested against the WT S protein prefusion trimer. 944 and 2,299 respectively showed positive signal (**Figure 27**).[112] The study on this cohort of vaccinees was conducted during the emergence of SARS-CoV-2 variants, including the Omicron variant which had already taken hold and caused the highest percentage of infections worldwide. Consequently, it became readily apparent that a broadly reactive human coronavirus neutralizing antibody (nAb) needed to be identified. To this aim, we decided to test mAb ability to neutralize the Omicron virus in the Biosafety Level 3 (BSL3) laboratory (data will be shown in Chapter 4).

Once we identified which antibodies had neutralizing properties vs. the Omicron virus, specifically a total of 52 nAbs from seropsitive and 16 nAbs from seronegative individuals, these were tested for the binding to the spike of SARS-CoV-1 and of MERS viruses. No binding signal was detected for the spike protein of MERS virus (data not shown), while 3 mAbs from seronegatives and 16 mAbs from seropositives recognized the SARS-CoV-1 S protein (**Figure 28**) [125].
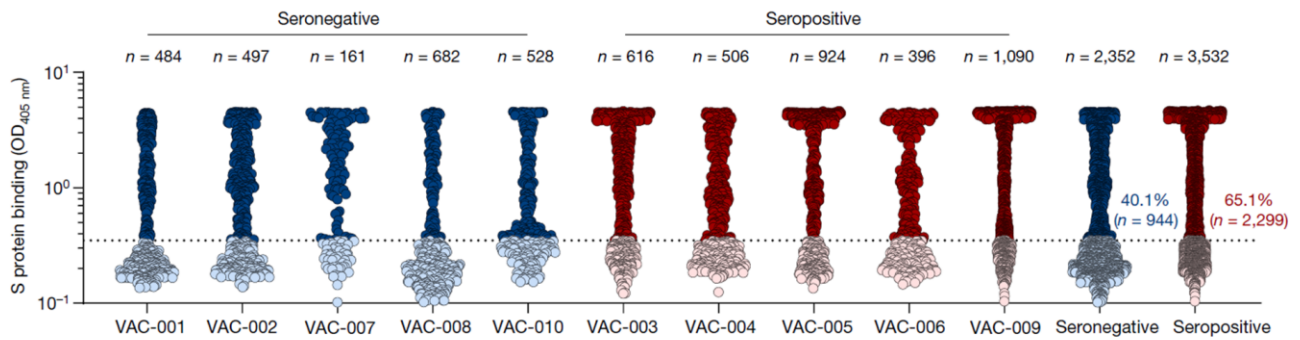
Figure 27. Identification of mAbs from the Hybrid cohort binding to SARS-CoV-2 S protein. *The graph represents supernatants tested for binding to the SARS-CoV-2 S protein antigen. Positivity was set at two times the value of the blank (dotted line). The dark blue and dark red spots represent mAbs that bind to the S protein in seronegative and seropositive vaccinees, respectively. The light blue and light red spots represent mAbs that are not bound to the S protein in seronegative and seropositive vaccinees, correspondingly. OD stands for optical density. Patients are indicated on the X axis.*
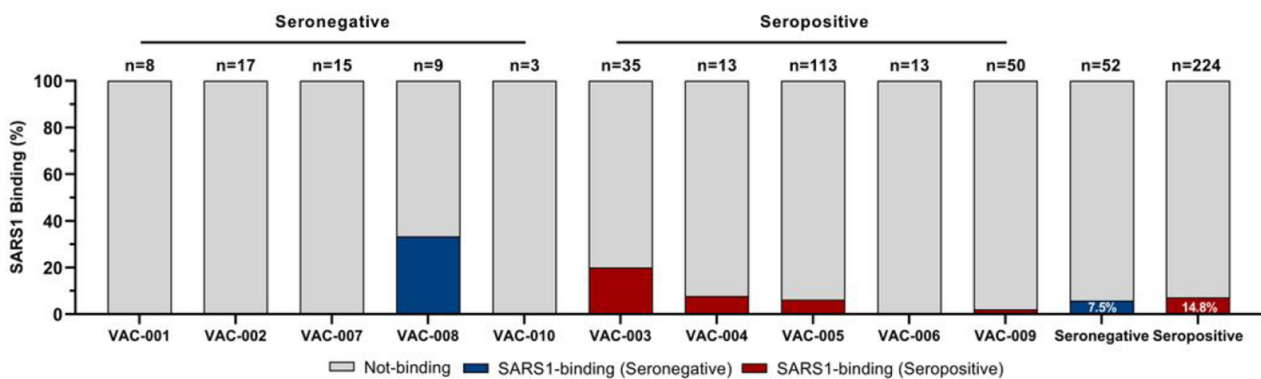
Figure 28. Binding of mAbs to SARS-CoV-1 S protein. *The percentages of not-binding antibodies (grey), SARS-CoV-1-binding nAbs from seronegative individuals (dark blue), and SARS-CoV-1-binding nAbs from seropositive people (dark red) are displayed in the bar graph. At the top of each bar is the total number (n) of antibodies tested for each participant. Patients are indicated on the X axis.*

Super Hybrid cohort: a total of 4,505 MBCs specific for the S protein were isolated from the super hybrid cohort. Supernatants from this group were screened for their capacity to neutralize pseudotype virus of the SARS-CoV-1 and Wuhan viruses (data will be shown in Chapter 2). A total of 544 nAbs were identified. A second ELISA assay was carried out using all of the spike proteins present in our library, including NL63, OC43, HKU-1,229E, SARS-CoV-1, and MERS, in addition to the WT spike protein of SARS-CoV-2 (**Figure 29**). As expected, the most prevalent binding signal detected in the assay was to the SARS-CoV-2 Spike. Approximately 10% of all neutralizing antibodies were able to

bind the SARS-CoV-1 S protein, whereas 0.7–1% of them bound the spike proteins of NL63, OC43, HKU-1, and 299E. No MERS targeting nAbs were found.
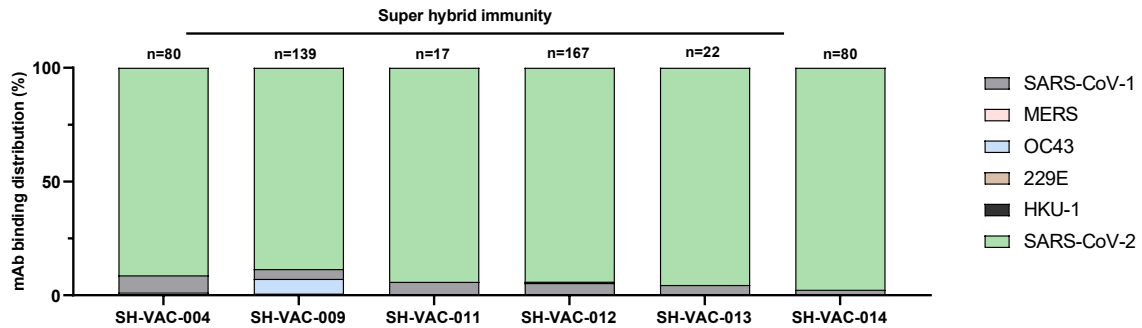
Figure 29. Monoclonal antibodies from Super Hybrid donors present different binding profiles to human coronavirus S proteins. *The percentage of SARS-CoV-2 binding nAbs (green), SARS-CoV-1-binding nAbs (grey), HKU-1-binding nAbs (black), OC43 binding nAbs (light blue) and 229E (light brown) are displayed in the bar graph. At the top of each bar is the total number (n) of antibodies tested for each donor. Patients are listed on the X axis.*

Spike variants BA 2.86 and XBB 1.5 shows a different binding profile between the Hybrid Cohort and the Super Hybrid Cohort

As in 2023 we decided to investigate primary versus a cross-immunity, we decided as first step to test our antibodies isolated from the Hybrid Cohort and the Super Hybrid Cohort for their possible binding versus BA.2.86 spike recombinant variant and XBB 1.5 (**Figure 30**).

Binding in ELISA using XBB 1.5 S-recombinant protein

A

Hybrid Immunity
- 95.14% No Binding
- 4.86% Binding

Super Hybrid Immunity
- 68.59% No Binding
- 31.41% Binding

Binding in ELISA using 2.86 S-recombinant protein

B

Hybrid Immunity
- 97.57% No Binding
- 2.43% Binding

Super Hybrid Immunity
- 79.77% No Binding
- 20.23% Binding
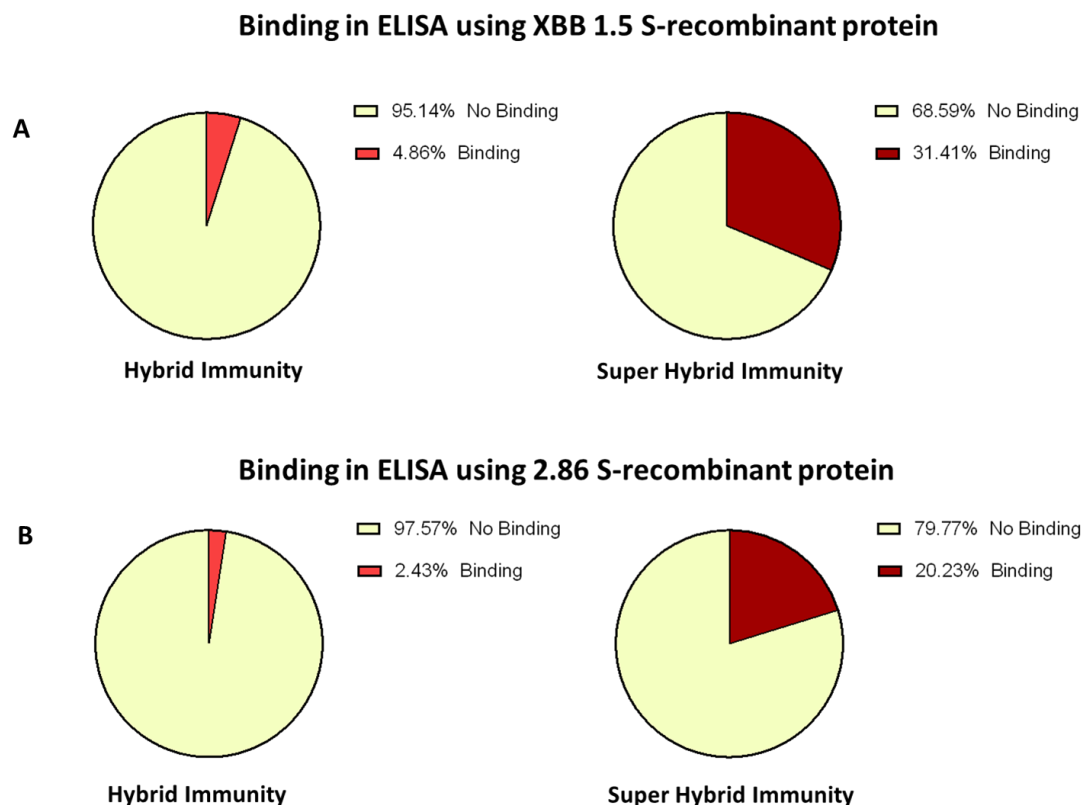
Figure 30. ELISA binding assay using BA 2.86 and XBB 1.5 spike recombinant protein. *The figure shows the percentage of binding for the XBB 1.5 spike protein (**A**) and the BA 2.86 protein (**B**) respectively with the antibodies derived from the Hybrid Cohort and the antibodies obtained from the Super Hubrid Cohort. The percentage of positive antibodies increase notably when the ELISA is conducted on the Super Hybrid subjects.*

Results indicated that the Super Hybrid subjects who subsequently contracted several Covid-19 infections (possibly from distinct variants) showed a considerable rise in immunity against the tested variants. Conversely, the response from Hybrid subjects to these tested variants is minimal, similar to how they responded to other Spikes of different HCoVs.

1.3 Discussion

Availability of high-quality reagents has been crucial for the discovery and development of countermeasures against the SARS-CoV-2 pandemic. Among these, the pure S protein has been instrumental for the design of vaccines and for the screening of anti-viral sera and mAbs with neutralizing activity [126]. Reagents and assays ought to be extremely specific for SARS-CoV-2 due to the widespread occurrence of similar coronaviruses in the human population (e.g. MERS-CoV, SARS-CoV-1, and common cold coronaviruses OC43 and HKU1).

The S protein, often referred to as Spike, is used in several published and ongoing serology assays that rely on the ELISA technology. Because of its intrinsic specificity [60], the spike protein is a prime candidate for both therapeutic interventions and serological research aimed at determining the frequency of immune responses to a specific coronavirus.

At the beginning of 2020, when I started my PhD program, generating and purifying high-quality soluble spike trimers were challenging tasks. A 0.5 mg/L yield was reported for this protein in one paper [126], whereas a 5 mg/L yield was suggested in another one [127]. However, multiple unpublished preprints showed consistent yields in the 1-2 mg/L range.

To reliably produce the SARS-CoV-2 S protein in amounts suitable for serology assays and structural biology, a robust method was optimized as described in this first part of the Results section. By changing the expression cell line to CHO and the harvesting time, the methods described here enabled our laboratory to greatly increase the manufacturing yield of the spike protein. The recombinant proteins were functional as antigens in ELISA assays, formed suitable trimeric structures, and were extremely pure when run in SDS PAGE.

The optimization of the expression and purification process was easily applicable not only to the Spikes of other known coronaviruses (OC43, NL63, 229E, HKU-1), but also to the multiple SARS-CoV-2 spike variants that have emerged over the years, thereby allowing the creation of a rich library of recombinant S proteins.

Furthermore, the development of a mutagenesis platform for the generation of spike VOCs increased the value of this work as it expanded the range of serological assays that assessed mAbs capacity to bind the protein target, with no need for the live virus.

Different results were obtained by comparing the ELISA results across the various cohorts under analysis. For instance, in the *COVID-19 convalescent donors cohort*, the ELISA binding assay used the sole SARS-CoV-2 spike WT protein and pinpointed numerous mAbs capable of binding the wild type antigen. On the other hand, in the *Hybrid cohort*, more antibodies were able to bind the SARS-CoV-2 spike protein. Additionally, plasma from seropositive participants demonstrated a higher binding activity to the S protein in comparison to plasma from seronegative participants. The analysis of the binding towards the SARS-CoV-1 spike revealed that only a very small proportion (roughly 14%) of the neutralising antibodies present in seropositive subjects were able to bind this protein. Additionally, not all subjects had antibodies that could bind the SARS-CoV-1 Spike; in contrast, the percentage dropped to about half (7%) in seronegative subjects.

Finally, the *Super Hybrid cohort* displayed a notable increase in the proportion of antibodies capable of binding the SARS-CoV-2 Spike, reaching 93.4% of all neutralising mAbs. Moreover, we observed

that each subject had expressed antibodies capable of binding the SARS-CoV-1 spike protein. With the exception of SH-VAC-013 and SH-VAC-014 donors, all subjects showed some, albeit slight, cross-reactivity with the spike proteins of the other three coronaviruses. The MERS spike protein was the only exception, as no cross-reacting antibody was found.

Overall, these data indicate that the presence of cross-neutralizing antibodies is favoured by the administration of multiple vaccine doses, and that this is more prevalent in people who have undergone both vaccinations and infections. The increase in the number of these cross-neutralizing antibodies in subjects who received more than two vaccine doses (the *Super Hybrid cohort*) highlights how vaccine booster is closely correlated with the development of a larger antibody repertoire.

1.4 Experimental procedures

Human sample collection

This work was possible thanks to the collaboration with the Azienda Ospedaliera Universitaria Senese, Siena (IT), which donated samples from donors who gave written agreement and were vaccinated against COVID-19 in both sexes. The research project received approval from the ethics committee of the Comitato Etico di Area Vasta Sud Est (CEAVSE) (Parere 17065 in Siena) and was carried out in compliance with the Helsinki Declaration (European Council 2001, US Code of Federal Regulations, ICH 1997) and appropriate clinical practices. This was not a randomized, unblinded study. The sample size was not predetermined using statistical techniques.

Expression and purification of spike recombinant proteins

The plasmid encoding SARS-CoV-2 S-2P construct, generously provided by Prof. Jason S. McLellan, was transiently transfected in Expi293F™ cells (Thermo Fisher) using ExpiFectamine™ 293 Reagent. Cells were grown for six days at 37°C with 8% CO_2 in shaking conditions at 125 rpm according to the manufacturer's protocol (Thermo Fisher). ExpiFectamine™ 293 Transfection Enhancers 1 and 2 were added 16 to 18 hours post-transfection to boost transfection, cell viability, and protein expression.

The same procedure was used to express the spike constructs from other HCoV: MERS, SARS-CoV-1, OC43, 229E, NL63, HKU-1 spike 2P proteins.

The plasmid encoding SARS-CoV-2 6P WT and all the spike VOCs generated in this work were transiently transfected in ExpiCHO-S cells (Thermo Fisher) using ExpiFectamine™ CHO Reagent. Cells were grown for six days at 37°C with 8% CO_2 in shaking conditions at 125 rpm according to the manufacturer's protocol (Thermo Fisher). ExpiFectamine™ CHO Enhancer and ExpiCHO™ Feed were added 18 to 22 hours post-transfection to boost transfection, cell viability, and protein expression.

Both types of cell cultures (for spike 2P S-protein and for spike 6P S-protein) were harvested five days after transfection and the proteins were purified by immobilized metal affinity chromatography (FF Crude) followed by dialysis into final buffer.

Cell culture supernatants were clarified by centrifugation (1,200 x g, 30 min, 4°C) followed by filtration through a 0.45 µm filter. Chromatography purification was conducted at room temperature using ÄKTA Go purifier system from GE Healthcare Life Sciences. Specifically, filtered culture supernatant was purified with a 5 mL HisTrap FF Crude column (GE Healthcare Life Sciences) previously equilibrated in Buffer A (20 mM NaH_2PO_4, 500 mM NaCl + 30 mM Imidazole pH 7.4).

The flow rate for all steps of the HisTrap FF Crude column purification was 5 mL/min. The culture supernatant of each spike protein was applied to a single 5 mL HisTrap FF Crude column. The column was washed in Buffer A with 4 column volumes (CV). spike proteins were eluted from the column by applying a first step elution of 5CV of 60% Buffer B (20 mM NaH_2PO_4, 500 mM NaCl + 500 mM Imidazole pH 7.4). Elution fractions were collected in 1 ml each and analyzed by SDS-PAGE. Fractions containing the S protein were pooled and dialyzed against PBS buffer pH 7.4 using Slide-A-Lyzer™ Dialysis Cassette 10K MWCO (Thermo Scientific) overnight at 4°C. The dialysis buffer used was at least 200 times the volume of the sample. The final spike protein concentration was determined by measuring absorbance at 562 nm using Pierce™ BCA Protein Assay Kit (Thermo Scientific™). Proteins were dispensed into 0.5 mL aliquots and stored at -80°C.

Cloning of SARS-CoV-2 spike VOCs

The plasmid encoding SARS-CoV-2 S-6P was digested with the appropriate restriction enzymes (New England BioLabs) for 2 hours at 37°C and each digestion was confirmed on 0.6 % agarose gel with FastRuler DNA Ladders (ThermoFisher Scientific). DNA was then precipitated with sodium acetate and ethanol. The DNA sequence of each SARS-CoV-2 spike VOCs was codon-optimised for *Homo sapiens* and ordered as a string on GeneArt (ThermoFisher). Each string was amplified with 5U of KAPA LongRange DNA Polymerase (0.125 µl Kapa polymerase, 0.5 µl dNTPs (10 µM), 1.25 µl F primer and 1.25 µl R primer specific for the string, 3 µl string template (10 ng/µl), 1.25 µl of 25 mM $MgCl_2$, and 5 µl of KAPA LongRange Buffer 5X).

PCR reactions were performed as follows: denaturation at 98°C/30 sec, 25 cycles composed of denaturation at 98°C/10 sec, annealing at 67°C/30 sec, extension at 72°C/1 min and a final extension at 72°C/1 min. Amplification was confirmed on 0.6 % agarose gel with FastRuler DNA Ladders (ThermoFisher Scientific). The resulting fragments were then extracted from gel using QIAquick Gel Extraction Kit (QIAGEN) and quantified. Each string was then digested with the appropriate enzymes and ligated using T4 DNA Ligase into the SARS-CoV-2 6P expression vector which was previously digested with the same restriction enzymes. The mixture (1µl SARS-CoV-2 S-6P (60 ng/µl), 8 µl synthetic string (25 ng/µl), 1 µl 10x DNA ligase buffer, 1 µl enzyme) was incubated at room temperature for 4 hours. The ligation reaction was transformed in TOP10 *Escherichia coli* chemically competent cells (ThermoFisher). Colonies were screened by colony PCR using primers Forward and Reverse specific for each synthetic string. Positive clones were grown overnight in LB medium supplemented with ampicillin, plasmid DNA was extracted with QIAprep Spin Miniprep Kit (Qiagen) and sent to Eurofins for Sanger sequencing. The correct clone was saved and the corresponding plasmid transfected into CHO cells for protein expression.

Table 4. Spike variants generated using a modular mutagenesis platform. *For each variant, mutations were mapped and introduced via DNA strings into the vector carrying the S encoding gene. Plasmids encoding variant S proteins were thus generated.*

Alpha   α (UK variant B1.1.7)

- String N: Δ69-70; ΔY144 | Kpn I / EcoRI fragment |
- String O: N501Y; A570D; P681H | AgeI/NheI fragment |
- String P: S982A; D1118H | XbaI/BamHI fragment |

Beta   β (South Africa variant B1.351)

- String I: L18F; D80A | Kpn I / EcoRI fragment |
- String L: D215G | EcoRI/AgeI fragment |
- String M: K417T ; E484K; N501Y | AgeI/NheI fragment |
- String Q: A701V | NheI/XbaI fragment |

Gamma   γ (Brazilian variant P1)

- String F: L18F; T20N; P26S; D138Y; R190S | Kpn I / EcoRI fragment |
- String G: K417T; E484K; N501Y; H655Y | AgeI/NheI fragment |
- String H: T1027I; V1176F | XbaI/BamHI fragment |

Kappa   κ (Indian variant 1.617.1)

- String S: L452R; E484Q | AgeI/NheI fragment |

Delta   δ (Indian variant 1.617.2)

- String R: L452R; T478K | AgeI/NheI fragment |

According to the literature [128], as the virus evolved over time, the number of mutations grew significantly. Therefore, starting from the BA.1 variant, we decided to order the complete constructs directly from GeneArt rather than carrying out the whole cloning procedure. This allowed us to accelerate the library construction process and save time for exploiting this tool into functional assays.

ELISA assay with SARS-CoV-2 S protein prefusion trimer

ELISA assay was used to detect SARS-CoV-2 S-protein specific mAbs. 384-well plates (384 well plates, microplate clear; Greiner Bio-one) were coated with 3 mg/mL of streptavidin (Thermo Fisher) diluted in coating buffer (0.05 M carbonate-bicarbonate solution, pH 9.6) and incubated at RT overnight. The next day, plates were incubated for 1 h at room temperature with 3 µg/ml of SARS-CoV-2 S protein diluted in PBS. Plates were then saturated with 50 µl per well of blocking buffer (phosphate-buffered saline and 1% BSA) for 1 h at 37°C. Supernatants were diluted 1:5 in PBS/BSA 1%/Tween20 0.05% in 25 mL/well final volume and incubated for 1 h at 37°C without CO_2. After 1 h of incubation, 25 µl per well of alkaline phosphatase-conjugated goat anti-human IgG (Southern Biotech) diluted 1:2,000 in sample buffer was added. Finally, S protein binding was detected using 25 µl per well of PNPP (p-nitrophenyl phosphate; Thermo Fisher) and the reaction was measured at a wavelength of 405 nm by the Varioskan Lux Reader (Thermo Fisher Scientific). After each incubation step, plates were washed three times with 100 µl per well of washing buffer (phosphate-buffered saline and 0.05% Tween-20). Sample buffer was used as a blank and the threshold for sample positivity was set at twofold the optical density (OD) of the blank.

1.5 Supplementary materials

Supplementary Table 1. List of plasmids used in this work.

Name	Type	Features	Resistance	Source
nCoV-1 nCoV-2P-F3CH2S (Spike 2P)	pcDNA 3.1 (+)	• Size: 8370 bp • Cloning site (KpnI,Age I, EcoRI, Nhe I, Xba I) are into the cloned gene under control of theCMV early enhancer + chicken β actin (CAG) promoter	Amp^R Ampicillin resistance gene	Jason McLellan Lab
SARS-CoV-2 S HexaPro (Spike 6P)	pcDNA 3.1 (+)	• Size: 8370 bp • Cloning site (KpnI,Age I, EcoRI, Nhe I, Xba I) are into the cloned gene under control of theCMV early enhancer + chicken β actin (CAG) promoter	Amp^R Ampicillin resistance gene	Jason McLellan Lab

2.   Pseudotyping: neutralization assay using pseudotyped viruses

2.1 Introduction

Coronavirus is an envelope virus composed of four structural proteins: spike (S) protein, membrane (M) protein, envelope (E) protein and nucleocapsid (N) protein [129].

The attachment and entry of the virus into the target cells, which start the infection process, are mediated by the S protein. S protein has a pivotal role in the stimulation and induction of protective human and cellular immunity following SARS-CoV-2 infection; accordingly, the S protein is the most desirable target [130][131].

Many strategies, most of which target the S protein, have been used to develop preventive and therapeutic measures in response to the novel coronavirus pneumonia epidemic of 2019. These strategies include whole inactivated vaccines, subunit vaccines, RNA-based vaccines, viral vectored vaccines, neutralizing monoclonal antibodies, and fusion inhibitors [132].

Since SARS-CoV-2 is highly transmissible and pathogenic, and it can only be handled in biosafety level 3 (BSL-3) facilities, this has hampered the development of antiviral treatments especially during the first years of the pandemic. Another significant obstacle to developing candidate vaccines and therapeutics when working with the SARS-CoV-2 virus is the accessibility to the live virus strain.[132]

Over the past five decades, several pseudotype virus-based neutralization assays for emerging and re-emerging viruses, including highly pathogenic ones like MERS-CoV, rabies virus, Ebola virus, and Marburg virus, have been developed to prevent dealing with authentic viruses[133–136]. The pseudotype platform provides the fast implementation of serosurveillance and antigenic characterisation studies at low containment levels upon virus emergence, hence aiding in the development of drugs, vaccines and antivirals. This is particularly beneficial for researching highly pathogenic zoonotic viruses, which are a serious threat to public health[137].

Viruses are biological agents able to introduce efficiently, subsequently to the infection, their genetic materials in a host cell and rely on the host for replication and propagation.

Viral vectors are developed in laboratory starting from infectious virus with the main difference that they carry genes of interest instead of original viral genes. As a result of these modifications, the ability to replicate and propagate independently is lost in viral vectors, but the ability to infect and transfer gene material into the host cell is retained.

Lentiviral vectors, produced from viruses that belong to the Retrovirus family (Retroviridae; Lentivirus type), are currently considered as the most efficient vectors for genetic transfer not only for basic research activity but also for gene therapy. This is due to their ability to integrate into the mammalian cell genome, independently from their proliferative state, ensuring long-term expression of the transgene.

Crucially, the envelopes of these viral particles normally share similar conformational structures to those of the wild type viruses, making them suitable for the evaluation of possible neutralizing antibodies and mechanistic research concerning viral entry. [109]

Although lentiviral particles can infect susceptible cells, they can only multiply once in the host cells that they infect, thus making them safer to handle in biosafety level (BSL)-2 laboratories than wild-type (WT) viruses, especially in the case of the SARS-CoV-2 virus.

Pseudoviral surface proteins, however, have an elevated level of structural homology with the original viral proteins, and they are capable of mediating viral entry into host cells.

This is a crucial point to consider since, in addition to avoiding the use of BSL-3, working with pseudotyped viruses makes it possible to characterize the spike protein's envelope as needed.

Some mutations in the SARS-CoV-2 spike (S) protein are very important to study as they have the ability to change the antigenic properties through various mechanisms, making them potentially more pathogenic, virulent, transmissible, or able to evade immunity brought on by prior infection or vaccination. [79,114,138]

In 2021, the Omicron variant emerged containing a total of 59 mutations in its genome, with as many as 37 mutations occurring in the spike protein, including S371L, K417N, N440K, G446S, S477N, T478K, E484A, Q493R, G496S, Q498R, N501Y, and Y505H. These single point mutations were already known to the scientific community for being present in lineages such as Alpha (B.1.17), Beta (B.1.351) and Gamma (P.1), and for conferring to these lineage higher affinity to ACE2 and increased infectivity, together with immune escape.

According to Cao's work from 2022 [139], Omicron may cause substantial humoral immune evasion and putative antigenic shifting, as evidenced by the escape of more than 85% of tested human-neutralizing antibodies. Consequently, since the beginning of 2022, our laboratory started to test antibodies obtained from various patient cohorts against the emerging variants related to the Omicron lineage, even though the live virus was not immediately available.

Thanks to an internship in Prof. De Francesco's group at the Instituto Nazionale di Genetica Molecolare (INGM), who has vast experience in developing lentiviral vector assays, I learnt how to prepare and run tests using the SARS-CoV-2 pseudotyped viruses platform. In addition, targeted mutagenesis of the gene encoding the spike protein allowed to create different envelopes associated to each variant of concern.

In this chapter I am presenting a full panel of lentiviral particles pseudotyped with the S proteins of six of the human coronaviruses. For every human coronavirus pseudotyped, production was optimized to provide good titres using the same lentiviral luciferase plus GFP system, enabling parallel investigations that were similar throughout the panel. Specifically, when the real virus was unavailable, these lentiviral vectors have been utilized to examine and characterize the mAbs obtained by each cohort.

Specifically, in this work I used a third-generation HIV-based lentiviral system to develop pseudotype virus exposing the spike protein of SARS-CoV-2 variants on their surface, in which the Green Fluorescent Protein gene (useful for the titration of pseudotype virus preparation) and Firefly Luciferase gene (essential for the quantification of the infection) were inserted into the genomic plasmid.

The SARS-CoV-2 pseudotype virus constructed with this methodology are replication-defective viruses, yet they are competent for a single round of infection in host cells in a similar way as authentic viruses. This work produced a pseudotype virus -based neutralization assay that is safe,

widely available, and effective for assessing vaccines and treatment candidates against SARS-CoV-2 variants.

2.2 Results

Six human coronavirus lentiviral pseudotypes were produced at high production titres following the production method reported by Conforti et al. [140] and Sampson et al. [141]
and the permissive cell lines reported in the papers have been used to verify the ability of the different pseudotype virus to infect.
SARS-CoV-1, HCoV-229E, HCoV-NL63, HCoV-OC43, and HCoV-HKU1 and several variants of SARS-CoV-2 have been generated and tested as pseudoparticles.

2.2.1 Construction of the recombinant plasmid expressing SARS-CoV-2 spike envelope

While the plasmid necessary for the envelope, encoding the full length spike of HCoV 229E, NL-63 and HKU-1 were kindly gifted by Prof. Nigel Temperon's lab and used for pseudotyped viruses preparation, the HCoV-OC43 pseudotype supernatant was kindly donated by Prof. Nigel Temperton, since the single spike plasmid was not available.

To produce the SARS-CoV-2 S pseudotyped virus, the full-length S gene from strain Wuhan-Hu-1 (GenBank: MN908947) with a deletion of 19 amino acids of the cytoplasmic tail was optimized for codon usage and inserted into a pcDNA3.1 plasmid. In this sequence was already inserted the D614G mutation, since starting from the beginning of 2020 the viral genome permanently incorporated this mutation. This plasmid and the plasmid encoding for the S BA.2 variant were gently provided by Prof. De Francesco's lab.

Starting from these Spike-encoding plasmids, I generated SARS-CoV-2 spike envelopes through a new multisite mutagenesis method, using the specific *QuickChange Lightning Multi Site-Directed Mutagenesis Kit ™.* Briefly, this mutagenesis kit method allows mutagenesis at multiple sites in a single round, working with a single oligonucleotide per site. Using the appropriate primers carrying the mutations of interest, it was possible to introduce mutations at five different sites simultaneously.

This kit allows the generation of several spike variants in a very short amount of time. **Figure 31** below reports some of the single-point mutations and deletions considered in this study.
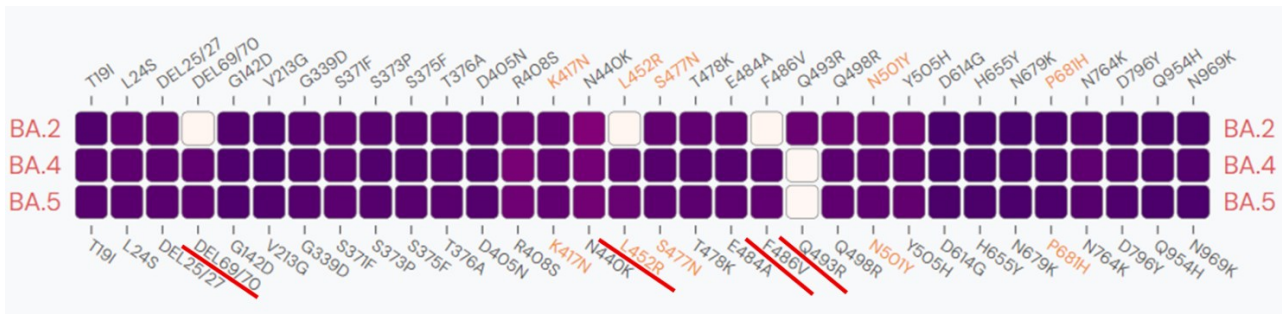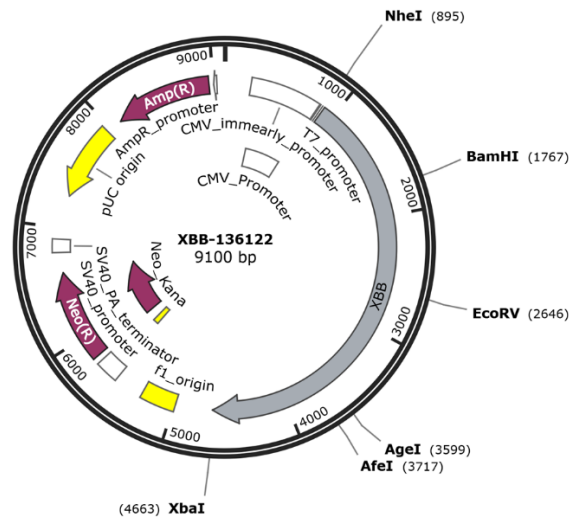
Figure 31. Sequence of the S gene of BA.2 and BA.4/5 SARS-CoV-2 variants. *The sequence of BA.2 and BA.4/5 differ from each other by only 4 major mutations: the disappearance of a deletion at amino acid 69-70, a lysine at position 452 being replaced by an Arginine, a Phenylalanine being replaced by a Valine at position 486, and a reversion of an Arginine back to a Glutamine as it was present in the original spike WT sequence, at position 493. It was possible to reproduce these single point mutations through a single round PCR using the BA.2 DNA plasmid as a backbone and three different primers (one primer carried both mutations F486V and R493Q), and in the final PCR the BA.4/5 DNA sequence was obtained.*

Using this methodology I was able to generate several spike plasmids (all carrying the del.19 AA corresponding to the C-terminal of the spike sequence), reported in **Table 5.** Each plasmid was used as envelope-encoding DNA to generate the appropriate pseudotype virus thereby obtaining a spike – pseudotyped viruses library of the several VOCs identified from 2020 to nowadays (Table 1 and Figure 2).

Table 5. The list of VOCs that we now have in our lab is separated into two categories: those that were created using mutagenesis and those that were received as whole plasmids from GeneArt when the mutations that needed to be introduced were too many (**Figure 32**).

A. Spike VOCs Envelope plasmid obtained through mutagenesis
BA.2.75
BA.2.75.2
BA.2.12.1
BA.4/5
CH.1.1
BF.7
BQ.1
XBB 1.5

B. Spike VOCs Envelope plasmid ordered from GeneArt
XBB
BA 2.86

Figure 32. Plasmid encoding spike XBB variant. *While ordering the plasmid for the XBB variant I introduced several restriction sites into the sequence of the S gene in order to be able to replace the wild-type sequence with restriction fragments containing new mutations, should new variants appear.*

The plasmid encoding for the envelope of SARS-CoV-1 Spike, named as "pcDNA3.3_CoV1_D28" was bought from AddGene from David Nemazee's lab (Addgene plasmid # 170447; http://n2t.net/addgene:170447). [142]

2.2.2 Optimization of S- lentiviral pseudotyped viruses production

To generate the various S- lentiviral pseudotyped viruses, all of the five different plasmids necessary for the creation of a third-generation vector were co-transfected into producer HEK293TN cells. Thirty hours after transfection, the supernatant was collected, clarified by filtration (0.45-mm pore-size), concentrated and each pseudotype virus was used to infect the corresponding cell line, to titrate and verify pseudotype virus activity.

Since the pseudotyped viruses exposed different spike proteins derived from different viruses, for each preparation I had to use the corresponding cell line for which they had tropism.

As mentioned above, plasmid for SARS-CoV-2 pseudotype virus derived from Prof. De Francesco's lab, which also provided us with the corresponding cell-line, hACE2 [140].

Regarding the other pseudotyped viruses, a very detailed work and screening has been described by Sampson et al[141] , who reported the infectious capacity of the lentivirus generated versus the different cell lines available in laboratories. Accordingly, the HUH7 and CHO – k1 cell lines together with the HEKT/17 cell line were kindly donated by Nigel Temperton's lab and used to evaluate the titre of the pseudotype virus of HCoV 229E, HKU-1 and NL-63 (**Figure 33**).
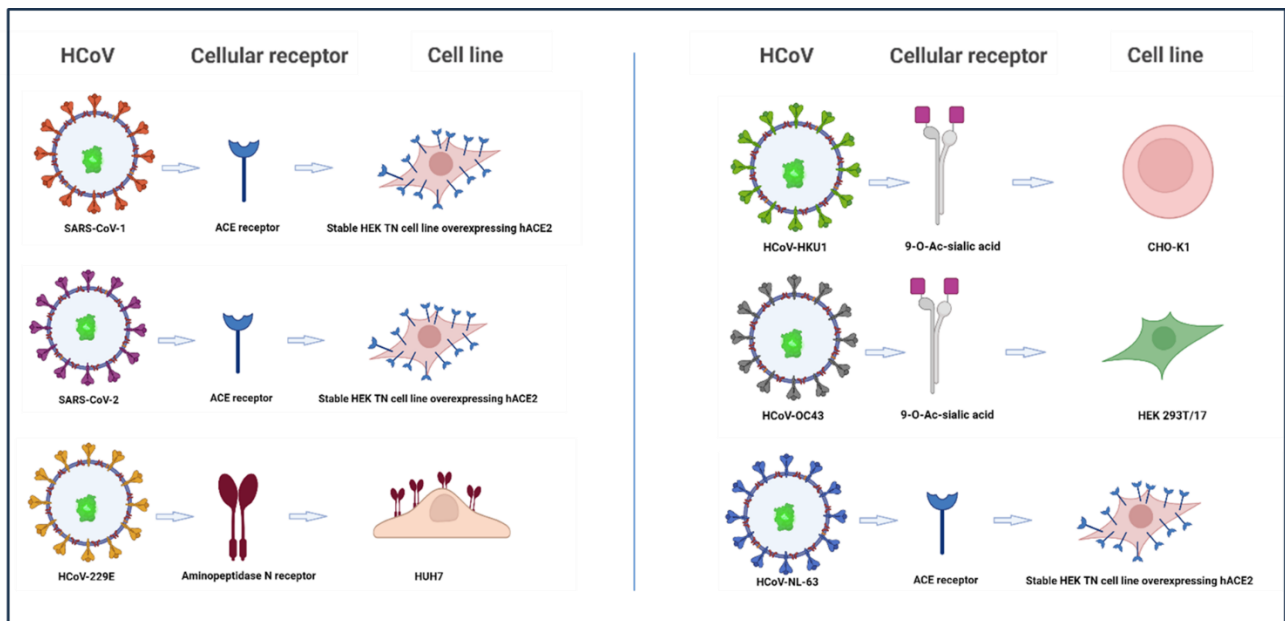
Figure 33. Cellular receptors and corresponding cell line for each h-CoV pseudotype virus. *Spike of SARS-CoV-1, SARS-CoV-2 and NL63 viruses showed tropism and affinity for ACE receptor, so cell lines overexpressing hACE2 receptor have been used to verify the ability to infect. Although HCoV HKU-1 and HCoV – OC43 share affinity for the same receptor, CHO-K1 cell line resulted permissive for HKU-1 pseudotyped viruses while, for OC-43 PVs, HEK 293T/17 cells were better transduced.*

hACE2 cells were infected with SARS-CoV-1, SARS-CoV-2 variants and with HCoV-NL63 for 72 hours, and then the viral titer was determined by measuring the GFP positive cells present in each well. h-CoV-229E was used to infect the HUH-7 cell line while HCoV-HKU-1 was used for the titration with CHO-K1 cell line.

The Luciferase gene and the GFP gene are the two major genes present in the pseudotyped viruses. The infected cell can produce fluorescence through the GFP protein as soon as the virion integrates into the genome, thus confirming the infection (**Figure 34 A, B**).

I introduced some modifications to the HCoV pseudotyped viruses, since the constructs that I utilized for co-trasfection differed from those reported in the publication were the methodology was described[141]. Since for these pseudotyped-vectors I used the construct coding for Luciferase gene plus GFP gene, I decided to titrate them using FACS analysis, as for the SARS-CoV-1 and SARS-CoV-2 variants, to count the number of GFP-positive cells in the cell cultures (**Figure 34, C**).
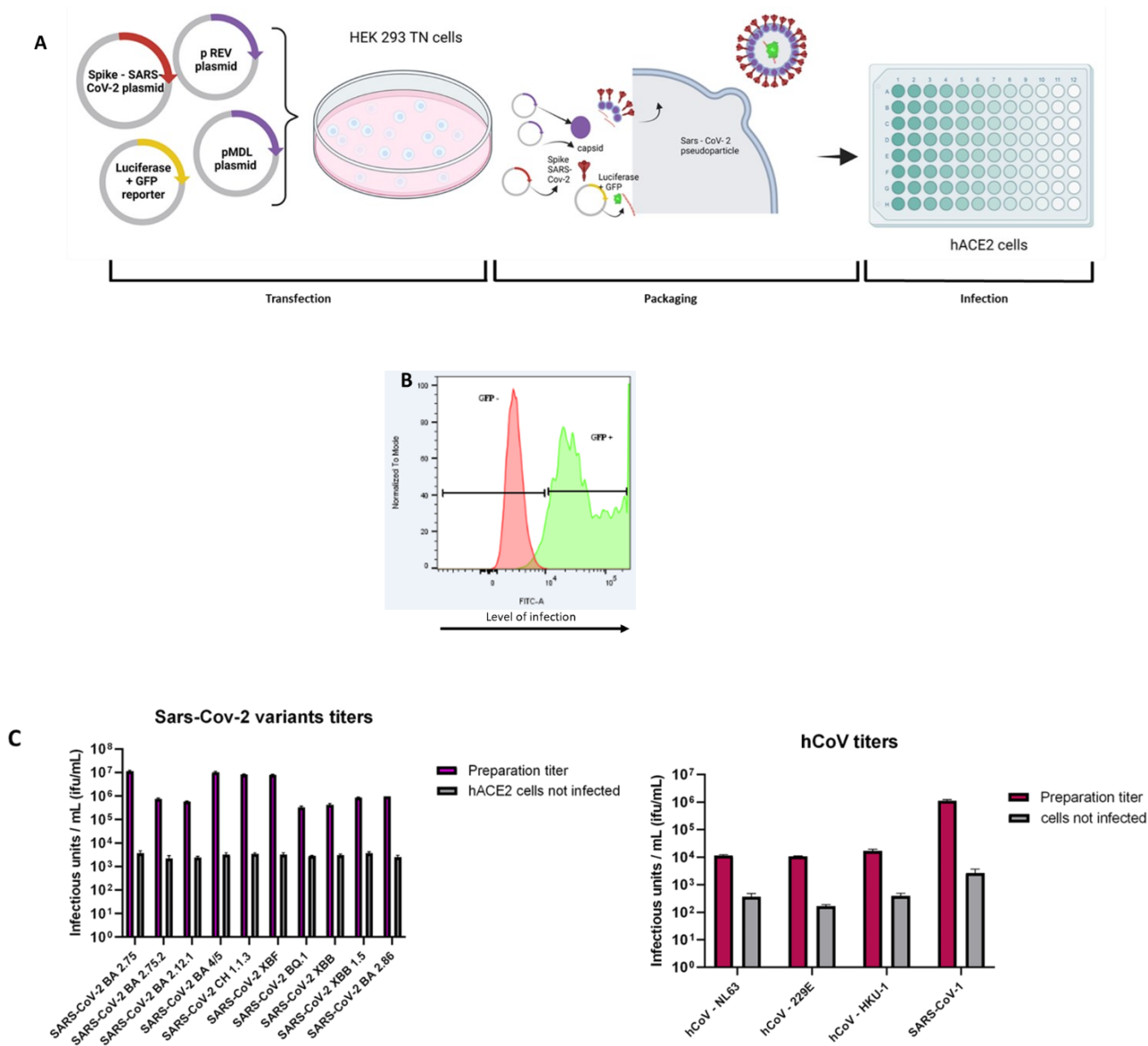
Figure 34. Schematic representation of pseudotyped viruses production and titration assay. (**A**) *The HIV backbone vector plasmids pMDLg/pRRE (Addgene #12251), pRSV-Rev (Addgene #12253), pAdVAntage™ Vector and reporter plasmid pLenti CMV-GFP-TAV2A-LUC Hygro, were co-transfected with different spike envelope-encoding plasmid depending on the type of virus, into HEK293TN cells, to package the pseudotyped lentiviral particles.*

The supernatants containing pseudotyped viruses *with the different S proteins were collected and then ACE2-293T cells or the other cell lines previously described were used to determine the pseudoviral titer. (**B, C**) Each pseudotype virus preparation was used to infect the corresponding cell lines and each infection was quantified by flow cytometry.*

2.2.3 Spike Omicron variants showed high immune evasion properties against mAbs derived from the COVID-19 convalescent cohort and Hybrid Cohort

As we reported in the published article[111] with the analysis of the cohort of *COVID-19 convalescent donors*, out of the 453 neutralizing antibodies that were tested and characterized, one antibody named J08 revealed extremely high neutralization potency against both the WT SARS-CoV-2 virus isolated in Wuhan and emerging variants containing the D614G, E484K, and N501Y mutations.

J08 mAb neutralized the authentic WT virus and emerging variants at picomolar concentrations *in vitro* and showed prophylactic and therapeutic efficacy in a SARS-CoV-2 hamster infection model when used at 0.25 and 4 mg/kg, respectively. The antibody described was a promising candidate for the development of a broadly affordable tool for prevention and therapy of COVID-19.

Since multiple reports have demonstrated that the unprecedented number of mutations carried on the Omicron S protein drastically reduced up to 40-fold the neutralizing efficacy of sera from infected and vaccinated people and that this VoC can evade more than 85% of nAbs described in literature, [139,143,144] including several antibodies approved for clinical use by regulatory agencies, it was imperative to test J08 as soon as the Omicron variant appeared.

In this case, since we didn't have the virus available in our BSL-3, we decided to test this mAb using pseudotyped viruses. Unfortunately, J08 lost its neutralization activity on the Omicron pseudotype variant, while, as expected, it was still active on the WT pseudotype virus of the SARS-CoV-2, exhibiting a neutralizing activity that was remarkably similar to what was observed when it was tested on the WT live virus **(Figure 35)**.
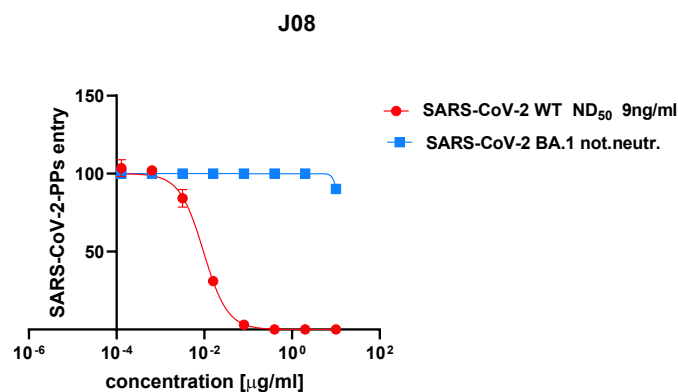
Figure 35. *Neutralization sensitivity of J08 on SARS-CoV-2 pseudotyped Omicron variant. Neutralizing curves of mAb J0 against pseudotyped SARS-CoV-2 variants. Data are representative of at least two independent experiments. Mean + SD is shown.*

This outcome demonstrated how crucial it was to keep looking for mAbs with broadly neutralizing potential against future appearance of SARS-CoV-2 variants.

In late 2021, to understand the impact of SARS-CoV-2 Omicron on antibody response, we evaluated the neutralization activity of 276 nAbs previously isolated from seronegative (n=52) and seropositive (n=224) donors from the *Hybrid Cohort.*

When tested on the Omicron live virus, 38 out of 224 nAbs from seropositives were able to neutralize this variant, whereas just 1 out of 52 nAbs from seronegatives had a medium-low neutralising potency against Omicron (data shown in Chapter 4).

We tested the antibodies that were found to be most effective in neutralising all of the previous variants (Alpha, Beta, Gamma, and Delta) on BA.2 and BA.2.12.1 pseudotype virus since the Omicron sub-variants became quickly prevalent on the original Omicron in few months.

Whereas a single antibody had been identified as most potent from the *COVID-19 convalescent cohort*, named M04, broad-neutralizing activity versus the several Omicron variants specifically of three antibodies named M04, G18, and O14 emerged from the *Hybrid cohort*. In details, two of the antibodies derived from the Hybrid subjects, notably the G18 and O14 antibodies, showed preservation of activity. Again, these results confirmed that the J08 antibody could no longer be used for the treatment of COVID-19 patients given the circulation of these new Omicron variants **(Figure 36).**
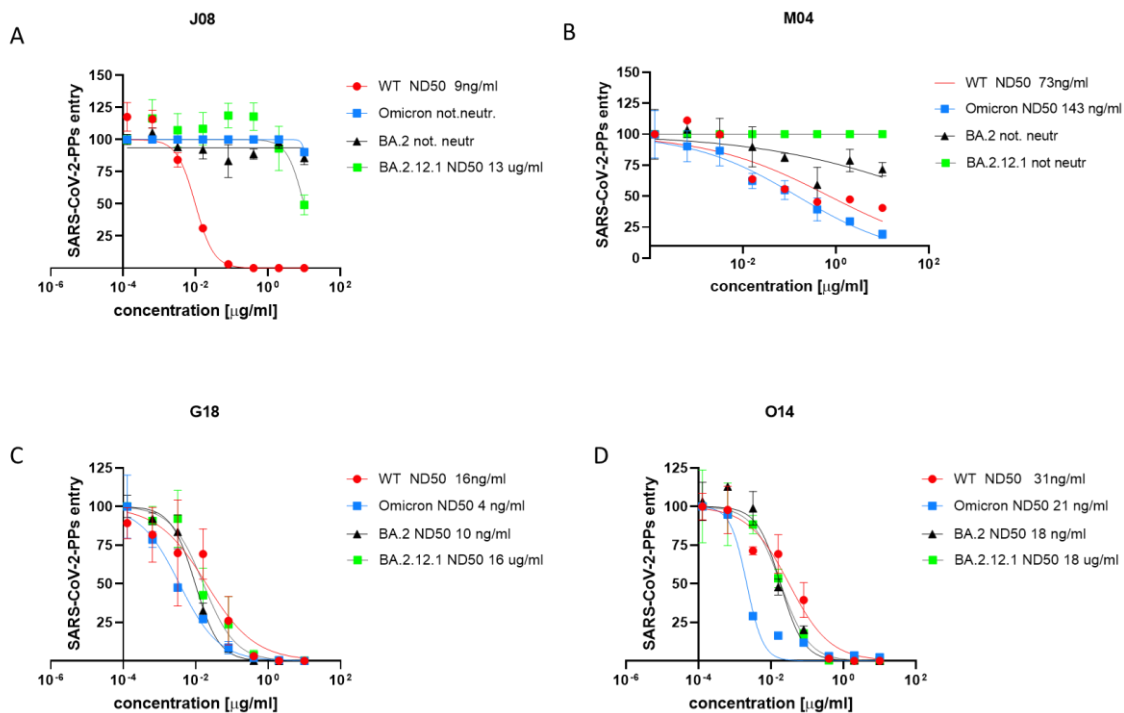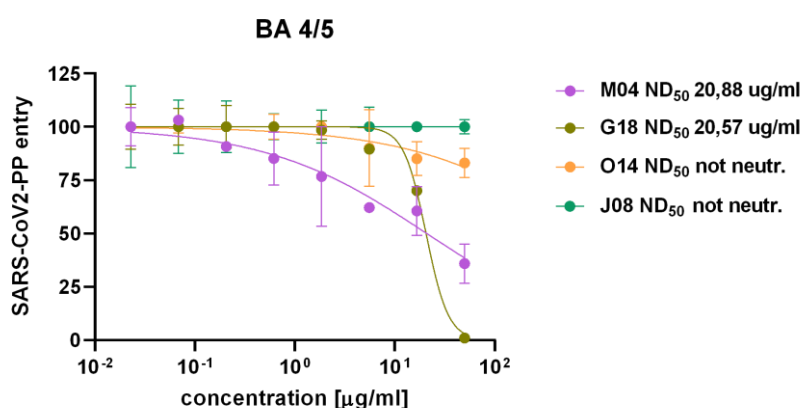

Figure 36. *Neutralization potency of J08, M04, G18 and O14 mAbs on SARS-CoV-2 pseudotyped Omicron variants.* *Neutralizing curves of mAbs against pseudotyped SARS-CoV-2 variants. The initial concentration for each sample was 10 μg/ml, followed by 3-fold serial dilutions. Data are representative of at least two independent experiments. mAb G18 shows high neutralization activity versus all the Omicron variants tested, compared to O14 and M04 (B, D) which lost their ability of neutralization versus the BA.2.12.1 and the BA.2 and BA 2.12.1, respectively.*

Only a few months after BA.1, almost at the same time as sublineage BA.2.75, BA.4 and BA.5 began to emerge in South Africa. These two variants show mutations in the S gene more similar to BA.2 than to the BA.1 strain, and carry specific mutations such as F486V, a new mutation that is only

present in these new variants, and a mutation identified as L452R, which has previously been reported in the Delta variant.

Since the L452R mutation is known to boost SARS-CoV-2 fusogenicity and infectivity[145], we tested mAb candidates on these variants.

When the antibodies were tested on these new pseudotyped viruses, their neutralising power was significantly reduced. The initial test was conducted as described above starting from 10 μg/ml; however, in this case, no neutralising activity was detected. Consequently, I increased the initial concentration to 50 μg/ml. I observed weak neutralising activity in the case of the M04 and G18 antibodies. J08 completely lost activity, as expected, and even for the O14 antibody the additional mutations present in Omicron BA 4/5 were deleterious **(Figure 37)**.


Figure 37. Loss of neutralization potency of J08, M04, G18 and O14 mAbs on SARS-CoV-2 pseudotyped Omicron BA 4/5 variants.* *Neutralizing curves of mAbs against pseudotyped Omicron BA 4/5 SARS-CoV-2 variants. The initial concentration for each sample was 50 ug/ml, followed by 3-fold serial dilutions. Data are representative of at least two independent experiments. mAbs M04 and G18 showed minor neutralization activity versus the Omicron variant tested, compared to O14 and J08 which lost their ability to neutralize variants B 4/5.*

These were the first results of a comprehensive investigation of these surging Omicron subvariants using the pseudotyped viruses library. When it comes to mAbs derived from vaccinated and boosted individuals, BA.2.12.1 is just slightly more resistant than BA.2, but BA.4/5 is significantly (2-fold) more resistant in the case of G18 mAb. Both BA.2.12.1 and BA.4/5 include a mutation at spike residue L452, which makes it easier to evade some antibodies that target the so-called class 2 and 3 areas of the receptor-binding domain. Although the F486V mutation in BA.4/5 reduces spike affinity for the viral receptor, it makes it easier to evade some class 1 and 2 antibodies, such as M04 and J08 antibodies here presented. Conversely, the R493Q reversion mutation increases the fitness of BA.4/5 by restoring receptor affinity, explaining its resistance to a broad class of antibodies.

2.2.4 Hybrid Cohort antibodies present very low broad-neutralization versus SARS-CoV-1 virus

From the moment we documented how significantly the Omicron variants affected the antibodies obtained from the convalescent donors cohort and the Hybrid cohort, we decided to evaluate if a third booster dose would improve the ability of nAbs to recognize and cross-neutralize the distantly related SARS-CoV-1 virus. Two of the four SN3 donors exhibited nAbs able to bind SARS-CoV-1 spike protein (Chapter 1, **Figure** 11). However, only 2.4% (5/206) and 0.9% (2/206) of all nAbs were able to bind the SARS-CoV-1 S protein and neutralize this sarbecovirus respectively, showing a lower frequency than the one observed in SN2 and SP2 nAbs **(Figure 38)**.
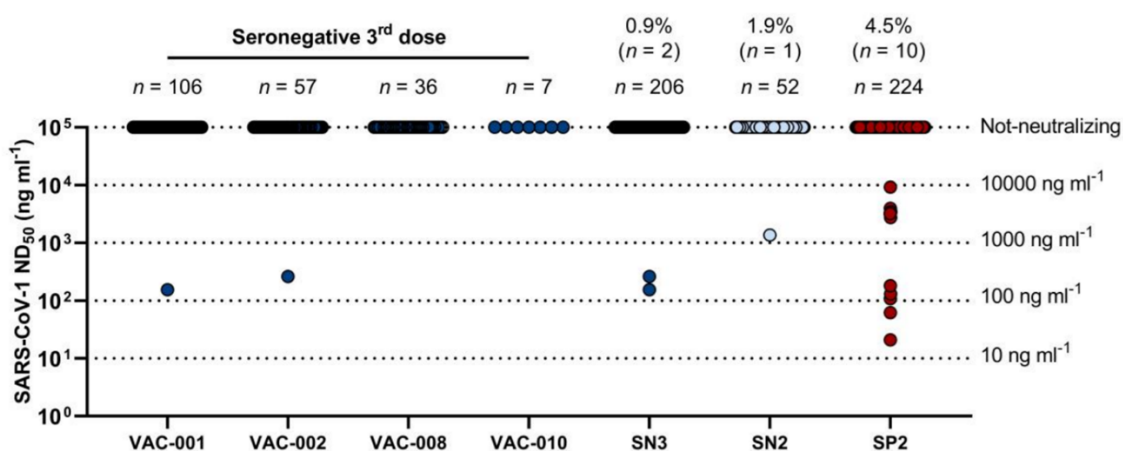
Figure 38. Functional characterization of SARS-CoV-1 nAbs. *Dot chart shows the neutralization potency, reported as 50% neutralizing dilution (ND$_{50}$ ng ml−1) of 57 nAbs isolated from SN3 (dark blue), SN2 (light blue) and SP2 (red), donors from the Hybrid Cohort. The number and percentage of nAbs from individuals who were seronegative and seropositive and neutralization ND$_{50}$ (ng ml−1) ranges (black dotted lines) are represented on the graph.*

2.2.5 Pseudotyped viruses platform to identify broadly neutralizing antibodies from Super Hybrid Cohort

The rising prevalence of variants of concern, such as the Omicron BA.2 and BA.4/5 strains that are partially resistant to the majority of vaccines and antibody therapies now on the market, has hindered the development of broad tools and strategies against SARS-CoV-2 [23,24].

Due to the ability of the Omicron variant sublineages to evade antibodies, in early 2023 we decided to carry out a study to examine the activity of mAbs isolated from donors who had previously received an mRNA vaccination and booster shot with the WT spike variant in addition to infections caused by the Omicron variants (Super Hybrid cohort). The SARS-CoV-2 virus has grown more transmissible and immune-evading from the Wuhan strain to the dominant Omicron strains of today. The ability of many mAbs to neutralise novel variants has been mostly or completely lost, including approved therapeutic ones that used to neutralise earlier variants. Therefore, the development of widely neutralising antibodies against the current Omicron variations and, hopefully, future variants that evolve is imperative. Moreover, it is possible for additional zoonotic coronaviruses to spread from their animal hosts and infect people. For instance, two coronaviruses that were previously only associated with animal infection—including a distantly related deltacoronavirus—were discovered in people who had flu-like symptoms lately [25,26]. These findings emphasise the need of focusing on antibodies directed versus potential conserved regions of coronaviruses that are less likely to mutate and can be functionally crucial.

To study the potential cross-reactivity of these antibodies with the several SARS-CoV-2 variants and the other human-coronaviruses, we performed a memory B cell screening using peripheral blood mononuclear cells collected from patients which had a history of COVID-19 first infection, SARS-CoV-2 vaccination plus Omicron breakthrough infection (*Super Hybrid Cohort*).

We chose to use a slightly different workflow in this instance than the one previously described in this thesis because, for this cohort, we had access to a larger library of live SARS-CoV-2 viruses in BSL3, ranging from the Wuhan variant to the most recent XBB 1.5 variant. As a result, the pseudotyped viruses SARS-CoV-2 library was not necessary for the screening or the neutralisation assays in the current study; for this first screening, the SARS-CoV-1 pseudotyped library and the pseudotyped viruses' libraries of the other four h-CoVs were actually required.

After collection of the PBMC of the donors, we conducted two main screenings: the first one was performed using the live Wuhan SARS-CoV-2 virus and in parallel the isolated S-protein⁺ MBCs were screened using SARS-CoV-1 pseudotype virus **(Figure 39).**

By following this strategy, we were able to concentrate our attention on the most broadly screened antibodies in the first step, and only those antibodies that showed promise in neutralising the Wuhan virus were the focus of the subsequent small-scale expression. Furthermore, early SARS-CoV-1 screening with pseudotype virus enabled us to promptly detect potential cross-neutralizing mAbs (when they demonstrated effectiveness against both tested viruses).
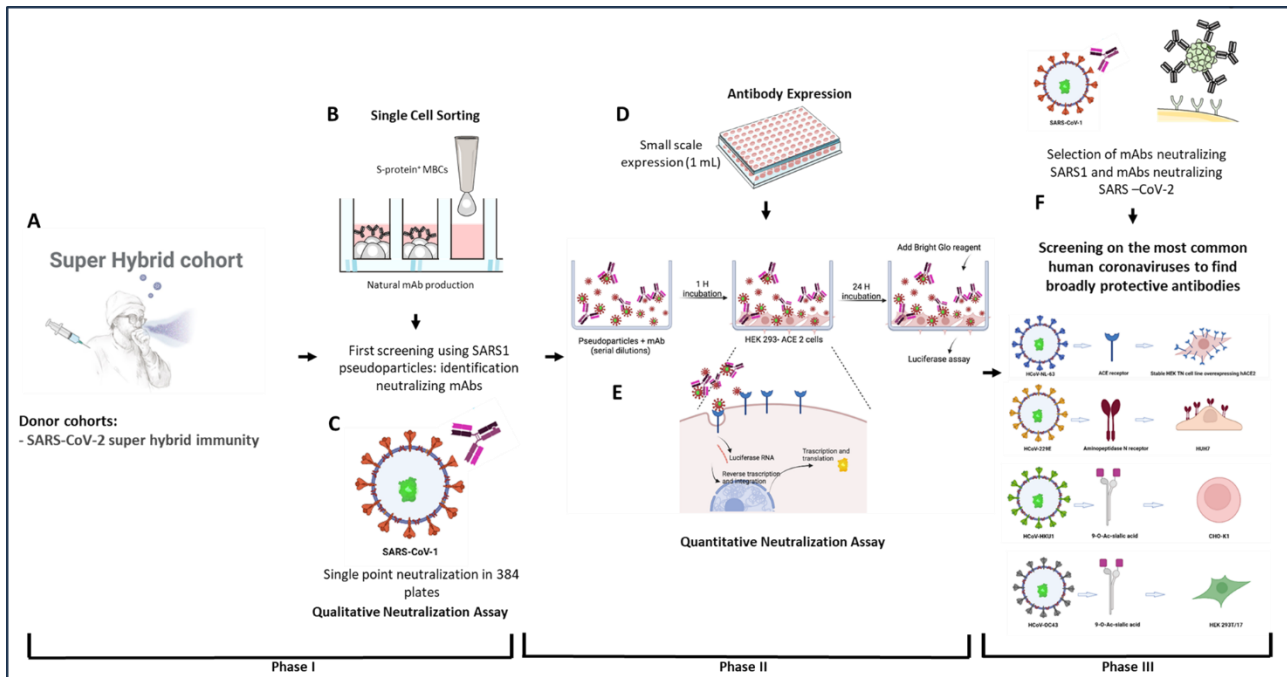
Figure 39. **Workflow for Super Hybrid Cohort screening.** *Samples were collected from Super Hybrid Cohort donors, presented by six COVID-19 convalescent donors who had the Covid-19 infection twice, vaccinated with 3 doses of BNT162b2 mRNA vaccine.*

*In Phase I memory B cells were single-cell sorted for a total of 6,001 cells (**A**) and following 2 weeks of incubation, antibodies were screened for their neutralization efficiency versus the SARS-CoV-1 pseudotype virus and in parallel versus the Wuhan Sars-CoV-2 virus (**B**).*

*Once neutralizing monoclonal antibodies (nAbs) were identified (n = 556) (**C**), phase II started. All specific mAbs were expressed on a small scale using 1ml of cell culture medium for each antibody (**D**), and subsequently they were tested against the SARS-CoV-1 pseudotype virus in a quantitative assay (**E**). At the same time, the same nAbs have been tested again on the SARS-CoV-2 live virus to identify their neutralization potency. Phase III starts with the identification and selection of the most promising mAbs able to neutralize SARS-CoV-2 and SARS-CoV-1 individually, and their screening on the h-CoV pseudotyped viruses library, specifically OC43 virus, HKU-1 virus and E229 virus (**F**). Finally, the most potent antibodies were identified and tested in synergy to detect possible synergic effect in combinations.*

2.2.6 Optimization of SARS-CoV-1 pseudotype virus assays in 384-well plates

The initial goal was to switch from utilising 96-well plates for the neutralisation experiments using SARS-CoV-1 pseudotype virus to 384-well plates; PBMC were sorted and stimulated for their maturation in 384-well plates, so it was suitable for the assay to simply transfer the supernatants into the new plate where SARS-CoV-1 pseudotype virus and hACE2 cells were seeded. As the neutralisation assay had previously required the use of 96-well plates, I optimized the protocol with this purpose.

The final volume containing the mAbs to test, the cells and the pseudotype virus was modified so that the final MOI ratio for infection was not changed.

81

We wanted to use as little as possible of the supernatant, so also the volume of supernatant to use was optimized to make the assay sensitive with no waste of materials.

The test was conducted using mAb S309, which was known as able to neutralize SARS-CoV-1 live virus and pseudotype virus, as a control [146].

According to the findings (**Figure 40**), the 384-well test was sufficiently sensitive to carry out qualitative screening on supernatants, although it may be slightly less sensitive than the 96-well plate assay.
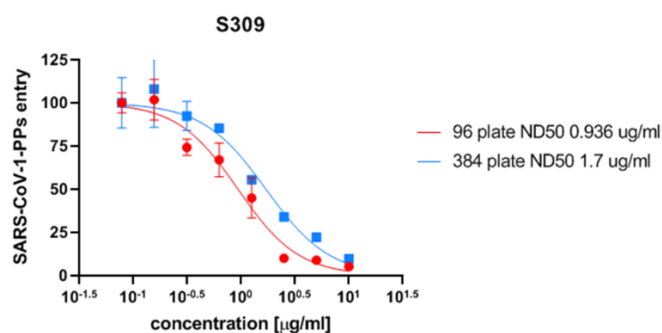
Figure 40. Optimization of pseudotype virus assays in 384-well plates. *The graph reports the mAb S309 [146] tested on SARS-CoV-1 pseudotype virus. S309 was tested in 3-fold dilutions in plate starting in both cases from 10 µg/ml. The two slopes here presented show the same profile, although in 384-well plate (blue coloured slope) there seems to be more background which may impact the final reading of the plate. Since the test to be carried out in 384-well plate involved a qualitative type of response, in this case this reduced sensitivity of the assay was negligible, also because the neutralization detected was able to reach up to about 1.7 µg/ml, well below what is normally expressed as antibodies in sorting plates.*

2.2.7 Qualitative screening of sorted supernatants of Super Hybrid Cohort subjects using SARS-CoV-1 pseudotype virus

A qualitative screening using SARS-CoV-1 pseudotype virus in 384-well plates was conducted. I assessed the neutralizing capacities of the antibodies present in the sorting plate derived from each subject using the SARS-CoV-1 pseudotype virus neutralization assay previously validated.

Most of the antibodies tested showed no inhibitory activity against SARS-CoV-1 pseudotype virus, only few of them had a good detectable responses, but the inhibition rates did not reach more than 80% with respect to mAb S309 used as a positive control **(Figure 41)**.

A total of 29 neutralizing antibodies were detected from this first qualitative screening; the percentage referred to the total antibodies screened is very low, but this data are not so surprising compared to the literature were the majority of SARS-CoV-1 neutralizing antibodies were isolated from patients with a previous history of SARS-CoV-1 infection [146,147].

On the other hand, remarkably, in our study some donors provided antibodies capable of neutralizing SARS-CoV-1 virus.
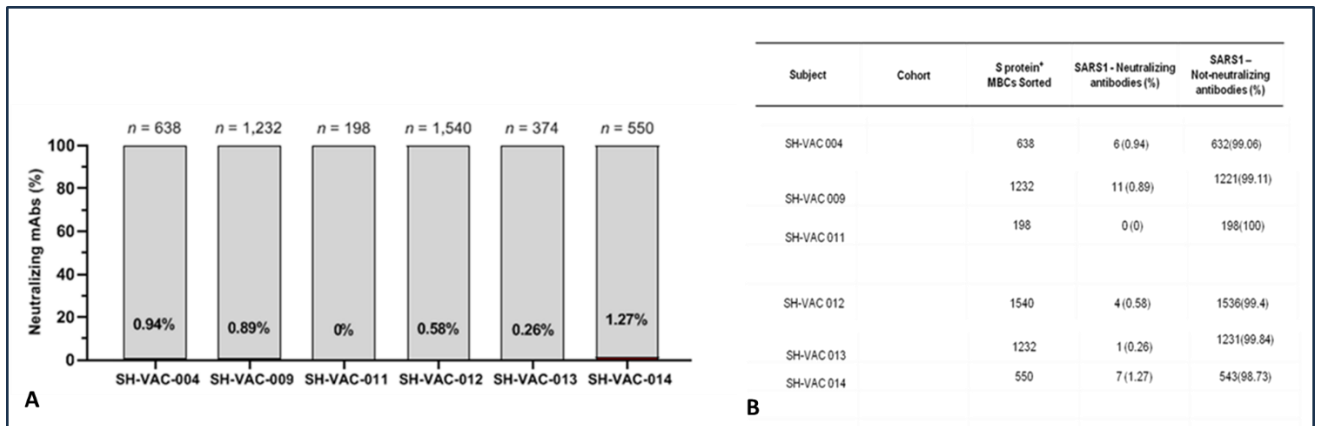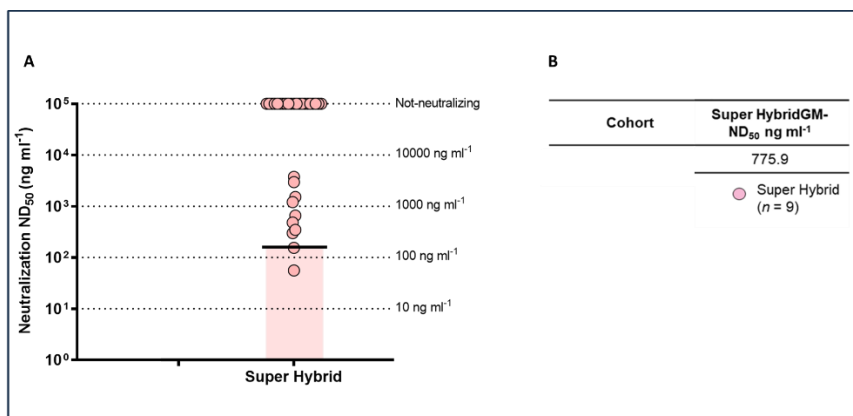
Figure 41. Positive antibodies anti SARS-CoV-1 pseudotype virus isolated from Super Hybrid Cohort. *In the graph (**A**) are reported the single percentage of antibodies able to neutralize SARS-CoV-1 pseudotype virus for each subject. In the Table on the right (**B**) is specified the number of the antibodies detected compared to the total number of PBMC sorted for each subject.*

2.2.8 Validation of neutralization potency of the antibodies identified versus SARS-CoV-1 pseudotyped virus

Following the identification of antibodies neutralizing SARS-CoV-1 virus pseudotype virus, the same antibodies were expressed in a small volume and tested in plate following 3-fold dilution to appreciate their neutralizing ability **(Figure 42)**.

As expected, most of the antibodies tested were able to neutralize SARS-CoV-1 pseudotype virus at a very high concentration, above 10 μg/ml, so we decided to classify this group of antibodies as not neutralizing. Nine other antibodies displayed a different neutralisation profile, with minimum neutralising concentrations ranging from tens of nanograms to one microgram. In addition to its capacity to neutralise SARS-CoV-1 (56 ng/ml), one antibody, known as mAb O07, merits special attention because it was found to be effective against all the SARS-CoV-2 variants, even at concentrations that varied by several hundred nanograms per millilitre. (further neutralization curves from this dataset are available in Supplementary Figure S1).

Figure 42. Neutralization potency of antibodies anti SARS-CoV-1 pseudotype virus. *In the Graph each dot corresponds to the specific antibody tested in the neutralization assay (**A**); many of the antibodies demonstrated a very low capacity of neutralization, while the average of the other 9 neutralizing antibodies is summed up in the Table (**B**) corresponding to 775.9 ng/ml. Just one antibody showed a very high neutralization potency: around 56 ng/ml. Data are representative of at least two independent experiments.*

2.2.9 Neutralization activity of cross-neutralizing mAbs on OC43, HKU-1 and 229E HCoV pseudotyped viruses

Since this Super Hybrid Cohort proved the presence of several broad-neutralizing antibodies against SARS-CoV-1, we decided to conduct an ELISA assay using the different spike proteins of the HCoV described in Chapter 1 of the Results, to identify other possible candidates with cross-neutralization activity.

Data from ELISA screening have been reported as mentioned in the previous chapter, and in this part of the results the neutralization data provided through the use of the HCoV pseudotype virus will be described. Specifically, the following antibodies showed binding versus the corresponding spike of the HCoV reported in **Table 5.**

Table 6. Number of antibodies able to bind each spike protein tested. The table indicates the spike tested and the number of the antibodies which showed positive binding in ELISA. The last column reports the percentage referred to the total number of antibodies identified able to neutralize Wuhan live virus.

HCoV	Binder (n)	Binder (%)	Neutralizing (%)
SARS-CoV-1	20	4,8%	45,0%
229E	2	0,5%	0,0%
HKU-1	1	0,2%	100%
OC43	7	1,7%	57,1%

After assessing the binding, we wanted to investigate whether the panel of mAbs identified could show neutralization activity versus lentiviral HCoV pseudotyped viruses.

HKU-1, 229E and OC43 pseudotyped viruses were incubated for one hour at 37°C together with the corresponding antibodies, prior to the addition of target cells. The neutralization of entry was inspected as a reduction in luciferase signal after 24h of incubation at 37°C.

For OC43 pseudotype virus, since I did not make the final construct but as previously reported the final supernatant was sent to us, I followed a protocol which included a longer time of incubation before reading the plate, about 48h of incubation [141].

The ND50 values for each sub-group against these PVs are shown in **Figure 43**, allowing to evaluate how, in each group, neutralisation is present but cannot be clearly detected at concentration in the nanogram/ml range by any antibody (further neutralization curves from this dataset are available in Supplementary Figure S2).
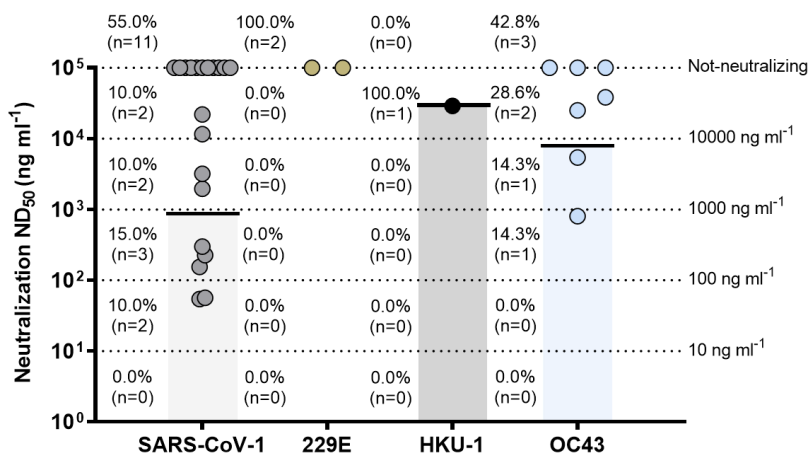
Figure 43. Neutralization potency of antibodies anti HCoV 229E, HKU-1 and OC43 pseudotyped viruses. *In the Graph each dot corresponds to the specific antibody tested in the neutralization assay; all the antibodies show neutralization versus the virus when used at very high dose, in the range of μg/ml.*

In each group, about 2 antibodies totally lost their ability of neutralizing the corresponding pseudotyped viruses for which they were testing for. Compared to the total percentage of neutralizing antibodies isolated, for each HCoV very few antibodies have been shown to retain potent neutralizing activity.

Table 7. Summary of the final data obtained from several neutralization assays using different preparations of pseudotyped viruses. Although the neutralizing activity is maintained relatively to the binding capacity of almost each mAbs, the neutralization observed was very low.

HCoV	Binder (n)	Binder (%)	Neutralizing (n)	Neutralizing (%)
SARS-CoV-1	20	4,8%	9	45,0%
229E	2	0,5%	0	0,0%
HKU-1	1	0,2%	1	100%
OC43	7	1,7%	4	57,1%

Specifically, the most potent antibodies were identified in the previously described SARS-CoV-1 group. For the remaining 3 groups, we were unable to identify enough neutralizing antibodies among the binders to be exploited for further investigation as potential cross-neutralizing mAbs for use in the clinic.

2.2.10 Identification of two broad-neutralizing antibodies against SARS-CoV-2 variants and some of the other Human Coronaviruses

When tested in neutralisation in BSL3 with various SARS-CoV-2 variants (BA.5, BA 2,75, BF.7, BQ 1.1, XBB 1.5, EG.5.1.1, BA 2.86) mAb 4 shown an outstanding reaction against each one, making it a remarkable antibody (data not reported). To determine whether it had cross-neutralizing activity versus other viruses, we decided to examine its activity on the other HCoV pseudotype virus available as well as pseudotyped SARS-1 viruses. Unexpectedly, although in ELISA this antibody presented binding with the spike of HKU-1 and 229E, in neutralizations with the corresponding pseudotyped viruses its activity was not as dramatically evident as against SARS-CoV-2 variants. (**Figure 44**).
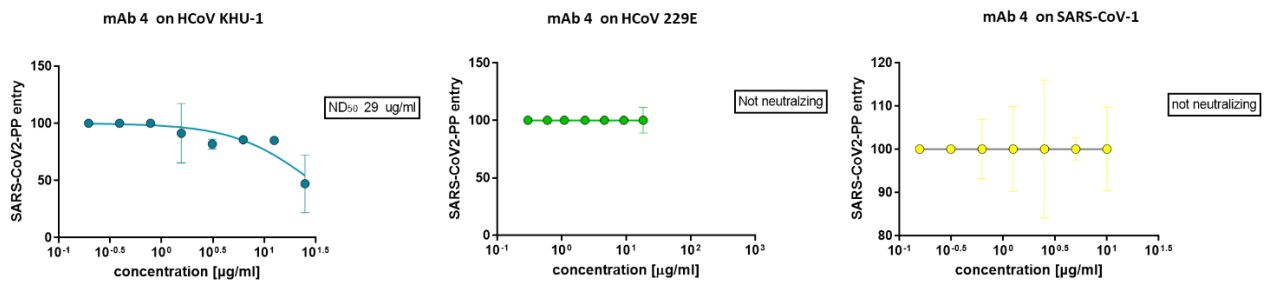

Figure 44. Neutralization data of mAb 4. *The two graphs report the neutralization potency of mAb 4 when tested on the Alpha coronavirus 229E and the two Beta coronavirus HKU-1. This mAb can neutralize only the HKU-1 pseudotype virus, and the concentration required to get the ND50 is really different between the HKU-1 and the 229E hCoVs, where in case of HCoV-HKU-1, is required at very high dose to exhibit its neutralizing activity, and several variants of SARS-CoV-2 live viruses, where it is functional in terms of nanograms or few micrograms. Data are representative of at least two independent experiments.*

However it was not surprising that an exceedingly wide cross-neutralising antibody could not be found: according to data published in the literature [147,148], antibodies that can neutralise both beta- and alpha-coronavirus at extremely low doses are extremely rare. Nevertheless, the fact that we

were able to identify an antibody from such a small number of subjects that can still neutralise various viruses is a crucial discovery that helps us understand how immunity develops after vaccination and infection with variant differences.

As previously reported, nAb 1 was one of the mAbs with strong action against SARS-CoV-1 pseudotype virus. This mAb was selected for further in-depth characterization since it was found to have a good neutralising capacity on SARS-CoV-2 variants of concern including BA.5, BA 2.75, BF.7, BQ 1.1. and XBB.1.5. Its neutralization efficiency appeared to be even higher when applied to SARS-CoV-1 PVs. (**Figure 45**). Regretfully, though, this antibody was evidently unable to neutralise any h-CoVs or bind any of their spike proteins (data not shown).
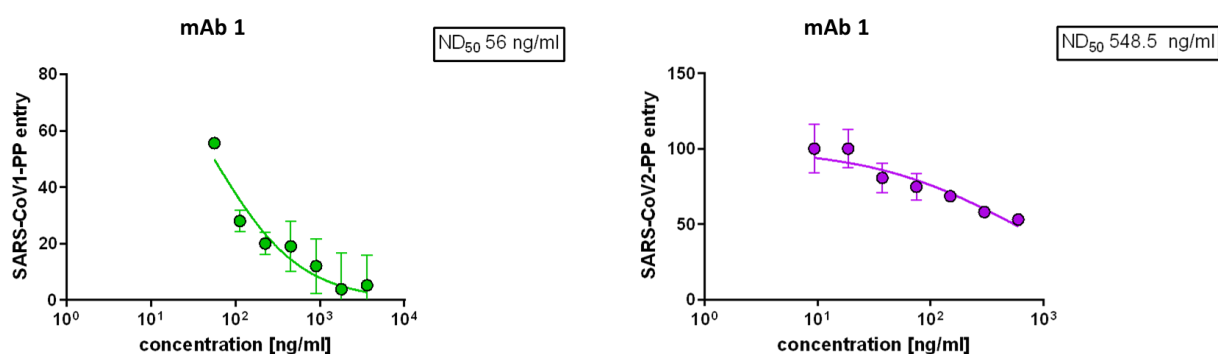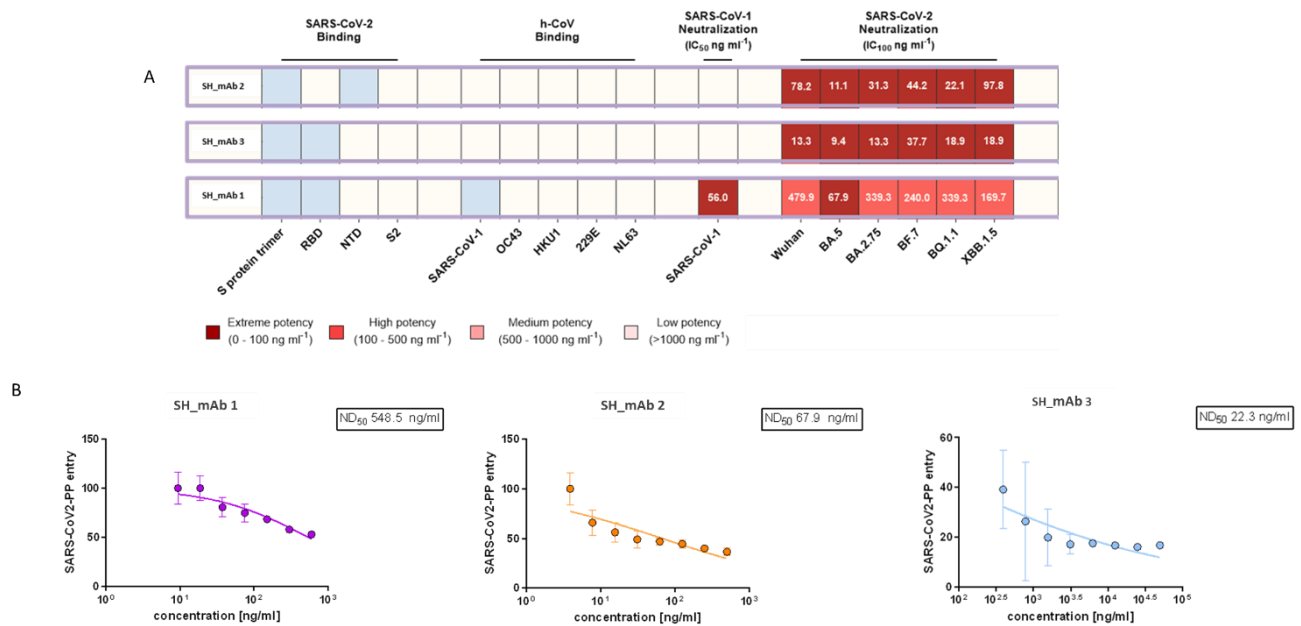

Figure 45. Neutralization potency of mAb 1 on SARS-CoV-1 and SARS-CoV-2 coronaviruses. *mAb 1 was firstly identified as one of the mAbs able to neutralize, in 384-well plate, SARS-CoV-1 pseudotyped viruses. When investigated more, once it was expressed in HEK293 cells, it confirmed its ability of neutralization (**A**) and compared to Wuhan virus (**B**) demonstrated a higher ability of neutralization on SARS-CoV-1 pseudotype virus.*

This broad spectrum defines mAb 1 and mAb 4 as potential attractive agents to fight the challenge of viral escape mutations and manage with a possible new coronavirus outbreak in the future. The neutralizing potency of mAb 1 against SARS-CoV-2 is lower than that some of other potent RBD-antibodies identified in our study from Super Hybrid Cohort (reported in Chapter 4). This phenomenon is consistent with influenza virus, in which the neutralizing potency of antibodies targeting the conserved haemagglutinin stem region is lower than the ones targeting the head region [149].

2.2.11 Establishment and validation of the most potent antibodies from Super Hybrid Cohort on Wuhan pseudotype virus of SARS-CoV-2

From the massive screening which has been conducted in BLS3 using several SARS-CoV-2 viruses available in each variants, three antibodies were selected for more detailed analysis. We observed that mAb 2, mAb 3 and mAb 1 could neutralize all the pseudotyped SARS-CoV-2 Wuhan virus in a

very similar range compared to the neutralization on the live virus (**Figure 46B**). Since pseudotype virus allow for more specific characterization assays than live virus, it is crucial to compare classical neutralisation and neutralisation on pseudotype. Additionally, it is essential to consider whether the level of neutralisation observed is comparable between the two different assays. With very little deviations in the final observed neutralising concentrations, the level of neutralisation in the two assays is entirely equivalent for these three antibodies (as well as all the antibodies previously described in this chapter).

A

| | SARS-CoV-2 Binding | | | | SARS-CoV-1 | h-CoV Binding | | | | SARS-CoV-1 Neutralization (IC_{50} ng ml^{-1}) | SARS-CoV-2 Neutralization (IC_{100} ng ml^{-1}) | | | | | |
	S protein trimer	RBD	NTD	S2	SARS-CoV-1	OC43	HKU1	229E	NL63	SARS-CoV-1	Wuhan	BA.5	BA.2.75	BF.7	BQ.1.1	XBB.1.5
SH_mAb 2											78.2	11.1	31.3	44.2	22.1	97.8
SH_mAb 3											13.3	9.4	13.3	37.7	18.9	18.9
SH_mAb 1										56.0	479.9	67.9	339.3	240.0	339.3	169.7

Extreme potency (0 - 100 ng ml^{-1}) High potency (100 - 500 ng ml^{-1}) Medium potency (500 - 1000 ng ml^{-1}) Low potency (>1000 ng ml^{-1})

B

SH_mAb 1 — ND_{50} 548.5 ng/ml

SH_mAb 2 — ND_{50} 67.9 ng/ml

SH_mAb 3 — ND_{50} 22.3 ng/ml

(graphs: SARS-CoV2-PP entry vs concentration [ng/ml])

Figure 46. Neutralization comparison between live virus and pseudotype virus neutralization. *Each antibody is reported with the corresponding neutralization IC_{100} in the table (A). The same antibodies tested in neutralization using SARS-CoV-2 WT pseudotyped virus are reported in the graph (B), with the corresponding ND_{50} described. The concentration identified for each assay are closely comparable.*

2.3 Discussion

Since SARS-CoV-2 variants are extremely hazardous coronaviruses, research with these viruses must be conducted in a biosafety level 3 laboratory with the appropriate qualifications. This requirement can slow the development of new drugs and vaccines. An alternative to actual viral neutralisation assay is represented by pseudotype virus neutralisation assay based on retroviruses or HIV backbones. These can be safely utilised and are convenient for drug screening and vaccine evaluation. The expression level of the viral envelope protein, the ratio of packaging plasmid combinations, the effectiveness of plasmid transfection, the growth state of HEK293TN cells prior to transfection, and the time interval between collecting pseudotyped viruses supernatants are just a few of the numerous variables that influence the packaging efficiency of PVs.

In this second chapter of the results, I have described how a screening platform composed of different types of pseudotyped viruses, related to SARS-CoV-2 and its variants, and also to other HCoVs, is now available in our laboratory thanks to these optimized experiments. Protocols for developing different envelopes so that the pseudotype virus coat could be modified, were optimized and led to the development and use of the lentiviral vectors of interest.

As a final outcome, we have developed a quick and effective system for evaluating the functional and antigenic impact of SARS-CoV-2 spike mutations.

This pseudoplatform system allows mapping of escape mutations from antibodies targeting any region of the spike and can be used as a first step to determine how mutations in the spike affect cell infection. Moreover, we demonstrated that our approach measures the impact of spike mutations on antibody neutralisation directly and that these results agree closely with conventional live virus neutralisation assays.

The process I describe here to create a lentiviral particle envelope through mutagenesis and pseudotyping may also be readily transferred to any virus that has an entrance protein amenable for lentiviral pseudotyping. This group of viruses comprises other coronaviruses, such as arenaviruses, ebolavirus, influenza viruses, filoviruses, and henipaviruses, all of which present a mechanism of receptor-binding and guaranteed by fusion proteins for which lentiviral pseudotyping. Without having to deal directly with the pathogenic virus, pseudotypes-based research offers a secure method of studying cellular infection and antibody neutralisation.

Having the ability to create many envelopes and alter them by introducing the desired mutations to achieve the target VOC is significantly beneficial in the case of the SARS-CoV-2 virus since it could provide valuable information for antigenic surveillance and vaccine design since the spike protein is the leading target of neutralizing antibodies.

I was able to demonstrate the effectiveness of a neutralisation assay to measure the various antibodies' neutralising ability against the H-CoV and SARS-CoV-2 pseudotype virus.

Using this methodology, it has been evaluated the effectiveness of using pseudotype virus systems to accelerate the creation of vaccines that would quickly protect populations against extremely harmful viruses.

Certain neutralising mAbs tested on SARS-CoV-2 and SARS-CoV-1 pseudotype virus, obtained from donors who have been passively or actively immunized versus SARS-CoV-2 virus, probably targeting

the conserved epitope of SARS-CoV-2, have been demonstrated to effectively cross-neutralize SARS-CoV-2 variants and SARS-CoV-1 pseudotype virus, confirming some data already showed by previous researcher [150] .

The viruses SARS-CoV and SARS-CoV-2 are both members of the Adenoviridae genus and family, which is related to the Coronavirus family. The N protein of SARS-CoV-2 virus has 90.52% homology with SARS-CoV, the S1 subunit has 64% homology with SARS-CoV, and the S2 subunit has 90% homology with SARS-CoV [55]. SARS-CoV-2 shares 79.6% sequence identity with SARS-CoV [129] . Both viruses utilize ACE2 as a receptor-entry for their host cell.

Based on all of this information, we can conclude that neutralising cross-antibodies can be obtained from convalescents who have contracted SARS-CoV-2 or, alternatively, from SARS-CoV-1; however, it is unlikely that these antibodies will be found in people who have not contracted these particular viruses or who have only ever been impacted during their lifetime by seasonal factors associated with the most significant HCoVs.

When evaluating the activity of the cross-neutralizing antibodies found, results demonstrated that anti-SARS-CoV-2 antibodies had a degree, although very low, of cross-reactivity against anti HKU1, OC43 and 229E pseudotyped viruses, probably indicating that HCoV-HUK1 and HCoV-OC43 antigens were similar to SARS-CoV-2 antigens: they have the ability to induce SARS-CoV-2 to produce antibodies against S protein and cross-react with it. Regarding the binding profile, the link between these antibodies and NL63 was very poor, so we decided not to investigate any further.

Regarding the different cohorts analyzed, in our study for the Hybrid Cohort we found that the third dose of mRNA vaccine induces an immune response similar to the immunity observed in people vaccinated after SARS-CoV-2 infection. The characteristics of this antibody response include a slight rise in antibodies that bind to S proteins, a significant increase in neutralising potency, and a noticeable increase in antibodies that can cross-neutralize newly developing variants, such as Omicron BA.1 and BA.2. The increased potency and breadth are due to a significant expansion of S protein-specific MBCs, which in subject with three vaccines doses is even higher than that observed in subjects with a vaccine dose plus an infection [125].

For this Hybrid Cohort we found that a third mRNA dose, nevertheless, did not elicit a robust response against the distantly related SARS-CoV-1. This suggests that additional doses of homologous vaccines against SARS-CoV-2 will concentrate the antibody response against this virus rather than extending cross-protection to other coronaviruses.

Super hybrid cohort (SH) antibodies likewise for the antibodies from the other cohorts, are particularly specific for SARS-CoV-2; on the other hand, this cohort shows the strongest and variants resistant neutralizing antibodies among the different cohorts tested.

The two neutralising antibodies that demonstrated a broad neutralising capacity against other h-CoVs, however moderate (except for mAb 1 for SARS-1 pseudotype virus), were actually derived from these subjects from the Super Hybrid cohort.

These results are supported by the observation that the Super Hybrid Cohort subjects demonstrated significantly more positive antibodies than the Hybrid Cohort subjects did during the initial qualitative screening test on SARS-CoV-1 pseudotype virus (**Figure 8** and **11**, respectively). The main difference between these two cohorts is the second infection, hence passive immunity, experienced by the Super Hybrid cohort subjects compared to the Hybrid Cohort subjects.

The fact that the subjects contracted the SARS-CoV-2 infection in 2022 and that the infection was most likely caused similarly by an Omicron variant raises the possibility that individuals who contracted the virus from different strains and received multiple booster doses of the mRNA vaccine can develop a far broader cross-neutralizing antibodies than subjects simply convalescing from wild type infection (Convalescent Cohort) or a single infection plus two or three doses of mRNA vaccines (Hybrid Cohort).

In summary, our research offers a detailed image of the main differences between the different efficiency of the several antibodies generated by a single infection from SARS-CoV-2 virus, a single infection followed by two doses of vaccinations and a third mRNA vaccination and a subsequent infection. Although significant parallels between hybrid immunity and super hybrid immunity were noted, our analysis reveals aspects of the antibody response that is generated exclusively following a second infection and a third mRNA vaccine administration. These are significant observations that need to be considered while developing new vaccines and administering booster doses.

Taken together our research has effectively demonstrated the use and near-necessity of lentiviral pseudotype virus systems for screening the isolated antibodies to determine which is the most potent and broadly neutralising. We assessed the feasibility of using pseudotype virus in the process of antibody isolation and discovery. Applying pseudotype virus in the neutralisation assay for SARS-CoV-2, SARS-CoV-1, and h-CoVs, the pseudotype virus system demonstrated convincing results for screening and neutralisation efficacy. Furthermore, we demonstrated the effectiveness of pseudovirions to be applied in antigenic property modifications by generating the several spike variants for the SARS-CoV-2 VOCs; this can be an important aspect to consider for Spike-antigen candidate selection for a new vaccine.

Above all, the pseudotype virus system ia associated with low biosafety risk and can be handled in a biosafety level 2 laboratory. By using this approach, we could reduce the amount of time needed for screening candidate mAbs to treat disease caused by COVID-19. Application to other new emerging viruses is foreseen.

2.4 Experimental procedures

Mutagenesis of spike Envelope to generate the spike SARS-CoV-2 variants

To produce the different envelope correlate to the spike protein variants of SARS-CoV-2 lentiviral pseudotyped particles the specific *QuikChange Lightning Multi Site-Directed Mutagenesis Kit ™* was used. The primers were designed as indicated from the kit-protocol between 25 and 45 bases in length, with a melting temperature (*T*m) of ≥75°C.

Each variant was created using the opportune primers used to amplify and insert the mutations of interest in the spike del19 WT plasmid, amplified with the *Multi Site-Directed Mutagenesis Kit ™* (1 µl QuikChange Lightning Multi enzyme blend, 1 µl dNTPs (10 µM), about 1 µl of each primer and 100 ng of template).

PCR reaction was performed as follows: denaturation at 95°C/2min, 30 cycles composed of denaturation at 95°C/20 sec, annealing at 55C°C/30 sec, extension at 65°C/4 min and a final extension at 65°C/5 min. After PCR the transformation using XL10-Gold Ultracompetent Cells was performed, following the protocol described in the kit.

Production of pseudotype virus based on lentiviral vectors

To generate SARS-CoV-2 lentiviral pseudotyped particles and NL63, 229E, HKU-1 pseudotype virus, HEK293TN (System Bioscience) cells were plated in 15-cm dishes with complete DMEM medium. The following day, 32 mg of reporter plasmid pLenti CMV-GFP-TAV2A-LUC Hygro, 12.5 mg of pMDLg/pRRE (Addgene #12251), 6.25 mg of pRSV-Rev (Addgene #12253), and 9 mg of pcDNA3.1_Spike_del19 were co-transfected using a calcium phosphate transfection. pcDNA3.1_Spike_del19 (Addgene #155297), and pLenti CMV-GFP-TAV2A-LUC Hygro were generously provided by Prof. De Francesco Lab.

spike pcDNA 3.1_229E, spike pcDNA 3.1_NL63, spike pc DNA 3.1_HKU-1 plasmids were kindly gifted by Prof. Nigel Temperton.

Twelve hours after transfection, the medium was replaced with complete Iscove. Thirty hours after transfection, the supernatant was collected, clarified by filtration (0.45-mm pore -size), and concentrated using Lenti-X Concentrator. Viral PP suspensions were aliquoted and stored at -80°C. H-CoV- OC43 pseudotype virus supernatant was generously supplied ready to be used by Prof. Nigel Temperton lab, since the plasmid encoding the corresponding spike was not available.

Titration of pseudotype virus produced

Pseudotype virus preparation was tested by titration in the opportune cell line, cells were seeded at 10,000 cells/well in 24 well plates in 1 ml of complete DMEM medium. After 24 hours, cell medium is replaced with medium containing pseudotype virus preparation diluted in 6 point in 3 fold dilution, in a final volume of 500 µl for each well in the 24 wells plate. The plate was then left in incubation at 37°C for 48 hours. After 48h from the infection, medium is removed and cells are detached using 150 µl of trypsin and then trypsin is inactivated with 100 µl of Medium. The cells are then resuspended carefully and moved in a MW96 bottom plate.

Cells are centrifuged at 1500 rpm (300g) for 3 min, supernatant discarded, cells resuspended and washed with 200 µl PBS (two times). After the last washing cells are resuspended in PFA 1% and wash in PBS before the FACS analysis. The FACS analysis is conducted using as negative control cells without pseudotype virus infection; since pseudotype virus containing GFP gene, cells resulted infected when they showed fluorescence. By counting positive cells and the volume used to infect each wells and their interpolation, the final pseudotype virus titers is determined.

Neutralization pseudotype virus assays

For the neutralization assay with pseudotyped virus, each cell lines corresponded to the cell line which is more willing to be infected by each PVs, were plated 10.000/well in white 96-well plates using DMEM medium complete (10% FBS, 2mM L-glutamine, 1% Pen-strep,1mM Sodium pyruvate, 1% Non-Essential Amino Acid, antibiotic if cells presented gene-antibiotic resistance).

24h later, cells were infected with 0.1 MOI of pseudotyped viruses that were previously incubated with serial dilution of purified or not purified (cell supernatant) mAb. In particular, a 7-point dose response curve (plus PBS as untreated control), was obtained by diluting mAb or supernatant respectively five-fold and three-fold. Thereafter, nAbs of each dose-response curve point was added to the medium containing pseudotyped viruses adjusted to contain 0.1 MOI.

After 1h at 37°C incubation, 50 µl of mAb + pseudotype virus mixture were added to each well in which HEK293TN- hACE2 were seeded the day before, and then plates were incubated at 37°C for 24h. Each point was tested in triplicate.

24h later luciferase activity was measured reading the plate on Varioskan™ LUX (Thermo Scientific™) using the Bright-Glo Luciferase Assay System (Promega), according to the manufacturer's recommendations.
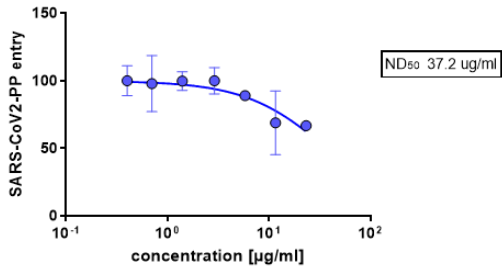
Percent inhibition was calculated relative to pseudotype virus-only control. ND_{50} (Neutralization Dose) values were established by nonlinear regression using Prism v.8.1.0 (GraphPad). The average ND_{50} value for each antibody was determined from a minimum of three independent technical replicates and two independent experiment.

For the assay conducted in 384 plates, the protocol was optimized using the same 0.1 MOI, adjusting the volume to fit the 394 wells.
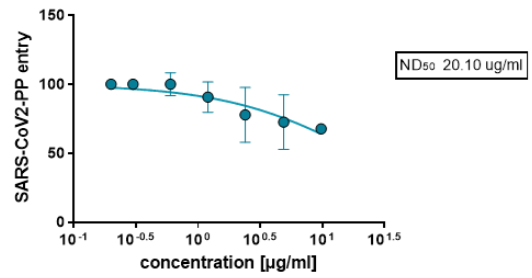
2.5 Supplementary materials
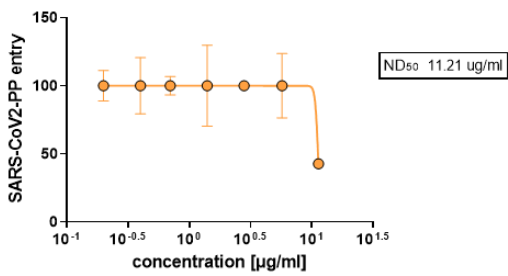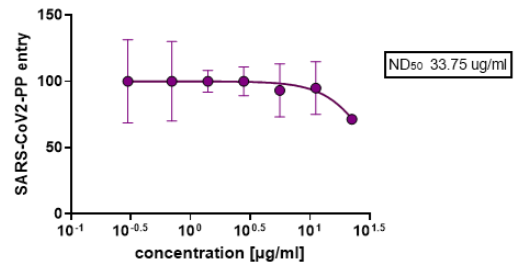
Pseudotype virus neutralization on HCoV 229 E

mAb 5

ND$_{50}$ 37.2 ug/ml

mAb 6

ND$_{50}$ 20.10 ug/ml

mAb 7

ND$_{50}$ 11.21 ug/ml

mAb 8

ND$_{50}$ 33.75 ug/ml

mAb 9

not neutralizing

mAb 10

not neutralizing

mAb 11

ND$_{50}$ 1.2 ug/ml

Positive Control mAb Cov44-62

ND$_{50}$ 5 ug/ml
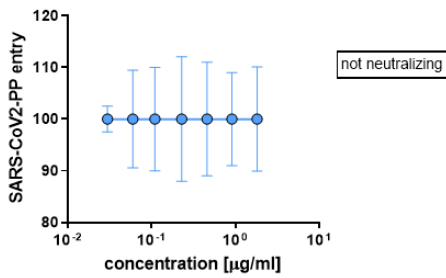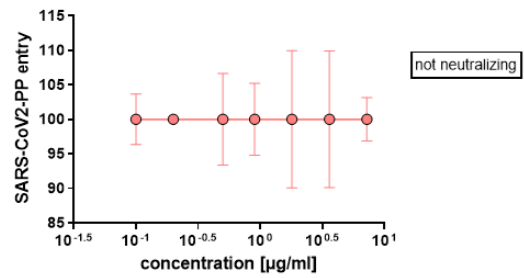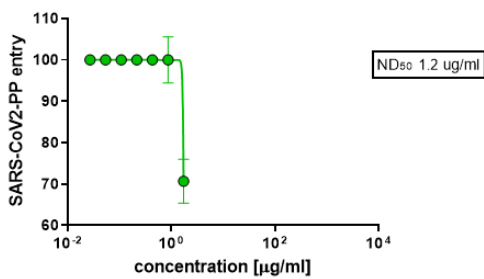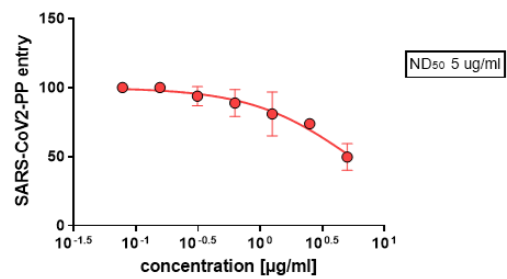
Pseudotype virus neutralization on HCoV HUK-1

mAb 5
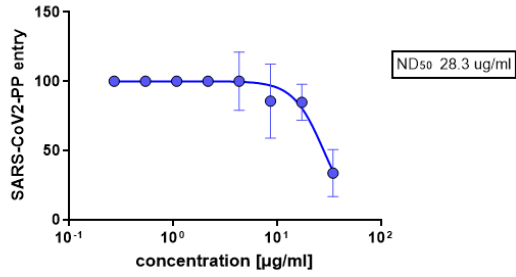
mAb 10
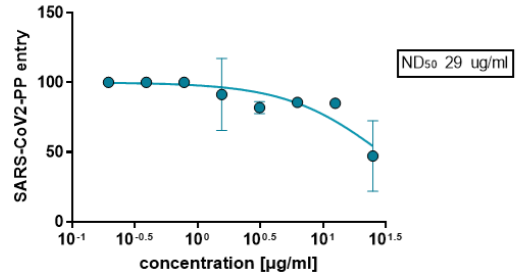
Positive Control mAb binding HKU-1
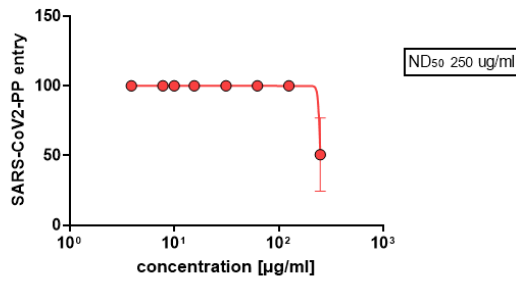
Negative Control mAb a-Shigella

Pseudotype virus neutralization on HCoV OC43

mAb 12 — NDso 51 ug/ml

Positive Control mAb Cov44-62 — NDso 103 ug/ml

Negative Control mAb a-Shigella

mAb 13 — ND50 2 ug/ml

mAb 14 — ND50 36 ug/ml

mAb 15 — ND50 0.8 ug/ml

mAb 16 — NDso 19ug/ml

mAb 10 — NDso 25ug/ml

mAb 17 — NDso 5ug/ml
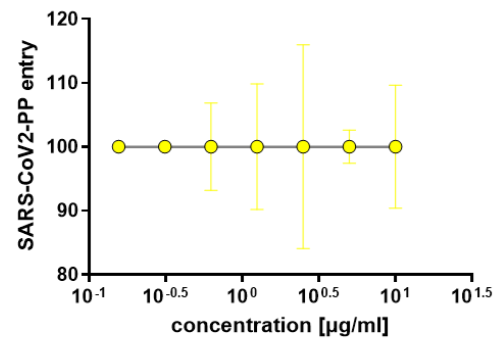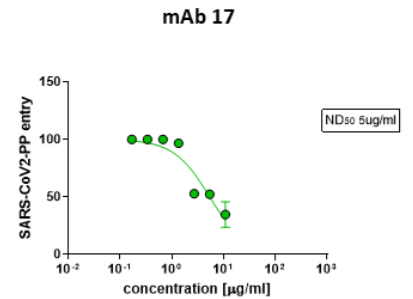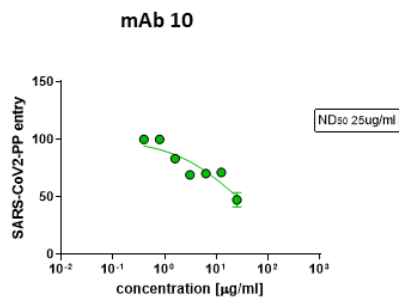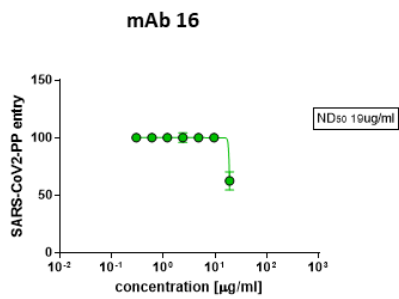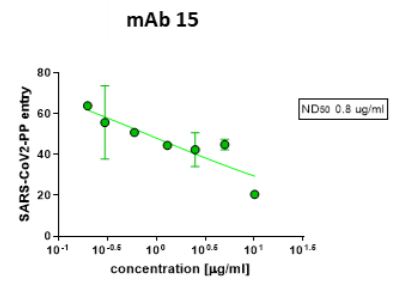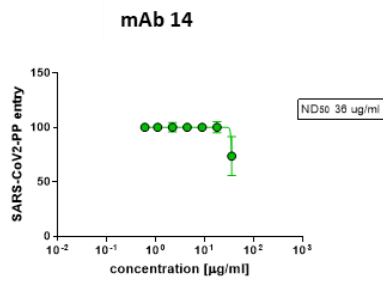
3.   Pseudotyping: measurement of synergistic neutralization by antibody combinations.

3.1 Introduction

Following the discovery of SARS-CoV-2 in Wuhan, the globe experienced a critical pandemic phase. Globally, infections have proliferated and vaccination has been identified as one of the most effective ways of preventing the epidemic. To protect citizens and combat the pandemic, governments have launched a COVID-19 immunisation programme [151][152]. Simultaneously, researchers discovered novel SARS-CoV-2 mutations that were influencing diverse pandemic epidemiological events. A few noteworthy variants have been designated as Variants of Concern/Variants of Interest (VOC/VOI) due to their increased transmissibility and higher risk of severe disease [68][153].

These VOC/VOI have mutations which confer to the virus characteristics including immune escape and decrease vaccination effectiveness[154]. Due to the significant mutations reported in the spike gene, several notable SARS-CoV-2 variants have appeared over the course of these four years.

These mutations may have altered some viral features. Pathogenicity, antigenicity, transmissibility, re-infectivity, and infectivity are a few important biological functions that may have been modified [68]. The 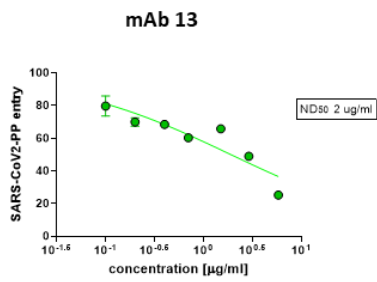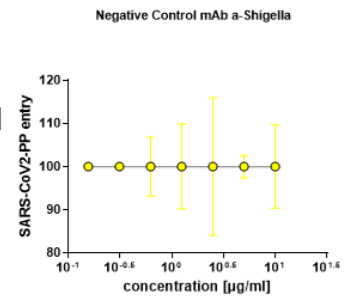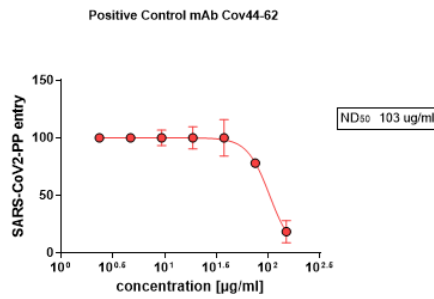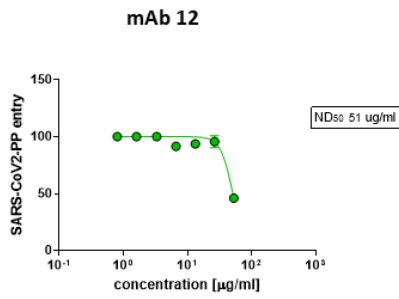D614G mutation in the S-glycoprotein, which was discovered in the early stages of the pandemic in 2020, was the first substantial mutation reported. [154,155]

The S-glycoprotein also underwent some other notable mutations responsible for the alteration of the biology of this virus. Further investigation is necessary to fully understand the significant mutations driving the emergence of these variants of SARS-CoV-2.

Every virus has the ability to mutate, which aids in its ability to elude the immune system and infect humans, as well as re-infect (infect the same patient twice or more). The term "viral escape" or "escape mutant" refers to this event [156,157] and represents an obstacle to the development of vaccines and antibodies.

Controlling this virus actually depends on studying the advent of new variations [158] and avoid their appearance. It was observed that the SARS-CoV-2 mutation rate was extremely stable at first. From December 2019 to October/November 2020, the evolution rate was estimated to be two mutations per month. Global awareness of the phenomenon was observed [159,160]. Following then, there were reports of high mutation rates, leading to the emergence of several variants. These variants are currently speeding around the globe and feature multiple notable variants [68].

Many researchers have documented the use of different nAbs in response to escape episodes caused by SARS-CoV-2 variants and their notable variants; alternatively a possible strategy to counteract pandemics caused by SARS-CoV-2 but also by other viruses worldwide would be to employ an antibody cocktail rather than a single mAb, as suggested by Xiong et al. [161].

However, the majority of the antibodies used as therapeutic treatments for Covid 19 have lost some of their potency or overall usefulness over time due to the emergence of variants, especially with the advent of Omicron. Unfortunately, even in our investigation, the introduction of various

VOCs throughout time resulted in loss of function of some mAbs that we had previously identified as possible therapeutic options.

In particular, some specific mutations present in the Omicron sublineage and first appeared in the previous VOCs, are being studied closely. In immunocompromised patients, the E484K mutation may be the cause of the immune escape occurrences [162]. A recent study remarked the antibody escape incidence using a mixture of two antibodies: this suggested that novel spike variants might trigger loss of neutralization to the antibody cocktail, representing the escape phenomenon even with combinations of antibodies[163]. Three significant mutations (E484K, K417N/T, L452R) have been reported [164]as responsible for different categories of antibody escape. It has been shown that K417N/T, present in P.1 lineage and in B.1.351 lineage, is responsible for class 1 antibody escape. Simultaneously, the E484K mutation, observed in several lineages such as B.1.526 lineage, P.1 lineage, P.2 and B.1.351 lineages, is accountable for class 2 antibody escape. Similarly, L452R spotted in the other lineages such as B.2.75 lineage and in some sequence of the BA.5 lineage is accountable for class 3 antibody escape.

In spite of these findings, using an antibody cocktail proved to be one of the most effective strategies for preventing the emergence of novel variations in immunocompromised patients.

In this Chapter, I present a matrix assay based on several papers [165] [156] and developed during my Ph.D., to test the effectiveness of a combination of antibodies, predominantly directed against the SARS-CoV-2 virus, to prevent this phenomenon and determine whether any of our antibodies could be still active if used in cocktail with a second one.

The rationale behind establishing this matrix system is to not rule out the use of an antibody that may have worked well against one variant but whose efficacy wanes with the emergence of another. In fact, it becomes apparent how some mutations disappear during the evolution of the variants and then reappear years later with a different variant. The purpose of developing a mAb cocktail for prevention and/or therapy is to identify antibodies that are effective when used alone to neutralise single point mutations, which are perhaps the most common, and then to combine them, so that we can neutralise the spike protein on different epitopes. In this way we could thereby neutralise the virus by preventing the formation of escape mutants and consequently new variants.

The ultimate objective of the work is to accurately determine the neutralisation value of a pair of antibodies on specific VOCs to evaluate them for possible clinical development.

3.2 Results

When the Omicron variant appared, the J08 nAb, isolated in 2020 from convalescent patients and which showed a high neutralization ability versus the spike VOCs emerged until that moment, was in Clinical Phase III. When tested on Omicron BA.1 variant pseudotyped and then live virus, it revealed total loss of function: the clinical trial was therefore interrupted.

3.2.1 J08 mAb does not improve its efficacy when used in combination with M04

The first data that we wanted to obtain was the possible use of J08 in combination with a second mAb, in order to continue to use it for emergency purposes. To verify this possibility, we decided to exploit a synergy assay to verify if these mAbs could synergize for virus neutralization, a phenomenon previously reported for SARS-CoV mAbs [165].

I started to compare J08 mAb against the other three preferred mAbs that were recovered from the Hybrid Cohort and previously mentioned (M04, G18, and O14) in Chapter 2 of the Results. Combination responses were tested (**Figure 47**); virus neutralization was measured in a classical luminescence reduction neutralization test. The test was conducted using SARS-CoV-2 BA.1 pseudoparticles on a hACE2 cell culture monolayers and these experimental values were compared with the expected responses calculated by synergy scoring models [157].

Unfortunately, the combination revealed that the cocktail of J08 + M04 on BA.1 variant was not synergistic (**Fig. 47B**) (with a synergy score of 3,071, where any score >10 indicates synergy).
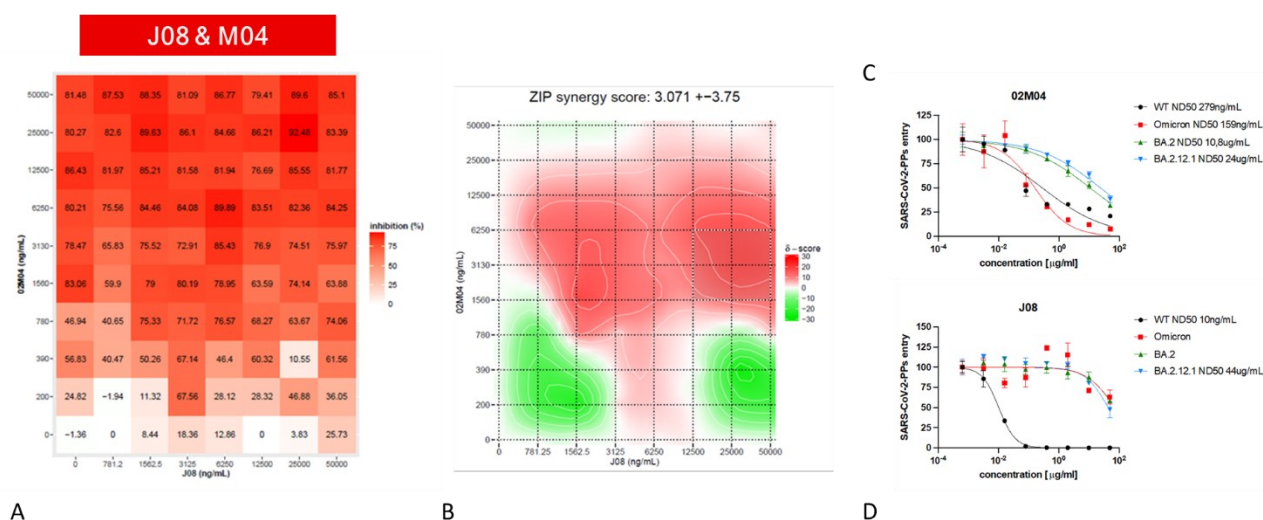
Figure 47. Evaluation of J08 and M04 neutralization activity against SARS-CoV-2 BA.1 pseudotype virus. *A.* Neutralization dose–response matrix of BA.1 variant from SARS-CoV-2 by J08 and M04. Axes indicate the concentration of each mAb, with the percentage of neutralization reported in each square. Data are from representative experiments from two independent replicates. The white-to-red heat map denotes 0% neutralization to 100% neutralization, respectively. *B.* The green-to-red synergy map denotes 0% neutralization to 100% neutralization, respectively. ZIP synergy score below -10, between -10 to 10, and above 10 denote an antagonistic, additive and synergistic activity

respectively. C, D. The red slope in the two graphs shows the dose-response curves for M04 (C) and J08 (D) against SARS-CoV-2 Omicron (BA.1) pseudotype virus. The x axes denote the concentration of each monoclonal antibody, with the percentage of neutralization shown on the y axes. Percent of inhibition was calculated relative to pseudotype virus -only control. Fifty percent neutralization dose (ND50) values were calculated by nonlinear regression using Prism v.8.1.0 (GraphPad). The average ND50 value for each antibody was determined from two independent replicates. The ND50 values are denoted on each graph.

3.2.2 When utilised in combination, none of the stronger antibodies from Hybrid Cohort exhibited a neutralising synergistic effect on BA.1 SARS-CoV-2 variant

After this first result, since we had already tested the loss of efficiency of mAbs G18 on BA.1 variant but from the same experiment we could appreciate that O14 mAb continued to show high neutralisation effect on this variant, we decided to test O14 mAb and G18 mAb in synergy with M04, to verify if one of these antibodies could enhance its neutralization potency on BA.1 variant. (**Figure 48**). Also in this case unfortunately no synergistic effect in neither of the two combinations was appreciated.
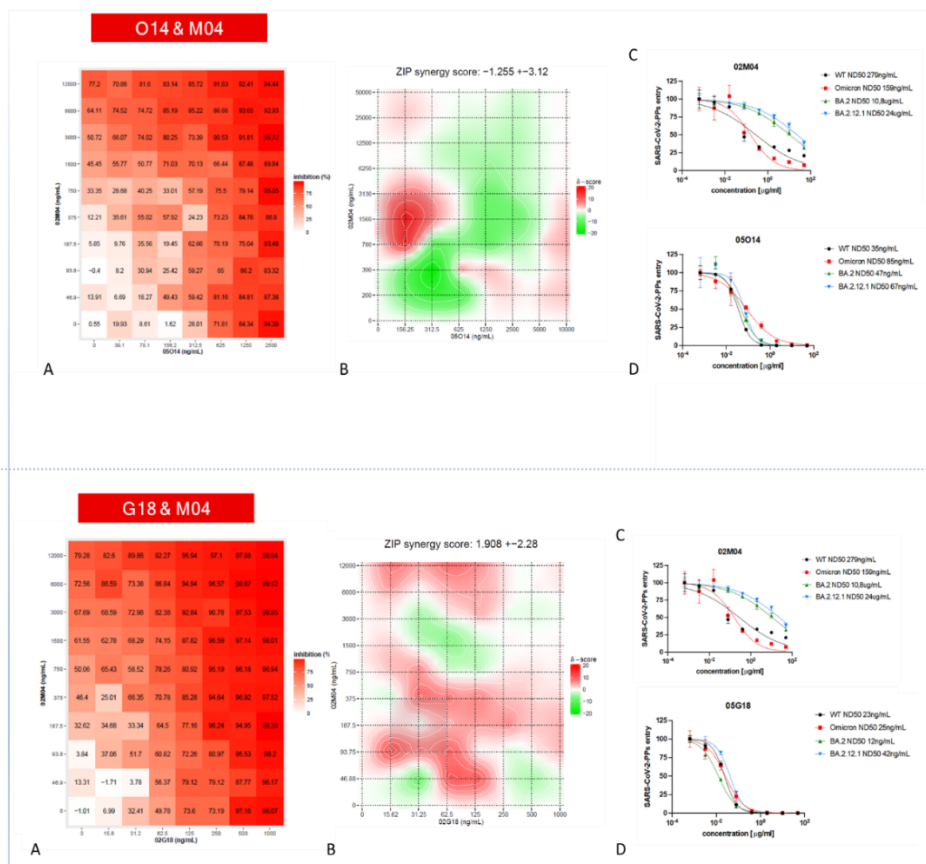
Figure 48. Evaluation of M04 respectively together O14 and G18 mAbs, activity against SARS-CoV2 BA.1 pseudotype virus. *The graphs were made using the same metrics as in Figure 1. No synergistic effect was observed with any combination.*

3.2.3 BA.2 and BA.2.12.1 SARS-CoV-2 variants can be neutralized by a synergistic action

Several sub-variants have emerged since Omicron arrived, culminating with the BA.1 variant. Consequently, we made the decision to keep testing these potential antibody combinations on the sub-variants that ensured the highest number of infections until September 2022: both BA.2 and BA.2.12.1.

Despite being part of the same sublineage, these three variants (BA.1, BA.2 and BA.2.12.1) differ from each other by some different point mutations. For instance, starting with BA.2, the well-known K417N mutation in the literature [166] becomes 93% predominant, when it was only roughly 60% present prior to BA.1. Moreover, the G496S and T547K mutations, present in BA.1 variant and which are similarly known to cause antibody evasion mechanisms, vanish from BA.2.

In this case, when tested on the BA.2 variant **(Figure 49, B & C),** two combinations, which included M04 & G18 and M04 & O14 antibodies, were synergistic, with an overall synergy δ-score of 14.15 and 10.82 respectively (where any score greater than 10 indicating synergy; **Figure 49**).

Specifically, for the combination M04 and G18 tested on BA.2 variant, a combined mAb dose of 1575 ng ml−1 (13 ng ml−1 of G18 and 1562 ng ml−1 of M04) had the same activity as 5000 ng ml−1 of M04 antibody (64% inhibition).

Concerning the M04/O14 combination tested on BA.2 pseudotype virus preparation, a combined mAb dose of 1612 ng ml−1 (50 ng ml−1 of O14 and 1562 ng ml−1 of M04) had the same activity as 5000 ng ml−1 of M04 antibody (61% inhibition).

Regarding the BA2.12.1 pseudotyped viruses, a combination of mAb M04 together with J08, G18 and O14 mAbs demonstrated an enhancement of neutralization ability, in all three cases **(Figure 50).**

Specifically, for the M04 plus J08 mixture, a combined mAb dose of 12.89 μg ml−1 (390 ng of M04 and 12.5 μg of J08) was effective for a 50% neutralization **(Figure 50A).** For M04 and G18 combination, combined mAb dose of 15.85 μg ml−1 (1560 ng of M04 and 25 μg of G18) showed a potency of 53% in neutralization **(Figure 50B)** and the cocktail of M02 and O14 revealed an efficacy dose of 3.163 μg ml−1 (31.25 ng of O14 and 3130 ng of M04) corresponding to a 70% inhibition effect **(Figure 50C).**

Even though these concentrations are ineffective for pharmaceutical therapy, they provide significant information on the possible synergistic effects of the tested antibodies.
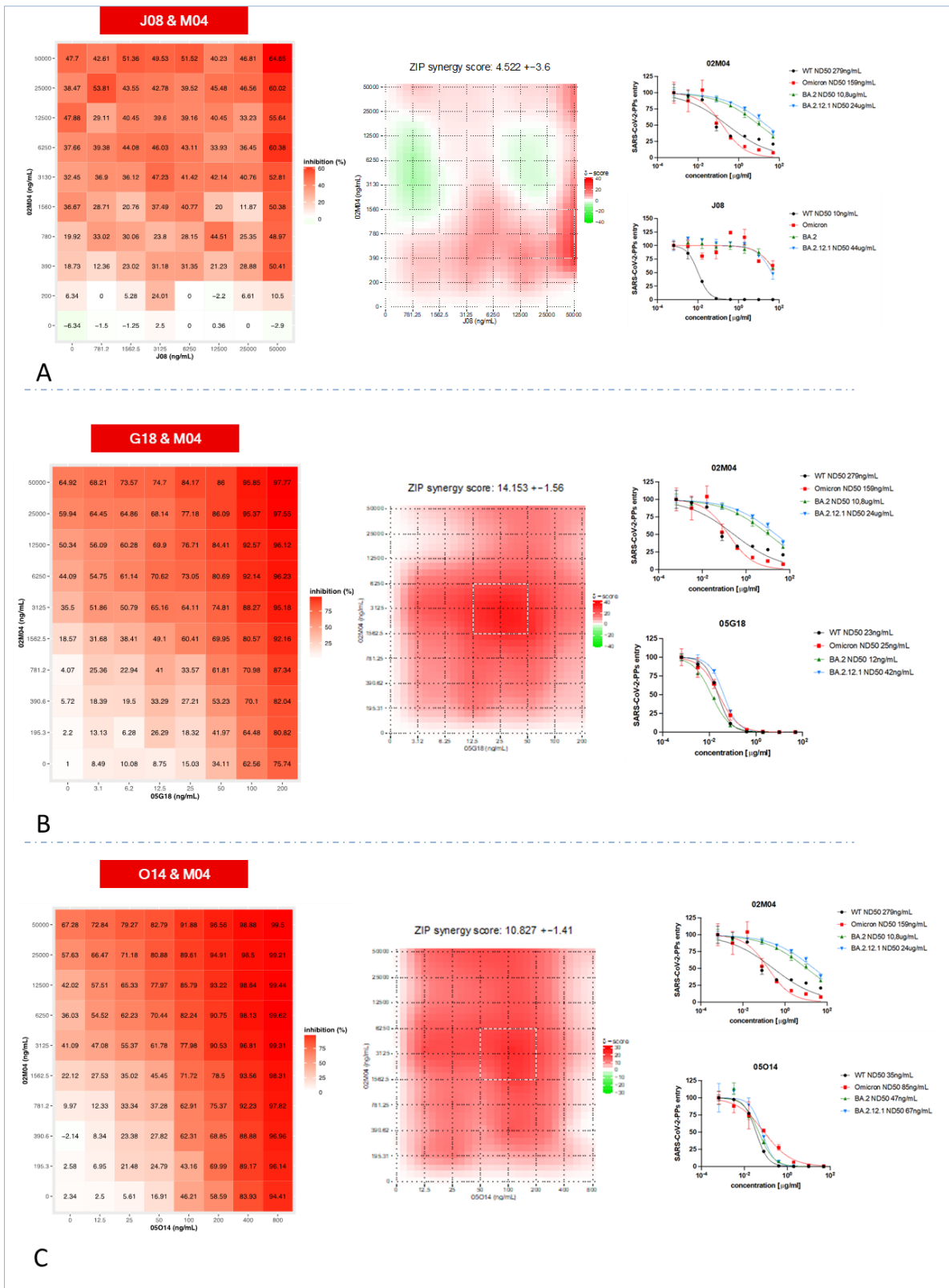
Figure 49. Evaluation of M04 activity together with J08, G18 and O14 mAbs, against SARS-CoV2 BA.2 pseudotyped viruses. *While for the combination of J08 and M04 no neutralizing effect was reported (A), for the cocktails composed of M04 and G18 (B) and M04 and O14 (C) a potent synergic effect is shown in the graphs. The black boxes in the centre of each table denote the area of maximum synergy between the two mAbs.*
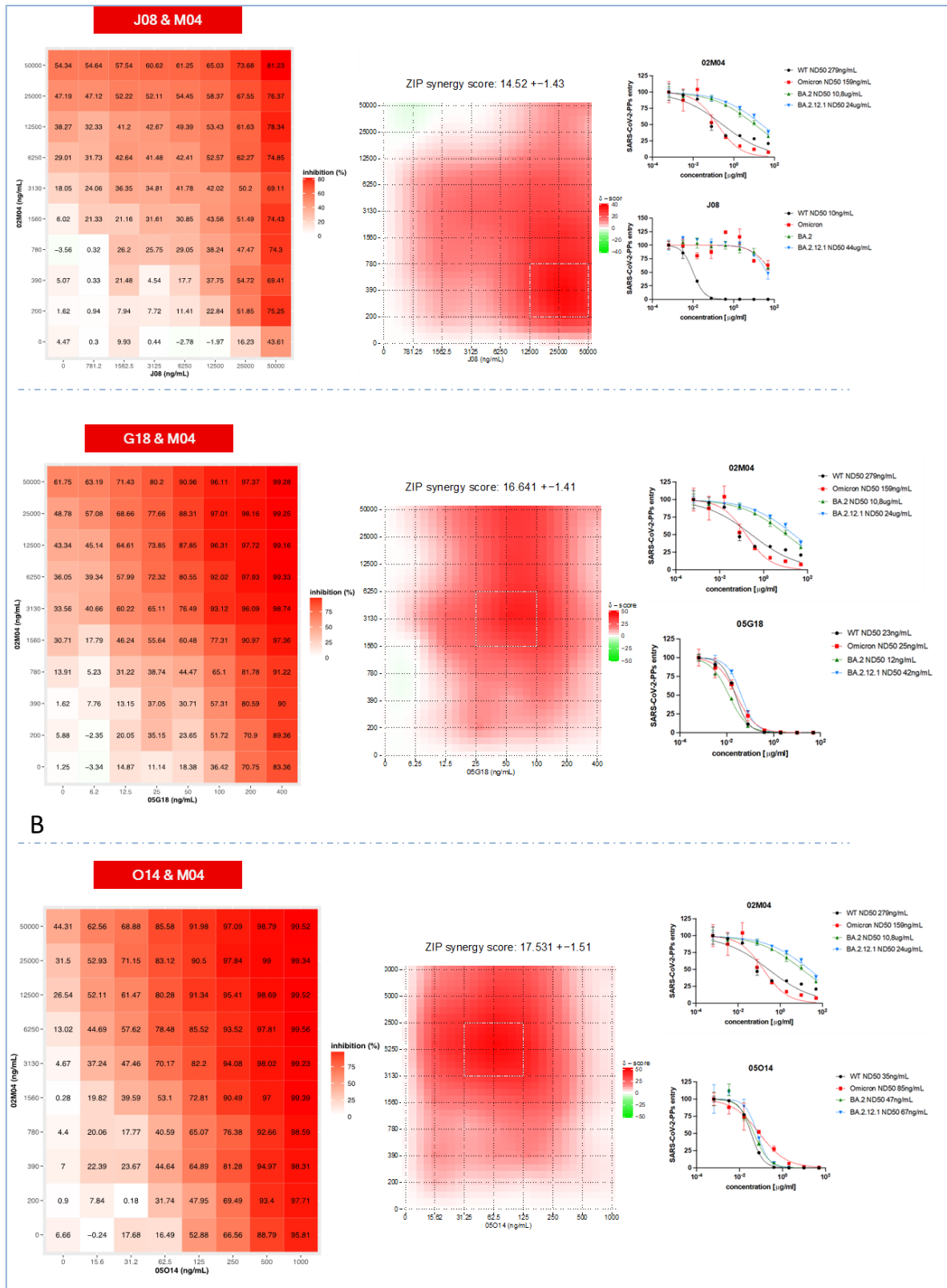
Figure 50. Evaluation of M04 activity together with J08, G18 and O14 mAbs, against SARS-CoV2 BA.2.12.1 pseudotyped viruses. *All of the three combinations of mAbs reported in the Figure show high synergistic effect. (A, B, C) The black boxes in the centre of each table denote the area of maximum synergy between each pair of mAbs.*

The ability of these antibodies to neutralize, when used in cocktails, the BA.2.12.1 variant is probably due to the different mutations that appeared in this variant: specifically, S704L and L452Q mutations first appeared with this variant, and the L452Q mutation (already present in a previous VOI variant, the "California variant") may indicate that the virus has evolved adaptively in response to the widespread epidemiological containment efforts implemented in the autumn of 2020, or to the increasing number of people who have become immune to the original viral variations through vaccination and/or recovery. Positive selection may therefore favour the virus's enhanced immune evasion, transmissibility, and/or infectivity. However, we can speculate that these mutations may cause a conformational change to the spike protein that would expose and make accessible the epitope that either or both of the antibodies are directed towards, given that the antibodies seemed functional when tested on this variant.

Regretfully, we decided to stop with synergy testing with these specific antibodies as soon as they stopped working with the arrival of the BA 4/5 variants (data shown in Chapter 2).

3.2.4 The most potent mAbs from Super Hybrid Cohort show low synergistic effect on SARS-CoV-2 Wuhan pseudotype virus

As mentioned in Chapter 2 and reported in details in Chapter 4 of Results, the screening from the Super Hybrid Cohort led to the isolation of a high number of antibodies able to neutralize the several SARS-CoV-2 variants tested, and three in particular were classified as the most potent antibodies identified: mAb 2, mAb 3 and mAb 1.

When tested on the SARS-CoV-2 Wuhan pseudotype virus, these antibodies showed a very similar behaviour to that reported on the live virus: to determine whether a hypothetical cocktail of these antibodies could boost their efficacy and, in parallel, limit the appearance of potential escape mutants, we decided to examine first the pseudotype virus in their wild-type version **(Figure 51).**
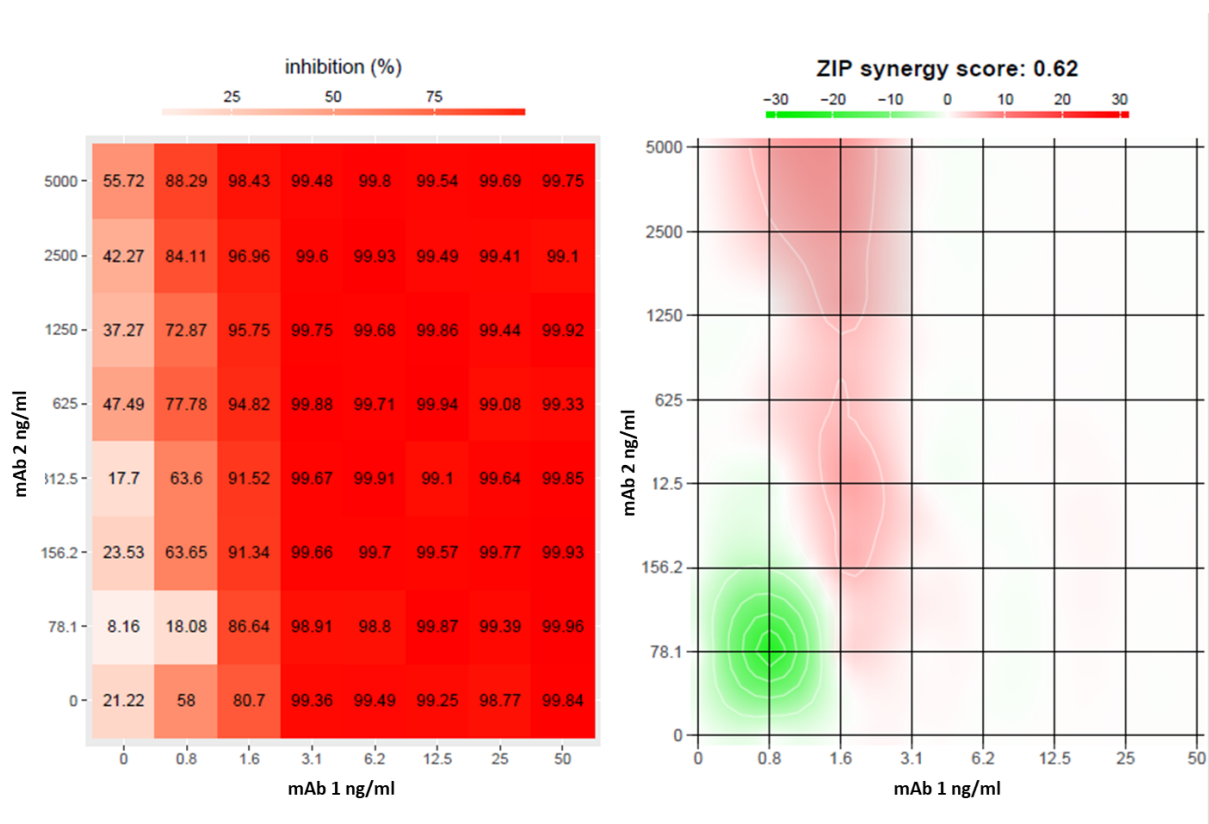
Figure 51. *Evaluation of* **mAb** *1 activity together with* **mAb** *2 against SARS-CoV-2 Wuhan pseudotype virus*. *In this assay, no synergic effect was observed, and the synergy δ-score so near to 0 results can indicate an antagonistic effect of the two antibodies when used together.*
Even the other mAbs combination tested (mAb 2 + mAb 3 and mAb 3 + mAb 1) didn't show any synergistic effect. (data not shown).

This three mAbs tested, as reported in **Figure 51**, didn't show any additive effect when used in combination, probably due to their strong neutralising action. Most likely, they should be used in considerably lower amounts to notice a synergistic effect.

3.3 Discussion

The coordinated activity of antibodies with various specificities and different epitope binding sites constitutes the natural human polyclonal response. It is reasonable to assume that employing properly designed cocktails made of recombinant human mAbs would more effectively mimic the response to pathogens than utilising single mAbs.

The hypothesis of combining several mAbs to improve their therapeutic effectiveness and to overcome the emergence of escape mutants is very appealing. To improve the efficiency of these promising therapies for infectious diseases, primarily caused by viruses and bacteria, numerous studies conducted over the past 30 years have assessed two or more mAbs in novel combinations. As evidence of their potential utility as future treatments, the majority of these mAb combinations had additive or synergistic neutralising effects. [168]

There are three possible outcomes when combining two or more drugs, like anti-viral mAbs: antagonism, which is defined as a reduction in efficacy; indifference, which is the result of one drug not enhancing or decreasing the efficacy of the other; and synergy, which occurs when the protective properties of the combined mAb preparation significantly outweigh the additive effect of the mixture's constituents.

A synergistic drug combination should facilitate the reduction of drug doses while maintaining efficacy. This is a critical aspect in the administration of mAbs since high-dosage monoclonals need hospitalisation of the patient; a possible dosage reduction would simplify the logistics.

In the discovery process for 7 anti SARS-CoV-2 drugs, understanding the mechanisms behind synergy and the implications for future screening and selection of effective neutralising mAb cocktails are greatly aided by the induction of synergistic neutralising effects by a mixture of non-neutralising mAbs. This is the case presented in paragraph 3.2.3. regarding J08 and M04 used as combined antibodies: in that case a cooperative action was studied, since each antibody when used alone was not able to neutralize the BA.2.12.1 variant. Since it's known that in case of the SARS-CoV-2, the efficacy of each antibody is strictly correlated with the exposure of the epitope which they bind to on the spike protein, this study can lead to understanding the mechanisms underlying this antibody-mediated synergy.

The neutralization of the several SARS-CoV-2 variants depends, at least in part, on functional "neutralizing" epitopes recognized by antibodies that inhibit the interaction of the spike protein with the ACE2 receptor expressed on human cells, and on the binding affinities of the antibodies. Therefore, the induction of neutralizing synergy might be explained by at least two mechanisms: first, the simultaneous binding of neutralizing mAbs to various functional sites on the spike protein; second, an increase in the affinity guaranteed by the mixture of mAbs compared with each mAb component. This was the case probably observed in the synergy assays conducted on the BA.2.12.2 variant: since each cocktail of antibodies seems to improve the neutralization efficacy, potentially the mutation presented in the BA.2.12.1 variant allowed a better affinity and improved exposure of the epitopes of interest for the antibodies tested.

Continuing to do research on potential antibody combinations is essential for SARS-CoV-2, at least as long as it continues to evolve over the months by introducing new mutations.

The pseudotype virus platform is helpful in this way, almost crucial. In fact, in our scenario, we do not have instruments in BSL3 that allow quantitative measurements of the experiments conducted using the live virus, but only a qualitative one.

Accordingly, luciferase detection within these virions enables accurate neutralisation readout and quantification.

The development of this synergy assay has made it possible for us to identify possible antibody combinations that could be helpful in the fight against COVID-19. Additionally, like any assay involving pseudotyped viruses, this assay can be extended to any type of virus, allowing for a thorough investigation of the antibody response to various pathogens.

3.4 Experimental procedures

Assessment of synergistic neutralization by a combination of antibodies

Synergy was described as a more potent neutralizing activity promoted by a cocktail of two mAbs when compared to that of single mAbs at the same total concentration of antibodies *in vitro*.

By using synergy-scoring models, the observed combination responses (dose–response matrix) were compared to the predicted responses to assess the magnitude of the advantageous effect from combining mAbs. The two mAbs were mixed at different concentrations, starting from 5 µg/ml and diluted step 1:2 for eight dilutions. The mix was prepared in a final volume of 25 µl and then incubated with 75 µl of different pseudotype virus for 1h at 37°C. After incubation 50 µl of the mAb cocktail + lentiviral vectors mixtures were added onto pre-coated wells with 10×10^3/well of HEK293TN- hACE2 and plates were incubated at 37°C for 24h. The control values included those for establishing the dose–response of the neutralizing activity measured separately for the individual mAbs, which were evaluated at the same doses as in the cocktail.

Afterwards, luciferase activity was measured using the Bright-Glo Luciferase Assay System (Promega), I then calculated the percentage of pseudotype virus neutralization for each condition and then calculated the synergy score value, which defines the interaction between these two mAbs in the cocktail. The synergic activity was measured using the SynergyFinder 3.0[3]. A synergy score of less than −10 indicates antagonism, a score from −10 to 10 indicates an additive effect, and a score greater than 10 indicates a synergistic effect.

Technical duplicates were performed for each experiment.

4. Neutralization assays with the authentic SARS-CoV-2 virus

4.1 Introduction

With over 799 million cases, over 6 million deaths and an estimated 50 trillion US dollars in worldwide economic losses, the severe acute respiratory syndrome coronavirus 2 (SARS-CoV-2) pandemic had an unprecedented impact.

The Food and Drug Administration (FDA) has granted emergency use authorizations (EUAs) for a number of SARS-CoV-2 vaccines and medications for the past four years to prevent and treat coronavirus disease 2019.

Despite this, we have seen that infectious waves are spreading over the world during the years that have passed, and more waves are probably going to follow in the next years. The constant appearance of novel SARS-CoV-2 mutations worldwide provides additional evidence for this.

Therefore, it is crucial to create therapeutic strategies against SARS-CoV-2 and its variants as soon as possible, in addition to vaccinations. As previously described in the Introduction of this Thesis, human monoclonal antibodies (mAbs) are among the several therapeutic possibilities that can be developed with the least amount of time.

Many groups have been working in the years of this emergency epidemic to isolate and characterise human mAbs from COVID-19 convalescent patients, and some of them have advanced swiftly to clinical trials for the treatment and prevention of SARS-CoV-2 infection.[142] [169] Each of these antibodies binds to the spike glycoprotein (S protein), neutralising the SARS-CoV-2 infection.

In most cases, the dose of mAbs employed in clinical trials against SARS-CoV-2 to date has been high, ranging from 50 to 8,000 mgs. This is in contrast to other mAbs in the field of infectious illnesses [170,171]. Two significant restrictions on the use of mAbs in the field of infectious illnesses are brought about by the high dose. First, this treatment intervention is exceedingly expensive and hence only available in high-income nations due to the high dosage related costs and the fact that it can only be administered intravenously. Furthermore, the prohibitive cost of this treatment has prevented mAbs from being widely accessible and from being used in different fields, like infectious diseases. The discovery and development of highly effective mAbs that can be injected subcutaneously or intramuscularly and utilised at lower dosages to save costs would be a potential approach to solve the problem. In this work, we decided to select just very strong antibodies with the goal of employing them at low dosage to make them easily and affordably administered by intramuscular injection, expanding the boundaries of mAb application to combat infectious diseases.

As previously mentioned, the primary focus of my Ph.D. work involved developing and implementing assays utilising recombinant spike proteins, pseudotyped SARS-CoV-2, and other HCoV. Occasionally, though, I also helped with antibody screening from different cohorts, by working in BSL3 with the live virus.

4.2 Results

In this Chapter I will present the neutralization screening conducted in BLS3 lab to identify and classify the neutralizing antibodies against SARS-CoV-2. Since during the three years of my PhD several cohorts of patients have been analyzed, as previously described in the Background section of this thesis, I will present the results divided by Cohort.

4.2.1 J08 mAb was identified as an extremely potent human mAb from COVID-19 convalescent patients

Covid-19 Convalescent Cohort: 453 neutralising antibodies were found by single-cell sorting 4,277 SARS-CoV-2 spike protein-specific memory B cells from 14 COVID-19 survivors. Specifically, the 1,731 supernatants containing S protein-specific mAbs were screened for their capability of neutralizing authentic SARS-CoV-2 virus through an *in vitro* microneutralization assay. They were examined for their capacity to shield the Vero E6 cell layer from the cytopathic effect caused on by SARS-CoV-2 infection. Supernatants were examined at a single-point dilution to boost our approach in high throughput, and a virus titer of 25 50% tissue culture infectious dose (TCID50) was employed to improve the sensitivity of our initial screening. A final panel of 453 (26.2%) mAbs out of the 1,731 mAbs examined in this study neutralised the real virus and prevented Vero E6 cells from becoming infected. From the panel of 453 nAbs, the heavy chain (HC) and light chain (LC) variable regions of 220 nAbs were recovered, and were expressed as full-length immunoglobulin G1 (IgG1) using the transcriptionally active PCR (TAP) approach [172] to characterize their neutralization potency against the live virus at 100 TCID50. In this screening process, mAbs were categorised as fully, partially, or non-neutralizing according to their capacity to inhibit Vero E6 cell infection (**Figure 52**). Only 1.4% (n = 3) of the expressed nAbs were grouped as extremely potent nAbs, showing an IC100 lower than 10 ng/mL (**Figure 53**).
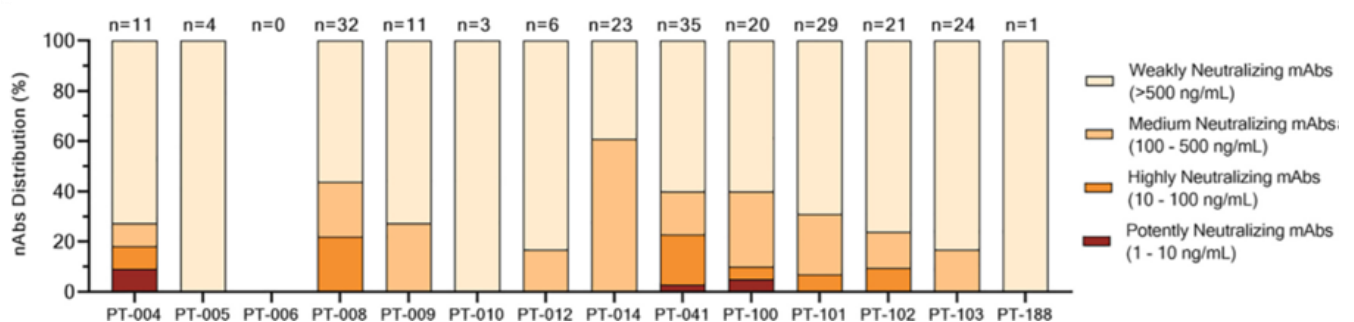
Figure 52. Distribution of neutralizing mAbs identified. *The bar graph shows the distribution of nAbs with different neutralization strengths. nAbs were grouped as weakly neutralizing (> 500 ng/mL; light orange), medium neutralizing (100 – 500 ng/mL; orange), highly neutralizing (10 – 100 ng/mL; dark orange) and extremely neutralizing (1 – 10 ng/mL; dark red). The total number of antibodies tested per individual is displayed on the top of each bar.*
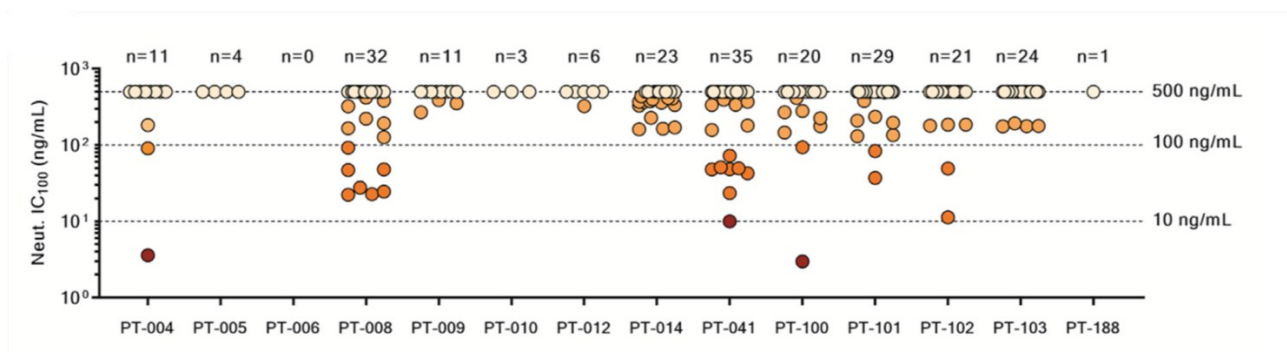
Figure 53. Potency neutralization of mAbs expressed as IgG. *The graph is divided in different dotted lines which limit different ranges of neutralization potency (500, 100, and 10 ng/mL). Dots are painted based on their neutralization potency and were categorised as weakly neutralizing (>500 ng/mL; light orange), medium neutralizing (100–500 ng/mL; orange), highly neutralizing (10–100 ng/mL; dark orange), and extremely neutralizing (1–10 ng/mL; dark red). The total number (n) of antibodies screened per individual is shown on top of each graph. A COVID-19 convalescent plasma and an unrelated plasma were used as positive and negative control, respectively, in all the assays.*

We found four distinct nAb groups against SARS-CoV-2. The first group (Group I) consists of the S1 RBD-specific nAbs (J08, I14, F05, G12, C14, and B07), (the data about the specific binding of the several portion of the spike protein are not shown here, but reported in the paper [111]) which demonstrated neutralisation effectiveness against the D614G mutation, and against the UK B.1.1.7. variant, one of the first variants detected in 2020, and the authentic wild type (WT) virus. Neutralising potency of S1 RBD-specific nAbs ranges from 3.9 to 157.5 ng/mL (**Figure 54A-3F**). nAb J08 demonstrated the ability to neutralise SARS-CoV-2 variants with the E484K mutation in addition to the D614G and B.1.1.7 variants [173]. I21, J13, and D14 were among the S1-specific nAbs in Group II, which did not bind the RBD. Although not as effective as S1 RBD-directed nAbs, these antibodies nonetheless demonstrated good neutralisation potency, ranging from 99.2 to 500.0 ng/mL (**Figure 54A-3F**). In this group a single antibody was unable to neutralise the B.1.1.7 variation (I21). The antibodies in the third group (Group III) can only bind the S-protein in its whole trimeric configuration (H20, I15, F10, and F20). Group IV, the last group, is made up of antibodies that only recognised the S2 domain. For Group IV, several antibodies with comparable characteristics were found; however, only nAb L19 is displayed. With 19.8 mg/mL for the authentic WT, 12.5 mg/mL against the D614G, and 9.9 mg/mL against the B 1.1.7 variant, Group IV nAb L19 exhibits the lowest neutralisation potency (**Figure 54A-3F**).
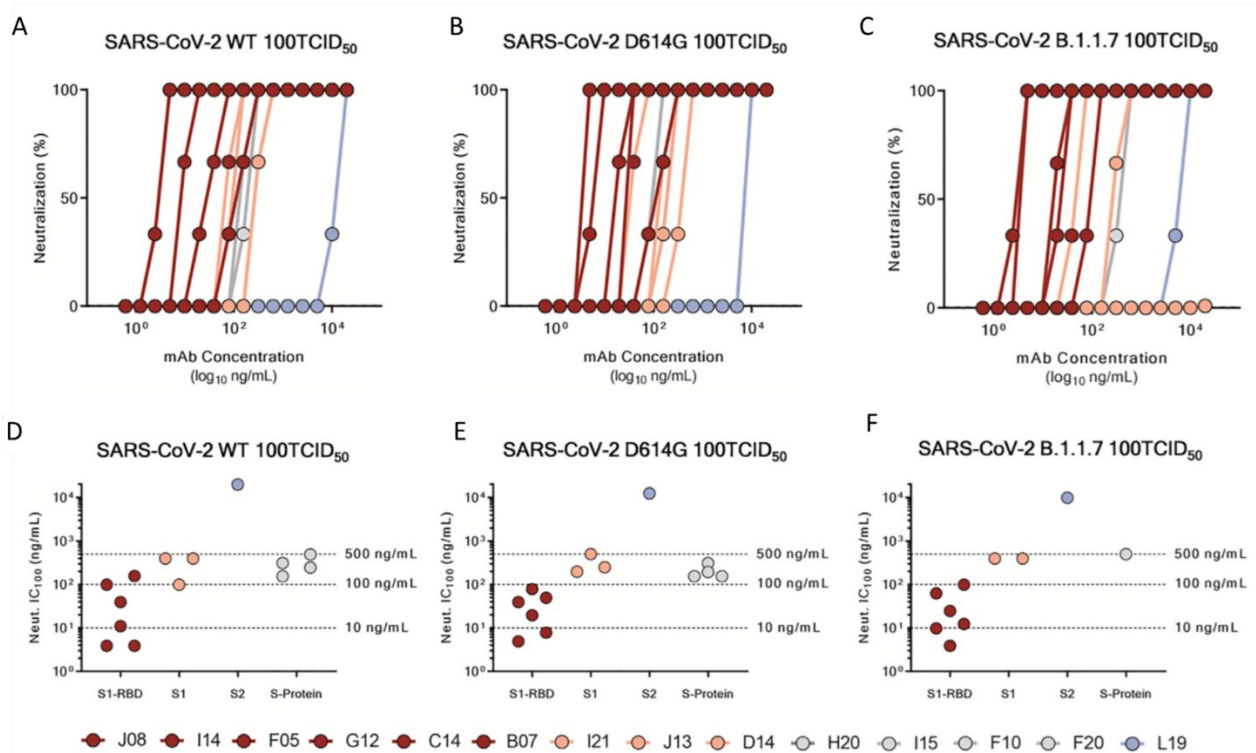
Figure 54. Neutralization potency of each selected mAb divided per SARS-CoV-2 variants. *A-C) Neutralization curves for selected antibodies are reported as percentage of viral neutralization against the authentic SARS-CoV-2 wild type (A), D614G variant (B), and the variant B.1.1.7 (C). Data are representative of technical triplicates. A neutralizing COVID-19 convalescent plasma and an unrelated plasma were used as positive and negative control, respectively. (D-F) Neutralization potency of 14 selected antibodies against the authentic SARS-CoV-2 wild type (D), D614G variant (E), and the UK variant B.1.1.7 (F). Dotted lines show different scales of neutralization potency (500, 100, and 10 ng/mL). In all graphs, the isolated antibodies are shown in dark red, pink, gray, and light blue based on their ability to recognize the SARS-CoV-2 S1 RBD, S1 domain, S protein trimer only, and S2 domain, respectively.*

From this massive screening, three mAbs were identified as the strongest ones, able to neutralize both the original wild-type virus and other strains tested with D614G, E484K, and N501Y mutations. These most potent mAbs were J08, I14 and F05. Given that the ultimate objective was to determine which of these would be clinically developed, Antibody-Dependent Enhancement (ADE) of disease had to be carefully avoided. In fact, a possible clinical risk after coronavirus infection is ADE disease [174].The three most potent nAbs (J08, I14, and F05) were therefore renamed J08-MUT, I14-MUT, and F05-MUT after five distinct point mutations were inserted in the constant region (Fc) to maximise the suitability for clinical development and lower the risk of ADE. To improve antibody half-life, tissue distribution, and persistence, the first two point mutations (M428L and N434S) were added [175] [176]. Three other point mutations (L234A, L235A, and P329G) were added to mitigate antibody dependent functions such as binding to FcγRs and cell-based activities [177] .

The cross-neutralization ability of the three modified antibodies was assessed by testing their binding specificity and neutralisation power against the WT, the widely distributed SARS-CoV-2 D614G variant, and the variant B.1.1.7 (**Figure 55**).
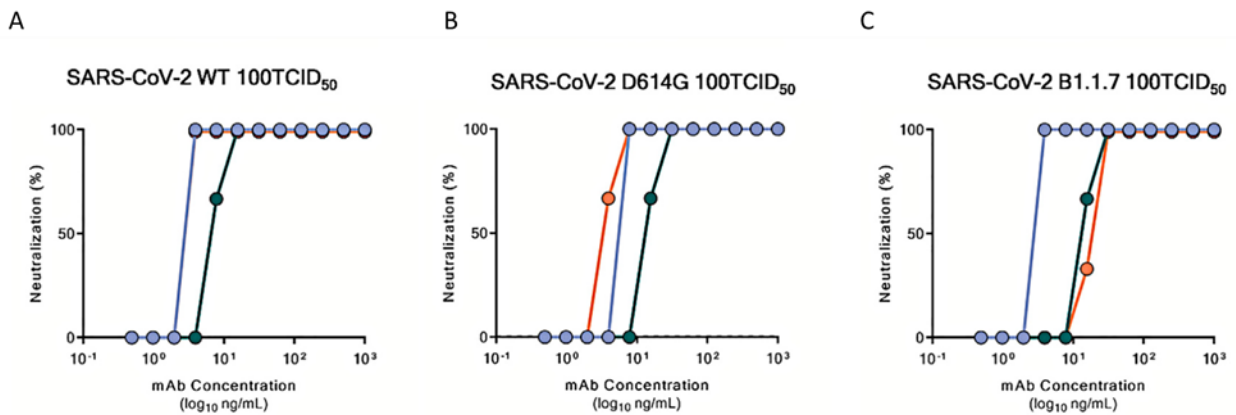
Figure 55. Neutralization potency of mAbs mutated. (A-C) *Neutralization curves against the authentic SARS-CoV-2 wild type, the D614G variant and the B.1.1.7 variant for J08-MUT, I14-MUT and F05-MUT shown in blue, green and red respectively. Data are representative of technical triplicates.*

After these screenings, J08 was chosen as the best candidate for development since, out of the three antibodies found, it demonstrated superior expression in HEK 293 and CHO cells even when expressed on a large scale and proved to be very stable following purification. Without Fc functions, its prophylactic and therapeutic effectiveness in the hamster model was noted at 0.25 and 4 mg/kg, respectively. All these data are reported in details in our paper published in 2021[111].

Unfortunately, J08 was withdrawn from clinical trials and emergency use in Italy after it was shown to be ineffective against Omicron variants, as previously reported.

4.2.2 Hybrid immunity is associated with improved antibody efficacy against SARS-CoV-2 variants but antiviral activity declines with the Omicron variant and its sublineages

Hybrid Cohort: During the year 2021 certain variants of SARS-CoV-2 virus have entirely replaced the original virus, which was initially identified in Wuhan, China. The viruses known as variants of concern (VoCs) include B.1.1.7 (Alpha), B.1.351 (Beta), B.1.1.248 (Gamma), and B.1.617.2 (Delta), which during that year was the most infectious variant. The advent of SARS-CoV-2 variants posed a threat to the efficacy of existing vaccinations and restricted the use of COVID-19 mAb-based therapy [178]. In this *Hybrid Cohort*, we examined the characteristics of the B cells and antibody responses at the single-cell level by analysing the memory B cells of five naive (classified as seronegative) and five recovering individuals (classified as seropositive) who received the BNT162b2 mRNA vaccination. Over 3,000 cells produced mAbs against the spike protein, over 400 mAbs neutralised the original SARS-CoV-2 virus that was first discovered in Wuhan, China, and over 6,000 cells were sorted. These mAbs developed by the isolated cells were specifically tested in a cytopathic effect-based microneutralization assay (CPE-MN) with the original live Wuhan - SARS-CoV-2 at a single point dilution to identify SARS-CoV-2 neutralizing human mAbs (nAbs). This first screening detected a total of 411 nAbs, of which 71 derived from participants who were seronegative and 340 were from seropositive.

All these data and experiments are reported in details in the two papers that we published in 2021 [112,125].

We attempted to express all 411 nAbs as IgG1 to more fully characterise and comprehend the potency and breadth of coverage of all nAbs against the SARS-CoV-2 virus discovered in Wuhan. For additional characterization, we were able to isolate and express 276 antibodies, of which 224 (89.8%) came from seropositive participants and 52 (10.1%) from seronegative participants. The antibodies were then tested by CPE-MN in serial dilution to determine their 100% inhibitory concentration (IC100) against the SARS-CoV-2 virus found in Wuhan and the VOCs including B.1.1.7 (Alpha), B.1.351 (Beta) B.1.1.248 (Gamma) and B.1.617.2 (Delta). Generally, nAbs obtained from seropositive vaccine recipients exhibited noticeably greater potency than those recovered from seronegative recipients (**Figure 56**). Furthermore, a greater proportion of nAbs from seropositive individuals maintained their ability to neutralise the VoCs. In fact, the ability to neutralise the Alpha, Beta, Gamma, and Delta variants was lost by 14%, 61%, 61%, and 29% of the nAbs from participants who were seropositive compared to 32%, 78%, 75%, and 46% of those from participants who were seronegative when nAbs were individually tested against all VoCs (**Figure 56**).
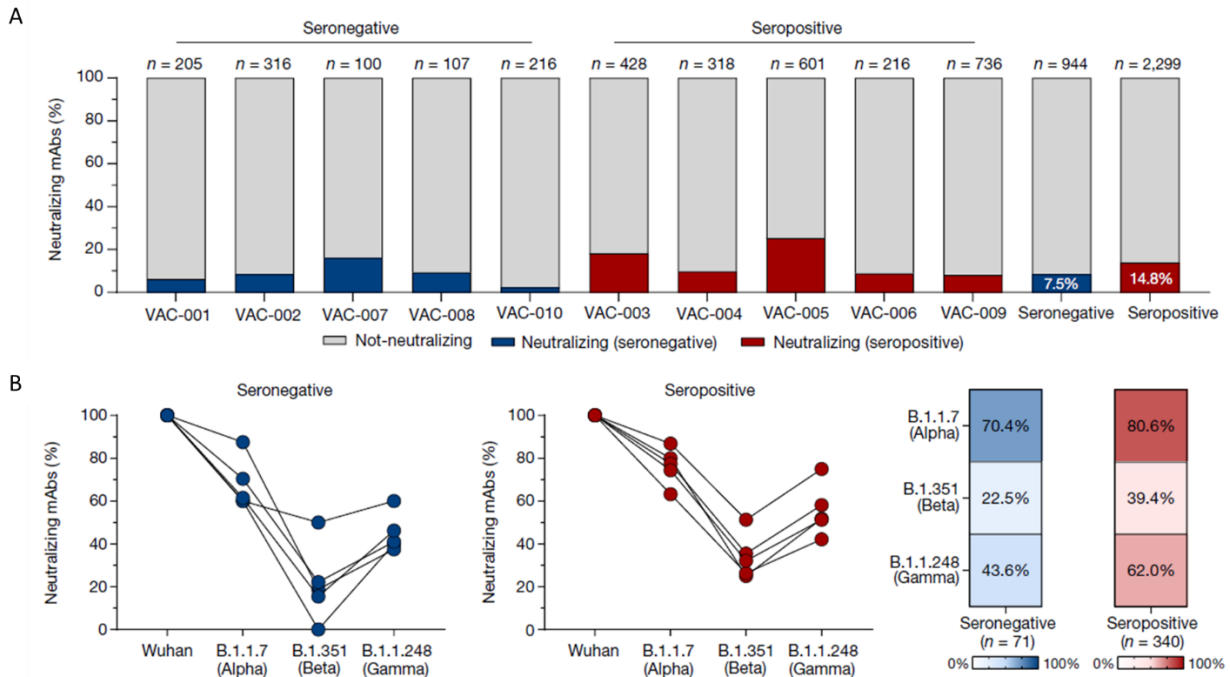
Figure 56. Identification of cross-neutralizing SARS-CoV-2 nAbs. *The bar graph reports the percentage of not-neutralizing antibodies (grey), nAbs from individuals who were seronegative (dark blue) and nAbs seropositive (dark red). The total number (n) of antibodies tested per donors is reproted on the top of each bar in A, B. The graphs show the fold-change percentage of nAbs in individuals who were seronegative (left) and seropositive (right) against the Alpha, Beta and Gamma VoCs compared with the original SARS-CoV-2 virus detected in Wuhan. The heat maps indicate the overall percentage of the SARS-CoV-2 nAbs identified in Wuhan that can neutralize the tested VoCs.*

Lastly, a significant distinction between seronegative and seropositive subjects was discovered in the class of nAbs with medium/high potency against all variants (IC100 of 11–100 ng ml−1 and 101–1,000 ng ml−1). In fact, the total nAb repertoire includes 71.0%, 62.5%, 23.7%, 22.8%, and 53.1% of nAbs from seropositive participants in these ranges, while the corresponding numbers for nAbs from seronegative donors were 48.1%, 38.5%, 17.3%, 17.3%, and 34.6% against the SARS-CoV-2 virus detected in Wuhan and the Alpha, Beta, Gamma, and Delta VoCs, respectively (**Figure 57).**

115
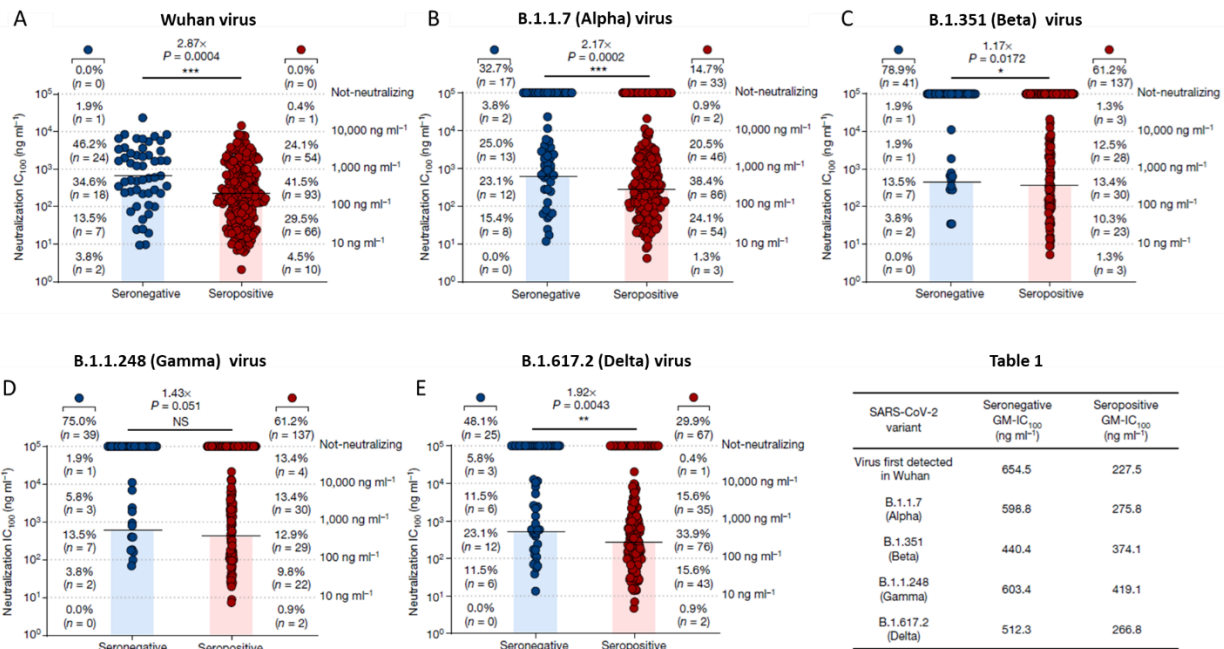
Figure 57. Potency and breadth of neutralization of nAbs against SARS-CoV-2 WT and VoCs. *A-E Dot charts show the neutralization potency, reported as IC100 (ng ml–1), of nAbs tested against the original SARS-CoV-2 virus and the VOCs. The number and percentage of nAbs from individuals who were seronegative versus seropositive, fold change, neutralization IC100 geometric mean (black lines, blue and red bars) and statistical significance are denoted on each graph. A non-parametric Mann–Whitney t-test was used to evaluate statistical significances between groups. Two-tailed P value significances are shown as *P < 0.05, **P < 0.01, ***P < 0.001. NS, not significant. The table 1 shows the IC100 geometric mean (GM) of all nAbs pulled together from each group against all SARS-CoV-2 viruses tested. Technical duplicates were performed for each experiment.*

The B.1.351 (Beta) and B.1.1.248 (Gamma) variants escaped almost 70% of these antibodies, while a much smaller portion was impacted by the B.1.1.7 (Alpha) and B.1.617.2 (Delta) variants. The overall loss of neutralization was always significantly higher in the antibodies from naive people.

As mentioned in Chapter 2, three antibodies (M04, O14, and G18) were chosen as the most effective; however, in 2022, with the introduction of Omicron (**Figure 58**) and its ensuing sublineages (**Figure 59**), their neutralising efficacy, along with that of all other antibodies examined, dramatically changed.
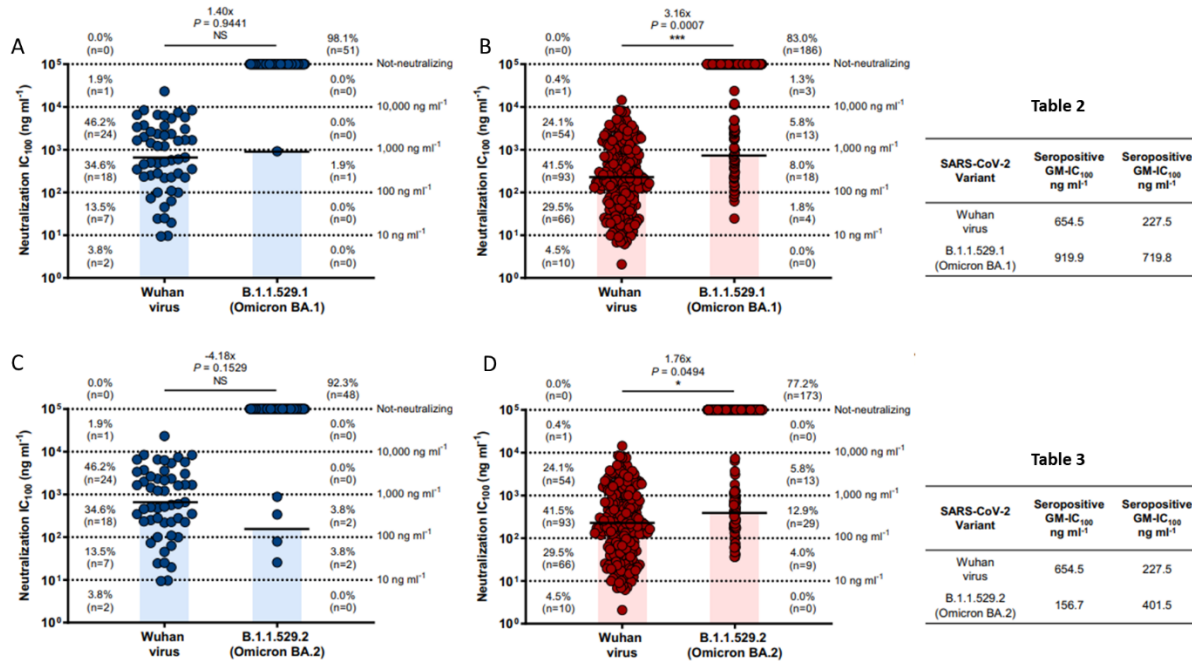
Figure 58. Neutralization potency of Omicron BA.1 and BA.2 nAbs. A-D. *Dot charts show the neutralization potency, reported as IC100 (ng ml−1), of nAbs tested against the original SARS-CoV-2 virus first detected in Wuhan, the BA.1 and BA.2 Omicron VoC for seronegatives (A, C, Table 2) and seropositives (B, D, Table 3). The number and percentage of nAbs from individuals who were seronegative versus seropositive, fold change, neutralization IC100 geometric mean (black lines, blue and red bars) and statistical significance are denoted on each graph. Technical duplicates were performed for each experiment. A non-parametric Mann–Whitney t-test was used to evaluate statistical significances between groups. Two-tailed P value significances are shown as *P < 0.05, **P < 0.01, ***P < 0.001. NS, not significant. Tables 2 and 3 show the IC100 geometric mean (GM) of all nAbs pulled together from each group against Wuhan, BA.1 (Table 2) and BA.2 (Table 3) viruses.*

The Omicron variants BA.1 and BA.2 caused a sharp decline in this cohort's antibody neutralizing activity. The graphs show that while seropositive subjects still exhibit some residual activity, although negligible, neutralization is lost in seronegative subjects.

We decided then to test the activity of these antibodies on all the Omicron sublineages we had access to during the last year to continue evaluating their action on the new variants: BA.5, BA 2.75, BF.7, BQ 1.1, XBB 1.5, EG 5.1.1, and BA 2.86 (**Figure 59**).
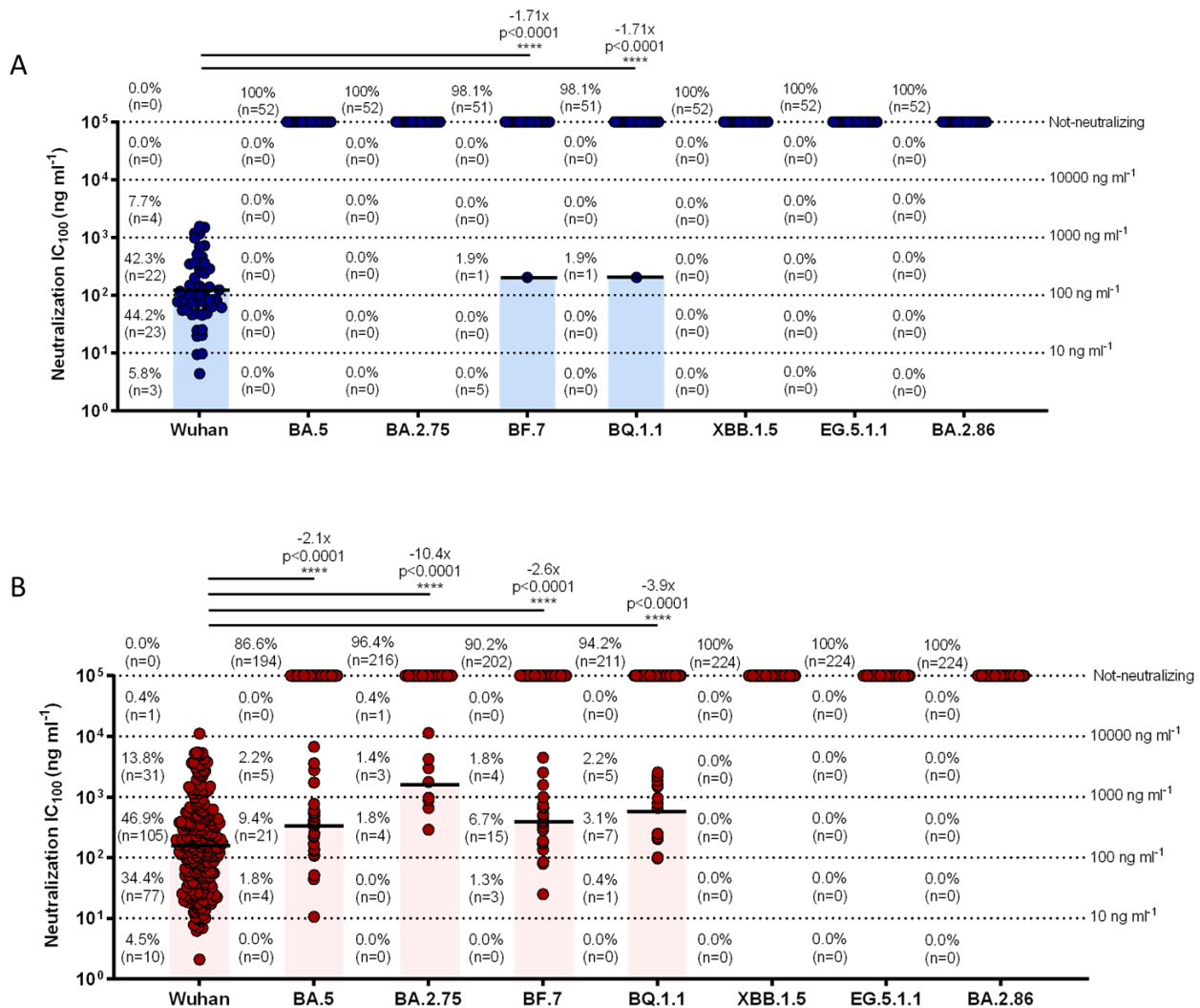
Figure 59. Neutralization potency on Omicron variants. *The graph with the dots shows the neutralization potency, reported as IC100 (ng ml−1), of nAbs tested against the original SARS-CoV-2 virus first detected in Wuhan, the BA.5 and all the other Omicron VoC for seronegatives (A) and seropositives (B). The number and percentage of nAbs from individuals who were seronegative versus seropositive, fold change, neutralization IC100 geometric mean (black lines, blue and red bars) and statistical significance are denoted on each graph. Technical duplicates were performed for each experiment. A non-parametric Mann–Whitney t-test was used to evaluate statistical significances between groups. Two-tailed P value significances are shown as *P < 0.05, **P < 0.01, ***P < 0.001. NS, not significant.*

Overall, no antibodies were effective against these new variants. More precisely, only two antibodies showed neutralisation against the BF.7 and BQ.1.1 variants for seronegative subjects; no other antibody in this group exhibited even weak neutralising activity against any of the other variants tested.

Conversely, among seropositive individuals, very little residual activity was observed, however the quantity of neutralising antibodies drastically decreased with each tested variant. Neutralising antibodies to the most recent variants EG.5.1.1, XBB 1.5, and 2.86, were not found in any group.

4.2.3 Super Hybrid immunity increases antibody potency against SARS-CoV-2 variants

Super Hybrid Cohort: in the Super Hybrid Cohort we studied the memory B cells of six COVID-19 convalescent donors who had the COVID-19 infection twice and were vaccinated with 3 doses of BNT162b2 mRNA vaccination. Over 4,000 cells were sorted. As mentioned in Chapter 2, for this cohort we decided to modify the workflow so that we could proceed faster in the identification of mAbs able to neutralize the Wuhan virus. The first step consisted in the classical microneutralization assay (CPE-MN) with the original live Wuhan SARS-CoV-2 at a single point dilution to identify SARS-CoV-2 neutralizing human monoclonal antibodies (nAbs). This screening detected a total of 544 nAbs (data not shown).

After that, 520 nAbs were successfully expressed as IgG1 and tested by CPE-MN in serial dilutions to determine their 100% inhibitory concentration (IC100) against the Wuhan SARS-CoV-2 and directly to the VOCs which are categorized as the more circulant nowadays: BA.5, BA 2.75, BF.7, BQ 1.1, XBB 1.5, EG 5.1.1, and BA 2.86 (**Figure 60**).

Figure 60. Identification of cross-neutralizing SARS-CoV-2 nAbs in the Super Hybrid Cohort. *The bar graph reports the percentage of neutralizing antibodies nAbs from each individual. Neutralization potency of the tested antibodies against the authentic SARS-CoV-2 wild type and all the Omicron variants tested. Dotted lines show different scales of neutralization potency (from 10 to 10000 ng/mL). The number and percentage of nAbs, fold change, neutralization IC100 geometric mean and statistical significance are denoted on each graph. Technical duplicates were performed for each experiment. A non-parametric Mann–Whitney t-test was used to evaluate statistical significances between groups. Two-tailed P value significances are shown as *P < 0.05, **P < 0.01, ***P < 0.001. NS, not significant.*
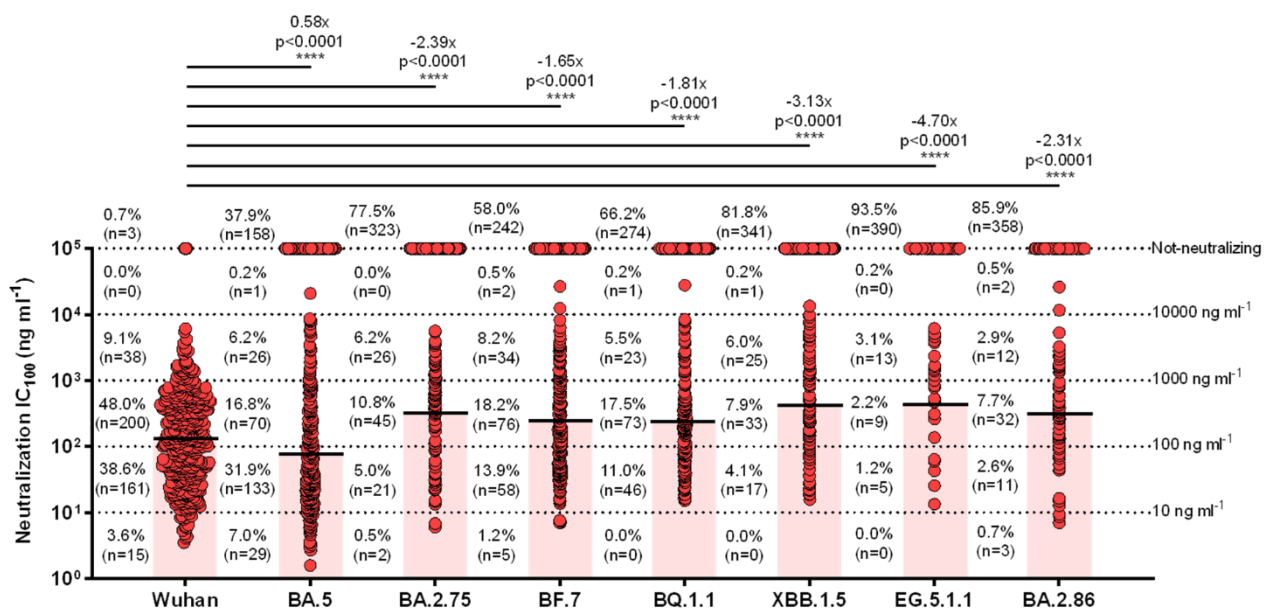
From the Super Hybrid Cohort, 3 antibodies were selected based on their neutralization potency on SARS-CoV-2 virus and its variants (**Figure 61**).

These antibodies were chosen to be characterized with the pseudotype platform (as previously reported) and to determine if they could work in combination to increment their neutralization potency (data already shown in Chapter 3).

	S protein trimer	RBD	NTD	S2	SARS-CoV-1	OC43	HKU1	229E	NL63	SARS-CoV-1 (IC$_{50}$)	Wuhan	BA.5	BA.2.75	BF.7	BQ.1.1	XBB.1.5
SH_mAb 2											78.2	11.1	31.3	44.2	22.1	97.8
SH_mAb 3											13.3	9.4	13.3	37.7	18.9	18.9
SH_mAb 1										56.0	479.9	67.9	339.3	240.0	339.3	169.7
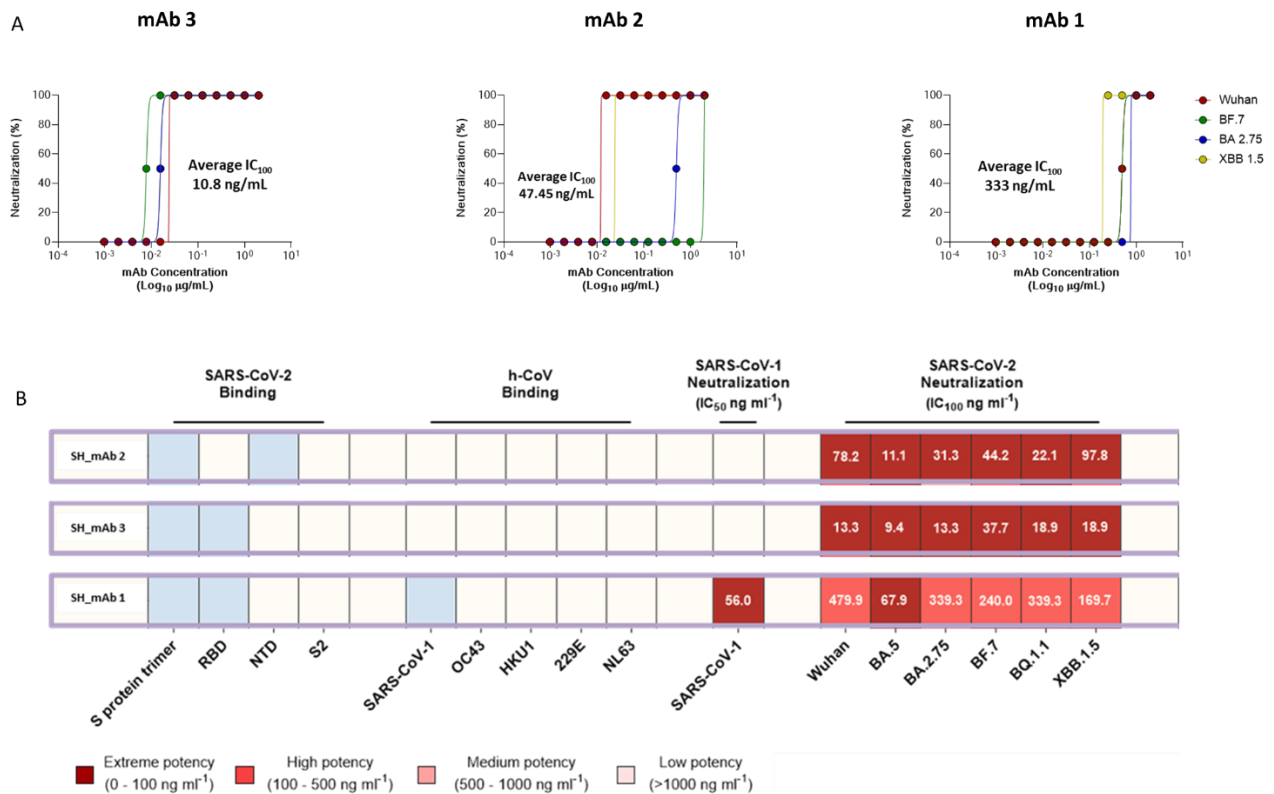
Figure 61. Identification of the most potent cross-neutralizing SARS-CoV-2 nAbs in the Super Hybrid Cohort. *A*. *The three graphs report the IC100 of each antibody presented, and the average value is reported in the graph. **B**. The table shows the precise neutralization potency of each mAb when tested with the corresponding SARS-CoV-2 variant. mAb 2 is the mAb which shows overall a higher neutralization efficacy but mAb 1 seems to be the more cross-reactive (since it is able to neutralize the SARS-CoV-1 virus).*

4.3 Experimental procedures

SARS-CoV-2 authentic viruses neutralization assay

Every SARS-CoV-2 authentic viral neutralising assay was carried out in the biosafety level 3 (BSL3) labs at Vismederi Srl, Siena, Italy, and at Fondazione Toscana Life Sciences, Siena, Italy. A Certified Biosafety Professional certifies BSL3 laboratories, and local authorities inspect them annually. Using a cytopathic effect-based microneutralization assay (CPE-MN), the neutralisation activity of the discovered nAbs against SARS-CoV-2 and for the several SARS-CoV-2 variants was assessed[111,112,125]. In summary, nAbs were incubated for one hour at 37°C and 5% CO_2 alongside a SARS-CoV-2 viral solution that contained 100 median Tissue Culture Infectious Dose (100 TCID50) of virus. A sub-confluent Vero E6 cell monolayer was previously placed into each well of a 96-well plate, and the mixture was then applied. After being cultured for three to four days at 37°C in a humidified atmosphere with 5% CO_2, plates were checked for CPE by two separate operators using an inverted optical microscope. Every nAb was diluted stepwise starting at a dilution of 1:5, with the IC100 determined by taking the original concentration into consideration. For every experiment, technical duplicates were carried out. Positive and negative controls were applied to each plate in the manner previously mentioned.

4.4 Discussion

To find highly effective mAbs against SARS-CoV-2 and several variants, screening of memory B cells from SARS-CoV-2 convalescent or vaccinated patients was undertaken.

In the case of Convalescent COVID-19 cohort, we found that only 10% of all B cells against the isolated S protein generated neutralising antibodies during the process of searching for strong antibodies.

However, the percentage of neutralising antibodies increased with the study of the other cohorts, indicating that vaccination, even if it occurs after illness, stimulates the establishment of a far more comprehensive immunity.

The most significant finding in the research concerning the Hybrid Cohort is that individuals who have previously been infected with SARS-CoV-2 produce more B-cell-producing antibodies after vaccination, which have a higher neutralization power and are more resistant to escape variants.

These data imply that a secondary immune response, which can be attained by vaccinating previously infected individuals or by administering a third booster dose, is necessary to elicit a meaningful proportion of cross-neutralizing antibodies among SARS-CoV-2 variants, after a primary immunisation with two doses of the vaccine in naive individuals.

Further studies supported by the study of the Super Hybrid Cohort were necessary to understand whether a booster dose in naive people can elicit a hybrid immunity-like antibody response and to define the molecular basis of cross-protection in the population.

The Super Hybrid cohort study confirmed the excellent immune response that is promoted by a third vaccination obtained after two COVID-19 infections. This immunization is highly cross-neutralizing, even against SARS-CoV-2 variants that the individual may not have experienced.

When compared with the immune response of the Hybrid cohort, the Super Hybrid cohort manifests a much higher number of antibodies capable of neutralizing Wuhan virus at low concentrations, and an interesting number of cross-reactive antibodies between different variants of the virus.

To enhance broad immunity, it is apparent that performing successive vaccine boosts with a version different from spike Wuhan can be even ideal. This leads to a very significant finding for the third vaccination boost.

Conclusions and future perspectives

During my PhD studies I developed tools and luminescence-based assays to support discovery and characterization of mAbs against the SARS-CoV-2 virus. Assays for neutralizing viruses are essential for the development and evaluation of vaccines and immunotherapies, as well as to conduct fundamental research on the immune system, disease pathogenesis, and transmission. However, the use of infectious viruses in neutralization assays is typically required, and these viruses must be handled carefully in a BSL-3 facility. This complicates the assay and limits its application to laboratories that have access to BSL-3 facilities. An alternative to employing infectious viruses in assays is represented by the use of pseudotype virus -based assays. Because the SARS-CoV-2 pseudotype virus only possesses the spike structural protein and only undergoes one cycle of replication upon infection, the experiment can be conducted under BSL-2 conditions without risk.

This thesis presents a pseudotype virus neutralization assay based on HIV backbones, which is a safer and more convenient alternative to actual viral neutralization assays for drug screening and vaccine evaluation.

Furthermore, the luciferase protein included in the genome of these pseudotyped viruses enables quantitative measurements of antibody properties, which can also be readily extended to a combination of antibodies in a matrix system.

This circumvents one of the primary drawbacks of the microneutralization assay carried out in BSL-3, since it depends entirely on the observation of CPE and is therefore unable to identify the minimal neutralizing capacity of a cocktail of antibodies of instance.

The most effective mAbs that were identified from the various patient cohorts that we examined and reported in this thesis were among the many that I used to validate the pseudotype virus neutralization assay. Results were in line with the assays conducted in BSL-3 using the live virus, indicating that this pseudotype virus -based neutralization assay is a valuable tool for the quick detection of neutralizing antibodies against SARS-CoV-2 and its variants in situations where BSL-3 facilities are not available.

Furthermore, the development of a library of recombinant spike proteins and their mutagenesis-assisted optimization to produce the desired SARS-CoV-2 variants in the quickest amount of time was also a crucial instrument that allowed screening mAbs isolated from individuals who were either actively or passively immunized and to subsequently evaluate their affinity.

These instruments allowed an extremely precise investigation of the various levels of immunity that resulted from a single COVID-19 infection, an infection followed by two vaccination doses, and a double infection followed by three vaccination doses. Although the vaccine boost does allow immunity against SARS-CoV-2 variants to expand, only the double infection confers extremely broad immunity against SARS-CoV-2 variants that are genetically more distant from the WT virus, as well as against other Spikes of distinct Coronaviridae, including SARS-CoV-1.

It is a remarkable accomplishment to have identified broadly reactive antibodies (mAb 1 and mAb 4) against pan-coronavirus genera, including Alpha and Beta coronaviruses, even with cohorts composed of only a few patients.

This work can provide insights for anyone interested in researching infectious diseases caused by viruses, employing pseudotyped viruses and recombinant proteins to assess the activity of mAbs.

To categorize the various levels of affinity that the most potent mAbs display vs the various spike VOCs, a characterization of the mAbs that were identified in our lab using all the Spike variants available in the spike Library by Biacore instrument will be done in the future.

Additionally, I reported in my thesis the detection of pseudotype virus neutralization using the Luciferase gene found in the virions' genomes. However, since the gene that encodes GFP is also present in the virions of the pseudotyped virus that we have produced in our lab, the detection of pseudotype virus using reporter GFP, utilizing sophisticated equipment like Opera Phenix, could ensure high-throughput application.

One aspect which was not deeply investigated here is the evaluation of the binding affinities of spike variants using an *in vitro* competitive pseudotype virus experiment [179]: the cell line HEK293T overexpressing hACE2 receptor could be incubated with a specific spike protein variants at different concentrations together with a pseudotype virus of another spike VOCs. Since our virions has dual reporter genes, GFP for visualization and luciferase for quantification of the infection, if the binding of spike protein variants to the receptor inhibits the infection of pseudotype virus it reduces the expression of reporter genes. This *in vitro* competitive pseudotype virus assay may be very helpful in assessing the various spike variants' binding affinities to the hACE2 receptor.

This could be a crucial experiment since determining the infectivity and rates of VOC transmission requires understanding the interaction between spike protein variants and the hACE2 receptors.

Having access to a comprehensive library of spike proteins and a pseudotype virus system offers researchers a useful tool for their work, simplifying the assessment of inhibitors that block viral entry and neutralizing antibodies.

Patent applications

The following patent applications related to the work presented in this PhD thesis, where I am listed as a co-inventor, were filed:

- Inventor of SARS-CoV-2 full-length human monoclonal antibodies Italian patent applications n. 102021000029528

- Inventor of SARS-CoV-2 full-length human monoclonal antibodies international patent system number PCT/IB2021/055755

- Inventor of SARS-CoV-2 full-length human monoclonal antibodies Italian patent applications n. 102020000015754 and 102020000018955.

Publication List

- *SARS-CoV-2 Spike protein suppresses CTL-mediated killing by inhibiting immune synapse assembly,* Anna Onnis, Emanuele Andreano, Chiara Cassioli, Francesca Finetti, Chiara Della Bella, Oskar Staufer, **Elisa Pantano**, Valentina Abbiento et al., J Exp Med 2023 Feb, doi: 10.1084/jem.20220906.

- *B cell analyses after SARS-CoV-2 mRNA third vaccination reveals a hybrid immunity like antibody response*, Emanuele Andreano, Ida Paciello, Giulio Pierleoni, Giulia Piccini, Valentina Abbiento, Giada Antonelli, Piero Pileri, Noemi Manganaro, **Elisa Pantano**, Giuseppe Maccari et al., Nat Commun., 2023 Jan, doi 10.1038/s41467-022-35781-6.

- *Anatomy of Omicron BA.1 and BA.2 neutralizing antibodies in COVID-19 mRNA vaccinees*, Emanuele Andreano, Ida Paciello, Silvia Marchese, Lorena Donnici, Giulio Pierleoni, Giulia Piccini, Noemi Manganaro, **Elisa Pantano**, Valentina Abbiento et al., Nat Commun., 2022 Jun, doi: 10.1038/s41467-022-31115-8.

- *Structural insights of a highly potent pan-neutralizing SARS-CoV-2 human monoclonal antibody*, Jonathan L Torres, Gabriel Ozorowski , Emanuele Andreano, Hejun Liu, Jeffrey Copps, Giulia Piccini, Lorena Donnici, Matteo Conti, Cyril Planchais, Delphine Planas, Noemi Manganaro, **Elisa Pantano**, Ida Paciello et al., Proc. Natl. Acad. Sci U S A, 2022 May, doi: 10.1073/pnas.2120976119.

- *Extremely potent human monoclonal antibodies from COVID-19 convalescent patients*, Emanuele Andreano, Emanuele Nicastri, Ida Paciello, Piero Pileri, Noemi Manganaro, Giulia Piccini, Alessandro Manenti, **Elisa Pantano**, Anna Kabanova, Marco Troisi et al., Cell, 2021 April doi: 10.1016/j.cell.2021.02.035.

- *Antibodies, epicenter of SARS-CoV-2 immunology*, Simone Pecetta, Mariagrazia Pizza, Claudia Sala, Emanuele Andreano, Piero Pileri, Marco Troisi, **Elisa Pantano**, Noemi Manganaro, Rino Rappuoli, Cell Death Diff., 2021 Feb, doi: 10.1038/s41418-020-00711-w.

- *SARS-CoV-2 escape from a highly neutralizing COVID-19 convalescent plasma*, Emanuele Andreano, Giulia Piccini, Danilo Licastro, Lorenzo Casalino, Nicole V Johnson, Ida Paciello, Simeone Dal Monego, **Elisa Pantano**, Noemi Manganaro et al., Proc. Natl. Acad. Sci U S A, 2021 Sep., doi 10.1073/pnas.2103154118.

- *Hybrid immunity improves B cells and antibodies against SARS-CoV-2 variants*, Emanuele Andreano, Ida Paciello, Giulia Piccini, Noemi Manganaro, Piero Pileri, Inesa Hyseni, Margherita Leonardi, **Elisa Pantano**, Valentina Abbiento, Linda Benincasa et al., Nature, 2021 Dec, doi 10.1038/s41586-021-04117-7.

- *Preprint: SARS-CoV-2 escape in vitro from a highly neutralizing COVID-19 convalescent plasma,* Emanuele Andreano, Giulia Piccini, Danilo Licastro, Lorenzo Casalino, Nicole V Johnson, Ida Paciello, Simeone Dal Monego, **Elisa Pantano**, Noemi Manganaro*, et al.,* Dic 2021, doi: 10.1101/2020.12.28.424451.

- *In publication: PNAS High-resolution map of the Fc-functions mediated by COVID-19 neutralizing antibodies, Ida Paciello, Emanuele Andreano, Elisa Pantano, Giuseppe Maccari, Rino Rappuoli, 2023.*

Acknowledgement

References

1. Information on COVID-19 Treatment, Prevention and Research. *COVID-19 Treatment Guidelines* https://www.covid19treatmentguidelines.nih.gov/.

2. Coronavirus disease (COVID-19). https://www.who.int/emergencies/diseases/novel-coronavirus-2019.

3. A Novel Coronavirus from Patients with Pneumonia in China, 2019 - PubMed. https://pubmed.ncbi.nlm.nih.gov/31978945/.

4. Chan, J. F.-W. *et al.* A familial cluster of pneumonia associated with the 2019 novel coronavirus indicating person-to-person transmission: a study of a family cluster. *Lancet* **395**, 514–523 (2020).

5. Wang, C., Horby, P. W., Hayden, F. G. & Gao, G. F. A novel coronavirus outbreak of global health concern. *Lancet* **395**, 470–473 (2020).

6. Sharma, A., Ahmad Farouk, I. & Lal, S. K. COVID-19: A Review on the Novel Coronavirus Disease Evolution, Transmission, Detection, Control and Prevention. *Viruses* **13**, 202 (2021).

7. Fehr, A. R. & Perlman, S. Coronaviruses: An Overview of Their Replication and Pathogenesis. *Coronaviruses* **1282**, 1–23 (2015).

8. Bentum, K. *et al.* Molecular phylogeny of coronaviruses and host receptors among domestic and close-contact animals reveals subgenome-level conservation, crossover, and divergence. *BMC Veterinary Research* **18**, 124 (2022).

9. Lau, S. K. P. *et al.* Severe acute respiratory syndrome coronavirus-like virus in Chinese horseshoe bats. *Proc Natl Acad Sci U S A* **102**, 14040–14045 (2005).

10. Corman, V. M. *et al.* Evidence for an Ancestral Association of Human Coronavirus 229E with Bats. *J Virol* **89**, 11858–11870 (2015).

11.   Castillo, G. *et al.* Molecular mechanisms of human coronavirus NL63 infection and replication. *Virus Res* **327**, 199078 (2023).

12.   Tang, G., Liu, Z. & Chen, D. Human coronaviruses: Origin, host and receptor. *J Clin Virol* **155**, 105246 (2022).

13.   Vijgen, L. *et al.* Complete genomic sequence of human coronavirus OC43: molecular clock analysis suggests a relatively recent zoonotic coronavirus transmission event. *J Virol* **79**, 1595–1604 (2005).

14.   Crossley, B. M., Mock, R. E., Callison, S. A. & Hietala, S. K. Identification and characterization of a novel alpaca respiratory coronavirus most closely related to the human coronavirus 229E. *Viruses* **4**, 3689–3700 (2012).

15.   Su, S. *et al.* Epidemiology, Genetic Recombination, and Pathogenesis of Coronaviruses. *Trends Microbiol* **24**, 490–502 (2016).

16.   Guan, Y. *et al.* Isolation and characterization of viruses related to the SARS coronavirus from animals in southern China. *Science* **302**, 276–278 (2003).

17.   Esper, F., Weibel, C., Ferguson, D., Landry, M. L. & Kahn, J. S. Evidence of a novel human coronavirus that is associated with respiratory tract disease in infants and young children. *J Infect Dis* **191**, 492–498 (2005).

18.   Zaki, A. M., van Boheemen, S., Bestebroer, T. M., Osterhaus, A. D. M. E. & Fouchier, R. A. M. Isolation of a novel coronavirus from a man with pneumonia in Saudi Arabia. *N Engl J Med* **367**, 1814–1820 (2012).

19.   Hijawi, B. *et al.* Novel coronavirus infections in Jordan, April 2012: epidemiological findings from a retrospective investigation. *East Mediterr Health J* **19 Suppl 1**, S12-18 (2013).

20.   Wise, J. Patient with new strain of coronavirus is treated in intensive care at London hospital. *BMJ* **345**, e6455 (2012).

21.   Middle East Respiratory Syndrome Coronavirus (MERS-CoV)- Kingdom of Saudi Arabia. https://www.who.int/emergencies/disease-outbreak-news/item/2023-DON484.

22.   Elena, S. F. & Sanjuán, R. Adaptive value of high mutation rates of RNA viruses: separating causes from consequences. *J Virol* **79**, 11555–11558 (2005).

23.   Sharma, A. & Lal, S. K. Is tetherin a true antiviral: The influenza a virus controversy. *Rev Med Virol* **29**, e2036 (2019).

24.   To, K. K. W., Hung, I. F. N., Chan, J. F. W. & Yuen, K.-Y. From SARS coronavirus to novel animal and human coronaviruses. *J Thorac Dis* **5 Suppl 2**, S103-108 (2013).

25.   Lam, T. T.-Y. *et al.* Identifying SARS-CoV-2-related coronaviruses in Malayan pangolins. *Nature* **583**, 282–285 (2020).

26.   Markov, P. V. *et al.* The evolution of SARS-CoV-2. *Nat Rev Microbiol* **21**, 361–379 (2023).

27.   Ghafari, M. *et al.* Purifying Selection Determines the Short-Term Time Dependency of Evolutionary Rates in SARS-CoV-2 and pH1N1 Influenza. *Mol Biol Evol* **39**, msac009 (2022).

28.   Ather, A., Patel, B., Ruparel, N. B., Diogenes, A. & Hargreaves, K. M. Coronavirus Disease 19 (COVID-19): Implications for Clinical Dental Care. *J Endod* **46**, 584–595 (2020).

29.   Cai, J. *et al.* Indirect Virus Transmission in Cluster of COVID-19 Cases, Wenzhou, China, 2020. *Emerg Infect Dis* **26**, 1343–1345 (2020).

30.   Phua, J. *et al.* Intensive care management of coronavirus disease 2019 (COVID-19): challenges and recommendations. *Lancet Respir Med* **8**, 506–517 (2020).

31.   Merad, M., Blish, C. A., Sallusto, F. & Iwasaki, A. The immunology and immunopathology of COVID-19. *Science* **375**, 1122–1127 (2022).

32.   Kasuga, Y., Zhu, B., Jang, K.-J. & Yoo, J.-S. Innate immune sensing of coronavirus and viral evasion strategies. *Exp Mol Med* **53**, 723–736 (2021).

33.   Blanco-Melo, D. *et al.* Imbalanced Host Response to SARS-CoV-2 Drives Development of COVID-19. *Cell* **181**, 1036-1045.e9 (2020).

34.   Hadjadj, J. *et al.* Impaired type I interferon activity and inflammatory responses in severe COVID-19 patients. *Science* **369**, 718–724 (2020).

35.   Sposito, B. *et al.* The interferon landscape along the respiratory tract impacts the severity of COVID-19. *Cell* **184**, 4953-4968.e16 (2021).

36.   Lucas, C. *et al.* Longitudinal analyses reveal immunological misfiring in severe COVID-19. *Nature* **584**, 463–469 (2020).

37.   Lee, J. S. *et al.* Immunophenotyping of COVID-19 and influenza highlights the role of type I interferons in development of severe COVID-19. *Sci Immunol* **5**, eabd1554 (2020).

38.   Witkowski, M. *et al.* Untimely TGFβ responses in COVID-19 limit antiviral functions of NK cells. *Nature* **600**, 295–301 (2021).

39.   Liao, M. *et al.* Single-cell landscape of bronchoalveolar immune cells in patients with COVID-19. *Nat Med* **26**, 842–844 (2020).

40.   Israelow, B. *et al.* Mouse model of SARS-CoV-2 reveals inflammatory role of type I interferon signaling. *J Exp Med* **217**, e20201241 (2020).

41.   Earle, K. A. *et al.* Evidence for antibody as a protective correlate for COVID-19 vaccines. *Vaccine* **39**, 4423–4428 (2021).

42.   Corti, D., Purcell, L. A., Snell, G. & Veesler, D. Tackling COVID-19 with neutralizing monoclonal antibodies. *Cell* **184**, 3086–3108 (2021).

43.   Wang, Z. *et al.* Naturally enhanced neutralizing breadth against SARS-CoV-2 one year after infection. *Nature* **595**, 426–431 (2021).

44.   Kemp, S. A. *et al.* SARS-CoV-2 evolution during treatment of chronic infection. *Nature* **592**, 277–282 (2021).

45.   Ng, K. W. *et al.* Preexisting and de novo humoral immunity to SARS-CoV-2 in humans. *Science* **370**, 1339–1343 (2020).

46.   Channappanavar, R. *et al.* Dysregulated Type I Interferon and Inflammatory Monocyte-Macrophage Responses Cause Lethal Pneumonia in SARS-CoV-Infected Mice. *Cell Host Microbe* **19**, 181–193 (2016).

47.   Livanos, A. E. *et al.* Intestinal Host Response to SARS-CoV-2 Infection and COVID-19 Outcomes in Patients With Gastrointestinal Symptoms. *Gastroenterology* **160**, 2435-2450.e34 (2021).

48.   Williamson, E. J. *et al.* Factors associated with COVID-19-related death using OpenSAFELY. *Nature* **584**, 430–436 (2020).

49.   Chakraborty, S. *et al.* Proinflammatory IgG Fc structures in patients with severe COVID-19. *Nat Immunol* **22**, 67–73 (2021).

50.   Takahashi, T. *et al.* Sex differences in immune responses that underlie COVID-19 disease outcomes. *Nature* **588**, 315–320 (2020).

51.   Li, W. *et al.* Angiotensin-converting enzyme 2 is a functional receptor for the SARS coronavirus. *Nature* **426**, 450–454 (2003).

52.   Shang, J. *et al.* Cell entry mechanisms of SARS-CoV-2. *Proc Natl Acad Sci U S A* **117**, 11727–11734 (2020).

53.   Matsuyama, S. *et al.* Efficient activation of the severe acute respiratory syndrome coronavirus spike protein by the transmembrane protease TMPRSS2. *J Virol* **84**, 12658–12664 (2010).

54.   Inoue, Y. *et al.* Clathrin-dependent entry of severe acute respiratory syndrome coronavirus into target cells expressing ACE2 with the cytoplasmic tail deleted. *J Virol* **81**, 8722–8729 (2007).

55.   Jaimes, J. A., André, N. M., Chappie, J. S., Millet, J. K. & Whittaker, G. R. Phylogenetic

Analysis and Structural Modeling of SARS-CoV-2 Spike Protein Reveals an Evolutionary Distinct

and Proteolytically Sensitive Activation Loop. *J Mol Biol* **432**, 3309–3325 (2020).

56.   Jackson, C. B., Farzan, M., Chen, B. & Choe, H. Mechanisms of SARS-CoV-2 entry into cells.

Nat Rev Mol Cell Biol **23**, 3–20 (2022).

57.   Bosch, B. J., van der Zee, R., de Haan, C. A. M. & Rottier, P. J. M. The coronavirus spike

protein is a class I virus fusion protein: structural and functional characterization of the fusion

core complex. *J Virol* **77**, 8801–8811 (2003).

58.   Watanabe, Y., Allen, J. D., Wrapp, D., McLellan, J. S. & Crispin, M. Site-specific glycan

analysis of the SARS-CoV-2 spike. *Science* **369**, 330–333 (2020).

59.   Tang, T., Bidon, M., Jaimes, J. A., Whittaker, G. R. & Daniel, S. Coronavirus membrane fusion

mechanism offers a potential target for antiviral development. *Antiviral Res* **178**, 104792 (2020).

60.   Wrapp, D. *et al.* Cryo-EM structure of the 2019-nCoV spike in the prefusion conformation.

Science **367**, 1260–1263 (2020).

61.   Bank, R. P. D. RCSB PDB - 6VYB: SARS-CoV-2 spike ectodomain structure (open state).

https://www.rcsb.org/structure/6VYB.

62.   Xia, S. *et al.* A pan-coronavirus fusion inhibitor targeting the HR1 domain of human

coronavirus spike. *Sci Adv* **5**, eaav4580 (2019).

63.   Huang, Y., Yang, C., Xu, X.-F., Xu, W. & Liu, S.-W. Structural and functional properties of SARS-

CoV-2 spike protein: potential antivirus drug development for COVID-19. *Acta Pharmacol Sin* **41**,

1141–1149 (2020).

64.   Robson, B. Computers and viral diseases. Preliminary bioinformatics studies on the design

of a synthetic vaccine and a preventative peptidomimetic antagonist against the SARS-CoV-2

(2019-nCoV, COVID-19) coronavirus. *Comput Biol Med* **119**, 103670 (2020).

65.   Andersen, K. G., Rambaut, A., Lipkin, W. I., Holmes, E. C. & Garry, R. F. The proximal origin of

SARS-CoV-2. *Nat Med* **26**, 450–452 (2020).

66.   Weissenhorn, W. *et al.* Structural basis for membrane fusion by enveloped viruses. *Mol

Membr Biol* **16**, 3–9 (1999).

67.   Zhang, H., Penninger, J. M., Li, Y., Zhong, N. & Slutsky, A. S. Angiotensin-converting enzyme

2 (ACE2) as a SARS-CoV-2 receptor: molecular mechanisms and potential therapeutic target.

Intensive Care Med **46**, 586–590 (2020).

68.   Harvey, W. T. *et al.* SARS-CoV-2 variants, spike mutations and immune escape. *Nat Rev

Microbiol* **19**, 409–424 (2021).

69.   Shen, X. *et al.* SARS-CoV-2 variant B.1.1.7 is susceptible to neutralizing antibodies elicited by

ancestral spike vaccines. *Cell Host Microbe* **29**, 529-539.e3 (2021).

70.   Sabino, E. C. *et al.* Resurgence of COVID-19 in Manaus, Brazil, despite high seroprevalence.

Lancet **397**, 452–455 (2021).

71.   Campbell, F. *et al.* Increased transmissibility and global spread of SARS-CoV-2 variants of

concern as at June 2021. *Euro Surveill* **26**, 2100509 (2021).

72.   Tegally, H. *et al.* Emergence of SARS-CoV-2 Omicron lineages BA.4 and BA.5 in South Africa.

Nat Med **28**, 1785–1790 (2022).

73.   Tao, K. *et al.* The biological and clinical significance of emerging SARS-CoV-2 variants. *Nat

Rev Genet* **22**, 757–773 (2021).

74.   Obermeyer, F. *et al.* Analysis of 6.4 million SARS-CoV-2 genomes identifies mutations

associated with fitness. *Science* **376**, 1327–1332 (2022).

75.   Peng, F., Yuan, H., Wu, S. & Zhou, Y. Recent Advances on Drugs and Vaccines for COVID-19.

Inquiry **58**, 469580211055630 (2021).

76.   Logunov, D. Y. *et al.* Safety and efficacy of an rAd26 and rAd5 vector-based heterologous

prime-boost COVID-19 vaccine: an interim analysis of a randomised controlled phase 3 trial in

Russia. *Lancet* **397**, 671–681 (2021).

77.   Lopez Bernal, J. *et al.* Effectiveness of the Pfizer-BioNTech and Oxford-AstraZeneca vaccines

on covid-19 related symptoms, hospital admissions, and mortality in older adults in England:

test negative case-control study. *BMJ* **373**, n1088 (2021).

78.   Yadav, T. *et al.* Recombinant vaccines for COVID-19. *Hum Vaccin Immunother* **16**, 2905–2912

(2020).

79.   Kuzmina, A. *et al.* SARS-CoV-2 spike variants exhibit differential infectivity and neutralization

resistance to convalescent or post-vaccination sera. *Cell Host Microbe* **29**, 522-528.e2 (2021).

80.   Analysis of a SARS-CoV-2 convalescent cohort identified a common strategy for escape of

vaccine-induced anti-RBD antibodies by Beta and Omicron variants - eBioMedicine.

https://www.thelancet.com/journals/ebiom/article/PIIS2352-3964(22)00209-2/fulltext.

81.   Tada, T. *et al.* Partial resistance of SARS-CoV-2 Delta variants to vaccine-elicited antibodies

and convalescent sera. *iScience* **24**, 103341 (2021).

82.   Liu, S. T. H. *et al.* Convalescent plasma treatment of severe COVID-19: a propensity score-

matched control study. *Nat Med* **26**, 1708–1713 (2020).

83.   Pecetta, S. *et al.* Antibodies, epicenter of SARS-CoV-2 immunology. *Cell Death Differ* **28**,

821–824 (2021).

84.   Traggiai, E. *et al.* An efficient method to make human monoclonal antibodies from memory

B cells: potent neutralization of SARS coronavirus. *Nat Med* **10**, 871–875 (2004).

85.   Baum, A. *et al.* REGN-COV2 antibodies prevent and treat SARS-CoV-2 infection in rhesus

macaques and hamsters. *Science* **370**, 1110–1115 (2020).

86.   Chen, P. *et al.* SARS-CoV-2 Neutralizing Antibody LY-CoV555 in Outpatients with Covid-19. *N Engl J Med* **384**, 229–237 (2021).

87.   Crowe, J. E. Human Antibodies for Viral Infections. *Annual Review of Immunology* **40**, 349–386 (2022).

88.   Shah, D. K. & Betts, A. M. Antibody biodistribution coefficients: inferring tissue concentrations of monoclonal antibodies based on the plasma concentrations in several preclinical species and human. *MAbs* **5**, 297–305 (2013).

89.   Charles A Janeway, J., Travers, P., Walport, M. & Shlomchik, M. J. The structure of a typical antibody molecule. in *Immunobiology: The Immune System in Health and Disease. 5th edition* (Garland Science, 2001).

90.   Viau, M. & Zouali, M. B-lymphocytes, innate immunity, and autoimmunity. *Clin Immunol* **114**, 17–26 (2005).

91.   Hifumi, T. *et al.* Clinical Serum Therapy: Benefits, Cautions, and Potential Applications. *Keio J Med* **66**, 57–64 (2017).

92.   The Nobel Prize in Physiology or Medicine 1901. *NobelPrize.org* https://www.nobelprize.org/prizes/medicine/1901/behring/article/.

93.   Burton, D. R. Antibody: the flexible adaptor molecule. *Trends Biochem Sci* **15**, 64–69 (1990).

94.   Lu, L. L., Suscovich, T. J., Fortune, S. M. & Alter, G. Beyond binding: antibody effector functions in infectious diseases. *Nat Rev Immunol* **18**, 46–61 (2018).

95.   Vidarsson, G., Dekkers, G. & Rispens, T. IgG subclasses and allotypes: from structure to effector functions. *Front Immunol* **5**, 520 (2014).

96.   Dondelinger, M. *et al.* Understanding the Significance and Implications of Antibody Numbering and Antigen-Binding Surface/Residue Definition. *Front Immunol* **9**, 2278 (2018).

97.   Ausserwöger, H. *et al.* Non-specificity as the sticky problem in therapeutic antibody

development. *Nat Rev Chem* **6**, 844–861 (2022).

98.   Zhao, J., Nussinov, R. & Ma, B. Antigen binding allosterically promotes Fc receptor

recognition. *MAbs* **11**, 58–74 (2019).

99.   Pantaleo, G., Correia, B., Fenwick, C., Joo, V. S. & Perez, L. Antibodies to combat viral

infections: development strategies and progress. *Nat Rev Drug Discov* **21**, 676–696 (2022).

100.   Rappuoli, R., Bottomley, M. J., D'Oro, U., Finco, O. & De Gregorio, E. Reverse vaccinology

2.0: Human immunology instructs vaccine antigen design. *J Exp Med* **213**, 469–481 (2016).

101.   Duvergé, A. & Negroni, M. Pseudotyping Lentiviral Vectors: When the Clothes Make the

Virus. *Viruses* **12**, 1311 (2020).

102.   Gao, D. *et al.* Cyclic GMP-AMP Synthase is an Innate Immune Sensor of HIV and Other

Retroviruses. *Science* **341**, 10.1126/science.1240933 (2013).

103.   Naldini, L., Trono, D. & Verma, I. M. Lentiviral vectors, two decades later. *Science* **353**, 1101–

1102 (2016).

104.   A Dictionary of Virology - Google Books.

https://www.google.it/books/edition/A_Dictionary_of_Virology/vYotjPWL_2IC?hl=it&gbpv=1&d

q=inauthor:%22Brian+W.J.+Mahy%22&printsec=frontcover.

105.   Clements, J. E. & Zink, M. C. Molecular biology and pathogenesis of animal lentivirus

infections. *Clin Microbiol Rev* **9**, 100–117 (1996).

106.   van Heuvel, Y., Schatz, S., Rosengarten, J. F. & Stitz, J. Infectious RNA: Human

Immunodeficiency Virus (HIV) Biology, Therapeutic Intervention, and the Quest for a Vaccine.

Toxins **14**, 138 (2022).

107.   The Lenti Viral Vector System: A New Way to Deliver Genetic Therapies. *Assay Genie*

https://www.assaygenie.com/blog/a-new-way-to-deliver-genetic-therapies-the-lenti-virus-

vector-system.

108.   La biosicurezza connessa all'utilizzo di vettori lentivirali nella sperimentazione

biotecnologica - INAIL. https://www.inail.it/cs/internet/comunicazione/pubblicazioni/catalogo-

generale/la_biosicurezza_connessa_utilizzo_di_vettori_lentivirali.html.

109.   Li, Q., Liu, Q., Huang, W., Li, X. & Wang, Y. Current status on the development of

pseudoviruses for enveloped viruses. *Rev Med Virol* **28**, e1963 (2018).

110.   Huang, S.-W. *et al.* Assessing the application of a pseudovirus system for emerging SARS-

CoV-2 and re-emerging avian influenza virus H5 subtypes in vaccine development. *Biomedical

Journal* **43**, 375–387 (2020).

111.   Andreano, E. *et al.* Extremely potent human monoclonal antibodies from COVID-19

convalescent patients. *Cell* **184**, 1821-1835.e16 (2021).

112.   Andreano, E. *et al.* Hybrid immunity improves B cells and antibodies against SARS-CoV-2

variants. *Nature* **600**, 530–535 (2021).

113.   Galipeau, Y. *et al.* Relative Ratios of Human Seasonal Coronavirus Antibodies Predict the

Efficiency of Cross-Neutralization of SARS-CoV-2 Spike Binding to ACE2. *eBioMedicine* **74**,

103700 (2021).

114.   Cui, Z. *et al.* Structural and functional characterizations of infectivity and immune evasion of

SARS-CoV-2 Omicron. *Cell* **185**, 860-871.e13 (2022).

115.   Walls, A. C. *et al.* Structure, Function, and Antigenicity of the SARS-CoV-2 Spike

Glycoprotein. *Cell* **181**, 281-292.e6 (2020).

116.   Cui, J., Li, F. & Shi, Z.-L. Origin and evolution of pathogenic coronaviruses. *Nat Rev Microbiol*

17, 181–192 (2019).

117.   Cicaloni, V. *et al.* A Bioinformatics Approach to Investigate Structural and Non-Structural Proteins in Human Coronaviruses. *Front Genet* **13**, 891418 (2022).

118.   Pallesen, J. *et al.* Immunogenicity and structures of a rationally designed prefusion MERS-CoV spike antigen. *Proc Natl Acad Sci U S A* **114**, E7348–E7357 (2017).

119.   Kirchdoerfer, R. N. *et al.* Stabilized coronavirus spikes are resistant to conformational changes induced by receptor recognition or proteolysis. *Sci Rep* **8**, 15701 (2018).

120.   Hsieh, C.-L. *et al.* Structure-based design of prefusion-stabilized SARS-CoV-2 spikes. *Science* **369**, 1501–1505 (2020).

121.   Korber, B. *et al.* Tracking Changes in SARS-CoV-2 Spike: Evidence that D614G Increases Infectivity of the COVID-19 Virus. *Cell* **182**, 812-827.e19 (2020).

122.   Gobeil, S. M.-C. *et al.* D614G Mutation Alters SARS-CoV-2 Spike Conformation and Enhances Protease Cleavage at the S1/S2 Junction. *Cell Rep* **34**, 108630 (2021).

123.   Zhang, L. *et al.* SARS-CoV-2 spike-protein D614G mutation increases virion spike density and infectivity. *Nat Commun* **11**, 6013 (2020).

124.   Huang, J. *et al.* Isolation of human monoclonal antibodies from peripheral blood B cells. *Nat Protoc* **8**, 1907–1915 (2013).

125.   Andreano, E. *et al.* Anatomy of Omicron BA.1 and BA.2 neutralizing antibodies in COVID-19 mRNA vaccinees. *Nat Commun* **13**, 3375 (2022).

126.   Krammer, F. & Simon, V. Serology assays to manage COVID-19. *Science* **368**, 1060–1061 (2020).

127.   Stadlbauer, D. *et al.* SARS-CoV-2 Seroconversion in Humans: A Detailed Protocol for a Serological Assay, Antigen Production, and Test Setup. *Curr Protoc Microbiol* **57**, e100 (2020).

128.   The effect of spike mutations on SARS-CoV-2 neutralization - PubMed. https://pubmed.ncbi.nlm.nih.gov/33713594/.

129. Chan, J. F.-W. *et al.* Genomic characterization of the 2019 novel human-pathogenic coronavirus isolated from a patient with atypical pneumonia after visiting Wuhan. *Emerg Microbes Infect* **9**, 221–236 (2020).

130. Du, L. *et al.* The spike protein of SARS-CoV--a target for vaccine and therapeutic development. *Nat Rev Microbiol* **7**, 226–236 (2009).

131. Jiang, S., He, Y. & Liu, S. SARS vaccine development. *Emerg Infect Dis* **11**, 1016–1020 (2005).

132. Nie, J. *et al.* Establishment and validation of a pseudovirus neutralization assay for SARS-CoV-2. *Emerg Microbes Infect* **9**, 680–686 (2020).

133. Fan, C. *et al.* A Human DPP4-Knockin Mouse's Susceptibility to Infection by Authentic and Pseudotyped MERS-CoV. *Viruses* **10**, 448 (2018).

134. Nie, J. *et al.* Development of in vitro and in vivo rabies virus neutralization assays based on a high-titer pseudovirus system. *Sci Rep* **7**, 42769 (2017).

135. Liu, Q. *et al.* Antibody-dependent-cellular-cytotoxicity-inducing antibodies significantly affect the post-exposure treatment of Ebola virus infection. *Sci Rep* **7**, 45552 (2017).

136. Zhang, L. *et al.* A bioluminescent imaging mouse model for Marburg virus based on a pseudovirus system. *Hum Vaccin Immunother* **13**, 1811–1817 (2017).

137. Bentley, E. M., Mather, S. T. & Temperton, N. J. The use of pseudotypes to study viruses, virus sero-epidemiology and vaccination. *Vaccine* **33**, 2955–2962 (2015).

138. Garcia-Beltran, W. F. *et al.* Multiple SARS-CoV-2 variants escape neutralization by vaccine-induced humoral immunity. *Cell* **184**, 2372-2383.e9 (2021).

139. Cao, Y. *et al.* Omicron escapes the majority of existing SARS-CoV-2 neutralizing antibodies. *Nature* **602**, 657–663 (2022).

140. Conforti, A. *et al.* COVID-eVax, an electroporated DNA vaccine candidate encoding the SARS-CoV-2 RBD, elicits protective responses in animal models. *Mol Ther* **30**, 311–326 (2022).

141.   Sampson, A. T. *et al.* Coronavirus Pseudotypes for All Circulating Human Coronaviruses for Quantification of Cross-Neutralizing Antibody Responses. *Viruses* **13**, 1579 (2021).

142.   Rogers, T. F. *et al.* Isolation of potent SARS-CoV-2 neutralizing antibodies and protection from disease in a small animal model. *Science* **369**, 956–963 (2020).

143.   VanBlargan, L. A. *et al.* An infectious SARS-CoV-2 B.1.1.529 Omicron virus escapes neutralization by therapeutic monoclonal antibodies. *Nat Med* **28**, 490–495 (2022).

144.   Planas, D. *et al.* Considerable escape of SARS-CoV-2 Omicron to antibody neutralization. *Nature* **602**, 671–675 (2022).

145.   Motozono, C. *et al.* SARS-CoV-2 spike L452R variant evades cellular immunity and increases infectivity. *Cell Host Microbe* **29**, 1124-1136.e11 (2021).

146.   Pinto, D. *et al.* Cross-neutralization of SARS-CoV-2 by a human monoclonal SARS-CoV antibody. *Nature* **583**, 290–295 (2020).

147.   Li, M. *et al.* Broadly neutralizing and protective nanobodies against SARS-CoV-2 Omicron subvariants BA.1, BA.2, and BA.4/5 and diverse sarbecoviruses. *Nat Commun* **13**, 7957 (2022).

148.   Chen, Y. *et al.* Broadly neutralizing antibodies to SARS-CoV-2 and other human coronaviruses. *Nat Rev Immunol* **23**, 189–199 (2023).

149.   Kallewaard, N. L. *et al.* Structure and Function Analysis of an Antibody Recognizing All Influenza A Subtypes. *Cell* **166**, 596–608 (2016).

150.   Kombe Kombe, A. J., Zahid, A., Mohammed, A., Shi, R. & Jin, T. Potent Molecular Feature-based Neutralizing Monoclonal Antibodies as Promising Therapeutics Against SARS-CoV-2 Infection. *Front Mol Biosci* **8**, 670815 (2021).

151.   Chakraborty, C., Sharma, A. R., Bhattacharya, M., Agoramoorthy, G. & Lee, S.-S. Asian-Origin Approved COVID-19 Vaccines and Current Status of COVID-19 Vaccination Program in Asia: A Critical Analysis. *Vaccines (Basel)* **9**, 600 (2021).

152. Chakraborty, C., Sharma, A. R., Bhattacharya, M., Agoramoorthy, G. & Lee, S.-S. All Nations Must Prioritize the COVID-19 Vaccination Program for Elderly Adults Urgently. *Aging Dis* **12**, 688–690 (2021).

153. Wang, H. *et al.* Mutation-Specific SARS-CoV-2 PCR Screen: Rapid and Accurate Detection of Variants of Concern and the Identification of a Newly Emerging Variant with Spike L452R Mutation. *J Clin Microbiol* **59**, e0092621 (2021).

154. Boehm, E. *et al.* Novel SARS-CoV-2 variants: the pandemics within the pandemic. *Clin Microbiol Infect* **27**, 1109–1117 (2021).

155. Kim, S.-J., Nguyen, V.-G., Park, Y.-H., Park, B.-K. & Chung, H.-C. A Novel Synonymous Mutation of SARS-CoV-2: Is This Possible to Affect Their Antigenicity and Immunogenicity? *Vaccines (Basel)* **8**, 220 (2020).

156. Zost, S. J. *et al.* Potently neutralizing and protective human antibodies against SARS-CoV-2. *Nature* **584**, 443–449 (2020).

157. Ianevski, A., Giri, A. K. & Aittokallio, T. SynergyFinder 2.0: visual analytics of multi-drug combination synergies. *Nucleic Acids Res* **48**, W488–W493 (2020).

158. Lauring, A. S. & Hodcroft, E. B. Genetic Variants of SARS-CoV-2-What Do They Mean? *JAMA* **325**, 529–531 (2021).

159. Duchene, S. *et al.* Temporal signal and the phylodynamic threshold of SARS-CoV-2. *Virus Evol* **6**, veaa061 (2020).

160. Worobey, M. *et al.* The emergence of SARS-CoV-2 in Europe and North America. *Science* **370**, 564–570 (2020).

161. Xiong, H. *et al.* The neutralizing breadth of antibodies targeting diverse conserved epitopes between SARS-CoV and SARS-CoV-2. *Proc Natl Acad Sci U S A* **119**, e2204256119 (2022).

162.   Jensen, B. *et al.* Emergence of the E484K mutation in SARS-COV-2-infected immunocompromised patients treated with bamlanivimab in Germany. *Lancet Reg Health Eur* **8**, 100164 (2021).

163.   Baum, A. *et al.* Antibody cocktail to SARS-CoV-2 spike protein prevents rapid mutational escape seen with individual antibodies. *Science* **369**, 1014–1018 (2020).

164.   Zhou, D. *et al.* Evidence of escape of SARS-CoV-2 variant B.1.351 from natural and vaccine-induced sera. *Cell* **184**, 2348-2361.e6 (2021).

165.   ter Meulen, J. *et al.* Human monoclonal antibody combination against SARS coronavirus: synergy and coverage of escape mutants. *PLoS Med* **3**, e237 (2006).

166.   Shrestha, L. B., Foster, C., Rawlinson, W., Tedla, N. & Bull, R. A. Evolution of the SARS-CoV-2 omicron variants BA.1 to BA.5: Implications for immune escape and transmission. *Rev Med Virol* **32**, e2381 (2022).

167.   Risk Assessment Summary for SARS CoV-2 Sublineage BA.2.86 | CDC. https://www.cdc.gov/respiratory-viruses/whats-new/covid-19-variant.html (2023).

168.   Diamant, E., Torgeman, A., Ozeri, E. & Zichel, R. Monoclonal Antibody Combinations that Present Synergistic Neutralizing Activity: A Platform for Next-Generation Anti-Toxin Drugs. *Toxins (Basel)* **7**, 1854–1881 (2015).

169.   Shi, R. *et al.* A human neutralizing antibody targets the receptor-binding site of SARS-CoV-2. *Nature* **584**, 120–124 (2020).

170.   Hooft van Huijsduijnen, R. *et al.* Reassessing therapeutic antibodies for neglected and tropical diseases. *PLoS Negl Trop Dis* **14**, e0007860 (2020).

171.   Sparrow, E., Friede, M., Sheikh, M. & Torvaldsen, S. Therapeutic antibodies for infectious diseases. *Bull World Health Organ* **95**, 235–237 (2017).

172.   Liang, X. *et al.* Transcriptionally active polymerase chain reaction (TAP): high throughput

gene expression using genome sequence data. *J Biol Chem* **277**, 3593–3598 (2002).

173.   Andreano, E. *et al.* SARS-CoV-2 escape in vitro from a highly neutralizing COVID-19

convalescent plasma. *bioRxiv* 2020.12.28.424451 (2020) doi:10.1101/2020.12.28.424451.

174.   Lee, W. S., Wheatley, A. K., Kent, S. J. & DeKosky, B. J. Antibody-dependent enhancement

and SARS-CoV-2 vaccines and therapies. *Nat Microbiol* **5**, 1185–1191 (2020).

175.   Zalevsky, J. *et al.* Enhanced antibody half-life improves in vivo activity. *Nat Biotechnol* **28**,

157–159 (2010).

176.   Pegu, A., Hessell, A. J., Mascola, J. R. & Haigwood, N. L. Use of broadly neutralizing

antibodies for HIV-1 prevention. *Immunol Rev* **275**, 296–312 (2017).

177.   Schlothauer, T. *et al.* Novel human IgG1 and IgG4 Fc-engineered antibodies with completely

abolished immune effector functions. *Protein Eng Des Sel* **29**, 457–466 (2016).

178.   Starr, T. N. *et al.* Prospective mapping of viral mutations that escape antibodies used to

treat COVID-19. *Science* **371**, 850–854 (2021).

179.   Mahalingam, G. *et al.* Correlating the differences in the receptor binding domain of SARS-

CoV-2 spike variants on their interactions with human ACE2 receptor. *Sci Rep* **13**, 8743 (2023).